5-10-2014

Characterization of Suf Pathway for Fe-S Cluster Assembly in Escherichia Coli

Yuyuan Dai
University of South Carolina - Columbia

CHARACTERIZATION OF SUF PATHWAY FOR FE-S CLUSTER ASSEMBLY IN *ESCHERICHIA COLI*

by

Yuyuan Dai

Bachelor of Science
Nanjing University, 2008

Submitted in Partial Fulfillment of the Requirements

For the Degree of Doctor of Philosophy in

Biochemistry

College of Arts and Sciences

University of South Carolina

2014

Accepted by:

F. Wayne Outten, Major Professor

Caryn E. Outten, Committee Member

Qian Wang, Committee Member

Mike Wyatt, Committee Member

Lacy Ford, Vice Provost and Dean of Graduate Studies

DEDICATION

Dedicated to my beloved mother

ACKNOWLEDGEMENTS

Ph.D. life is a tough journey. There are so many professors and so many friends who encouraged me, supported me and helped me during this journey. Without them, I probably would end up with quitting or in depression.

I would like to express my deepest appreciation to my advisor, Dr. F. Wayne Outten for his inspiring guidance, his endless support and his sincere encouragement throughout this work. He was always patient to me, to my upset and to my research. He is a mentor and also a friend who always thinks the best for me. I am so grateful to have him as my Ph.D. advisor.

I wish to thank my research committee members Dr. Cayn E. Outten, Dr. Qian Wang and Dr. Mike Wyatt for their time and valuable advice during my graduate studies. I would like to acknowledge Dr. Laura S. Busenlehner and Dr. Harsimran Singh from University of Alabama for the collaboration on my research project. I mst acknowledge NIH grant for the financial support.

I would like to thank all my former and present colleagues for their help and enjoyable company. In particular, I want to thank Haoran Li, Carla Ayala-Castro, Suning Wang, Avneesh Saini, Harsimranjit Chahal, and Leslie L. Lovelace for their technical guidance and valuable research suggestions. I would also like to thank the staff members at Department of Chemistry and Biochemistry, USC for their support.

I must thank all my friends (Chunxue Wang, Haoran Li, Shu Liu, Chen Zhao, Li Wang and Bing Gu) at USC for all the happiness they brought to my life and all the

difficult time we have been through together. I would like to give my special thanks to my best friend Xiaohan Wang for always being at my side giving me advice, encouragement and strength.

At last, I must express my tender thanks to my family in China, my grandparents Qiaozhu Sun and Anyun Wang, my parents Yuelin Wang and Tiecheng Dai, my aunt Yueping Wang and my uncle Qingjun Cui, my sister Yumei Wang and her husband Xinyu Qiao, and my lovely niece Han Qiao. They love me so much and give me strength to overcome all the difficulties I encountered. Special thanks go to my mother for her endless love and all the precious memories with her. Hope I made her proud.

ABSTRACT

Fe-S clusters are critical metallocofactors required for cell function. Because of the toxicity of ferrous iron and sulfide to the cell, in vivo Fe-S cluster assembly is carried out by multiprotein biosynthetic pathways. *Escherichia coli* contains a stress-responsive Fe-S cluster assembly system, the SufABCDSE pathway, working under iron starvation and oxidative stress conditions. The cysteine desulfurase SufS and its accessory protein SufE work together to mobilize persulfide from L-cysteine. We collaborated with Dr. Laura S. Busenlehner to use hydrogen/deuterium exchange mass spectrometry (HDX-MS) to characterize SufS-SufE interactions and protein dynamics. HDX-MS analysis shows that SufE binds near the SufS active site to accept persulfide and initiates allosteric changes in other parts of the SufS structure. SufE enhances the initial L-cysteine substrate binding to SufS and formation of the external aldimine required for early steps in SufS catalysis. HDX-MS analysis suggests a more active role for SufE in promoting SufS reaction for Fe-S cluster assembly and provides a new picture of the SufS-SufE sulfur transferase pathway, which is different from IscS-IscU sulfur system in Isc pathway working under normal conditions. To determine why the Suf pathway is favored under stress conditions, we directly compared the stress response SufS-SufE sulfur transfer pathway and the basal housekeeping IscS-IscU pathway. We found that SufS-SufE cysteine desulfurase activity is significantly higher than IscS-IscU at physiological cysteine concentrations and after exposure to H_2O_2. Mass spectrometry analysis demonstrated that IscS-IscU is more

susceptible than SufS-SufE to oxidative modification by H_2O_2. These results provide biochemical insight into the stress resistance of the Suf pathway. We also found an interesting mutant SufE(D74R), which can interacts stronger with SufS and better enhance SufS activity compared to SufE. Besides the SufS-SufE system, there are two cluster scaffold candidates in Suf pathway, $SufBC_2D$ complex and SufA. Both of them can be purified and reconstituted with Fe-S cluster in vivo and in vitro respectively. To distinguish their relative roles, we used a combination of protein-protein interaction and in vitro Fe-S cluster assembly assays and found that SufA works as a shuttle protein to accept Fe-S clusters formed de novo on the $SufBC_2D$ complex.

TABLE OF CONTENTS

LIST OF TABLES

LIST OF FIGURES

Chapter 1

Introduction

Iron

Iron is abundant in biology and is a necessary transition metal found in nearly all living organisms, ranging from the evolutionarily primitive arch to humans. Iron exists in a wide range of oxidation states, -2 to +6, although +2 and +3 are the most common. Iron can bind proteins in mono- and di-iron reaction centers; can be incorporated into porphyrin rings to form heme, which participates in many biological oxidations and in oxygen transport; and can be combined with elemental sulfur to form iron-sulfur (Fe-S) centers. In these various forms, iron is required for certain key biochemical pathways that are essential for life on Earth, most notably nitrogen fixation, photosynthesis, and respiration [1].

Iron-withholding, a major non-immune defense system is a general strategy in humans to protect them against pathogen invasions. Under normal conditions, iron availability is controlled through binding to high iron-affinity proteins and the concentration of free iron is reduced to extremely low levels. Free iron in body fluids is usually held below 10^{-12} μM. However, most microbial pathogens have high iron requirements for growth. Gram-negative bacteria, like *E.coli* requires iron concentration of 0.3 – 1.8 μM for growth.

In *E.coli*, one cell contains about 1.2 X 10^6 atoms of iron [2], most of which is bound to iron-containing proteins or iron storage proteins[3]. Only 1% of total cellular iron contributes to the labile free iron pool. This is due to the toxicity brought by high reactivity of the free reduced iron through the Fenton reaction[4] (Figure 1.1).

The hydroxyl radicals produced from the Fenton reaction can damage different biological target molecules such as DNA, proteins, or lipids. So the maintenance of iron homeostasis and iron availability is very important and highly regulated in vivo [5].

How does the microorganism including the pathogen bacterial adapt to the iron-restricted environment? It is an intriguing question. One of the questions our lab tries to answer is how *E.coli* survives in iron-limiting conditions. The long term goal is to characterize the genetic and biochemical systems utilized by bacterial pathogens to preserve intracellular iron homeostasis during stress.

Sulfur

Sulfur is one of the nonmetallic elements essential for life. It is the eighth most abundant element in the human body by weight. Sulfur is required for the biosynthesis of several essential compounds like amino acids (cysteine and methionine), vitamins (biotin, thiamin), and prosthetic groups (Fe-S clusters) in all organisms. In humans, methionine is an essential amino acid that must be ingested. The other sulfur-containing compounds like cysteine in the human body can be synthesized from methionine. In plants and microorganisms, the predominant mechanism for sulfur incorporation is through cysteine biosynthesis via sulfate assimilation. Sulfur in cysteine can be utilized for other sulfur containing cofactor synthesis through a group of enzymes called desulfurase that include

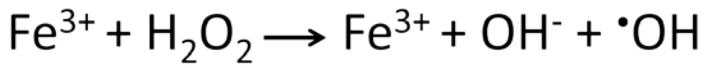

Figure 1.1 Fenton reaction. Hydrogen peroxide is decomposed to hydroxyl ion (OH^-) and highly reactive hydroxyl radical ($^{\bullet}OH$) in the presence of ferrous iron (Fe^{2+}), which undergoes oxidation to ferric iron (Fe^{3+}).

NifS, IscS and SufS in *E.coli*. My research in Dr.Wayne Outten's lab mainly focuses on the desulfurase study.

Iron-Sulfur Clusters

Influential theories of evolution have invoked a role for iron sulfides in the iron-sulfur word theory. The Günter Wächtershäuser proposes iron–sulfur world theory between 1988 and 1992. The theory proposes that early life may have formed on the surface of iron sulfide minerals. Iron is the fourth most abundant element by weight in the Earth's crust. The more soluble Fe^{2+} form was stabilized by the reducing atmosphere of the early Earth and primordial organisms incorporated iron as a cofactor for multiple biochemical reactions. In particular, Fe-S clusters are thought to be one of the earliest iron cofactors used in biology.

Iron sulfur clusters (Fe–S) represent one of nature's most ubiquitous, dynamic and likely most ancient prosthetic groups necessary to perform distinct cellular functions. In most Fe–S proteins, the clusters function as electron transfer groups, but alternative functions have been described over the years including maintenance of protein structure, enzyme catalysis, metabolic regulation and regulation of gene expression.

Fe–S cluster assembly in microbes is achieved via complex protein systems that construct nascent clusters on scaffold proteins and then transfer the cluster into recipient apo-proteins. Three genetic Fe–S cluster assembly systems are conserved among bacteria: the *nif* operon (nitrogen fixation), the *isc* operon (iron–sulfur clusters) and the *suf* operon (mobilization of sulfur) [3, 4].

Many organisms possess more than one system, although the *suf* system is the only system in certain bacteria and cyanobacteria [2-4]. The sulfur used by Fe–S systems is

usually procured from L-cysteine with the help of cysteine desulfurases such as NifS, IscS and SufSE. However, some Achaea like *Methanococcus* may use sulfide as a proximal sulfur donor[5]. The source of iron for the Fe–S cluster, however, remains controversial[6]. Recent work suggests that Fe–S clusters are part of a cellular chelatable iron pool (CIP).

Cluster Types

Iron sulfur clusters are the most ancient cofactors due to the availability of iron and sulfur in the early reducing anaerobic environment. With the development of diagnostic tools for identification and characterization, different structural types of clusters were identified, and some of them are quite complicated. The most common form is binuclear Fe_2S_2 and cubane-type Fe_4S_4 with cysteinyl sulfur completing tetrahedral Fe coordination (Figure 1.2). Cubane-type Fe_3S_4, linear Fe_3S_4 and double-cubane-type Fe_8S_7 clusters have subsequently been characterized [6]. And besides cysteine, histidine, aspartate and serine are also found to coordinate Fe-S clusters in different Fe-S cluster proteins.

Cluster Functions

Sulfur in the cluster is S^{2-}. However, iron can have different valence as Fe^{2+} and Fe^{3+}. So the same Fe and S content can produce clusters with different oxidation states. The different cluster types can interconvert to each other. The most established function of Fe-S clusters is as cofactors for oxidoreductases (an electron transporter, electron donor and acceptor). The first iron sulfur cluster protein identified in the 1960's was an electron donor, ferredoxin [6] followed by many dehydrogenases that were found with clusters. Since then, over 160 iron-sulfur cluster containing enzymes have been identified and characterized.The functions of clusters have been expanded a lot and are quite critical

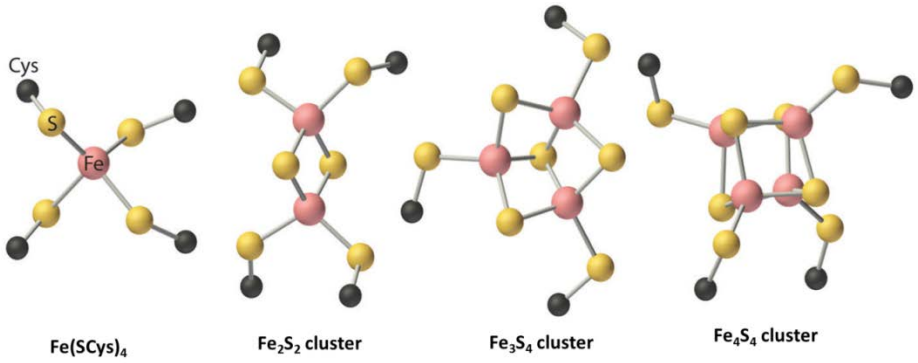

Figure 1.2 Different types of cluster.

for all living organisms. For example, the components in the respiration chain are all cluster containing proteins except Complex IV and electron transport depends on the series of the clusters (Figure 1.3) [7].

The assembly and disassembly properties of clusters also make them a very good sensor for protein regulators under different environments and conditions. Iron-sulfur cluster reduction potentials depend on cluster type and protein environment around the coordination site. This property can make the cluster vulnerable to reductive agents, oxidative agents and iron chelating agents leading to disassembly. Rather than being a detriment, some metalloregulatory proteins exploit the cluster sensitivity by using cluster oxidation or disassembly as an allosteric switch to regulate their activity. Oxidative stress is the most common stress where Fe-S clusters are used as sensors and may have arisen when cells switched to the aerobic environment during evolution of oxygen. For example, in *E.coli* FNR controls the switch between aerobic and anaerobic respiration through oxygen sensing clusters [8]. The O_2-sensing mechanism involves oxidative $Fe_4S_4^{2+}$ to $Fe_2S_2^{2+}$ cluster conversion. For the cluster assembly, you need the iron and sulfur so the cluster proteins can also sense the iron and sulfur availability. The sulfur-limiting situation is rare. However, the iron limiting strategy is usually used for host defense of the pathogen attack. Sensing the iron availability and initiating a corresponding change in gene regulation is very important for the pathogen.

Due to the specific tetrahedral coordination of iron and the varied cluster geometries depending on cluster types, a protein with and without a cluster should have a very different conformation around the cluster binding site. This leads to another function of the cluster, which is stabilizing protein structure for proper function and even to prevent

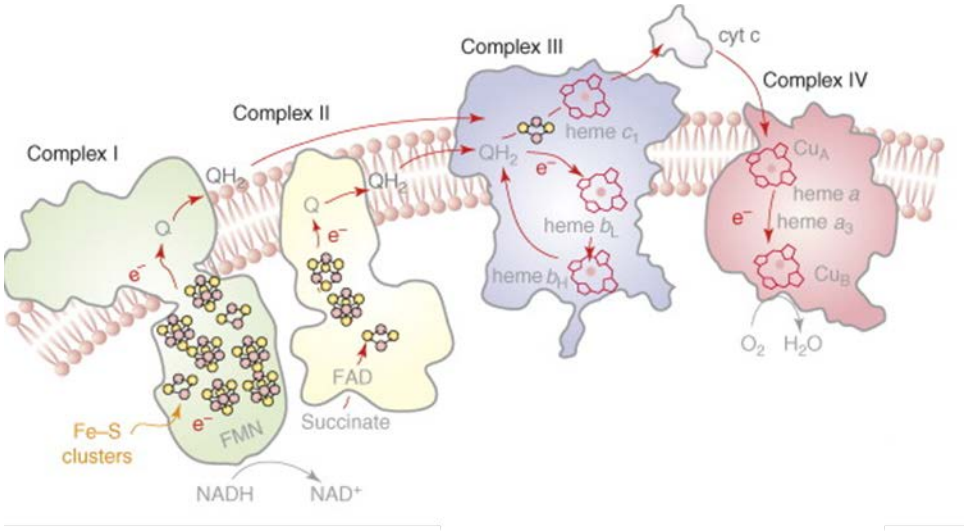

Figure 1.3 Respiratory chain. The clusters are illustrated in different complexes [7].

degradation. Another function of iron-sulfur proteins was addressed based on the observation of multi-clusters sitting in one protein, which has no specific enzyme function [9]. So the hypothesis is this protein may function as a cluster storage protein providing cluster for certain targets or for cluster repair and even may function as an iron storage protein to minimize the Fenton reaction damage to the organism.

Cluster Assembly Machinery and Regulation

In vitro, if you provide ferrous iron, sulfide and the reducing agent DTT, most Apo proteins can be reconstituted spontaneously with a cluster due to the thermodynamic stabilization of the cluster in the binding site. However, genetic studies have clearly demonstrated that Fe-S cluster proteins do not mature in vivo without the assistance of Fe-S cluster biogenesis proteins. This may be due to the fact that ferrous iron as a "free" iron source in vivo is high toxic via the Fenton reaction like I mentioned before. Hydrogen sulfide H_2S is a metabolic toxin because it binds tightly to the iron of cytochromes, poisoning the respiratory chain. High concentration would cause death of the tissue [10]. H_2S can be produced by nonenzymatic breakdown of cysteine. In *E.coli*, sulfide aggravates the hydrogen peroxide-induce killing since iron sulfide is more efficient catalyzed Fenton reaction than ferrous iron [11]. Due to iron and sulfide toxicity, cluster assembly in the cells is strictly regulated and accomplished by specific cluster assembly machinery. There are multiple Fe-S cluster assembly pathways throughout the three kingdoms of life. The maturation of bacterial Fe-S proteins was most intensely studied in *Escherichia coli* and the azototrophic (nitrogen fixing) *Azotobacter vinelandii*. Three different pathways for the biogenesis for bacterial Fe-S proteins were identified, which are the Nif (*ni*trogen *f*ixation) system, for specific maturation of nitrogenase in

azototrophic bacteria; and the Isc (*i*ron *s*ulfur *c*luster) assembly and Suf (*su*lfur *f*ormation) systems, for the generation of Fe-S proteins under normal and stress (oxidative stress and iron limiting) conditions, respectively (Figure 1.4) [12].

All three systems utilize a cysteine desulfurase enzyme (NifS, IscS, and SufS/E) to liberate sulfide from free cysteine during cluster assembly. All three systems also contain members of the A-type carrier (ATC-II) family of Fe-S biosynthesis proteins ($IscA^{Nif}$, IscA, and SufA) that contain three conserved cysteine residues involved in Fe-S cluster coordination. Despite some early controversy concerning the role of ATC-II proteins, all recent biochemical and genetic analyses suggest that they bind Fe-S clusters in vivo and are able to transfer the clusters to target apoproteins [13].

The model organism *E. coli* carries the *isc* operon used for housekeeping cluster assembly and the *sufABCDSE* operon that is required for stress-responsive Fe-S cluster assembly.

In *E. coli,* the core Suf pathway consists of six proteins, SufA, SufB, SufC, SufD, SufS, and SufE, organized in a single transcription unit, the *sufABCDSE* operon. The *suf* operon is controlled at the transcriptional level by the hydrogen-peroxide sensor OxyR, by the iron metalloregulatory protein Fur, and by the Fe-S transcription factor IscR. The sum of their regulation is that *suf* is strongly activated by oxidative stress, particularly hydrogen peroxide, and by iron limitation stress (Figure 1.5) [12].

Regulation of Fe-S cluster assembly pathways in *E. coli* under stress conditions. During oxidative stress or iron starvation, apo-IscR will predominate as the Isc proteins are titrated away by increased demand for cluster assembly. This will relieve *isc* repression and induce the operon. Simultaneously, apo-IscR will activate *suf* transcription

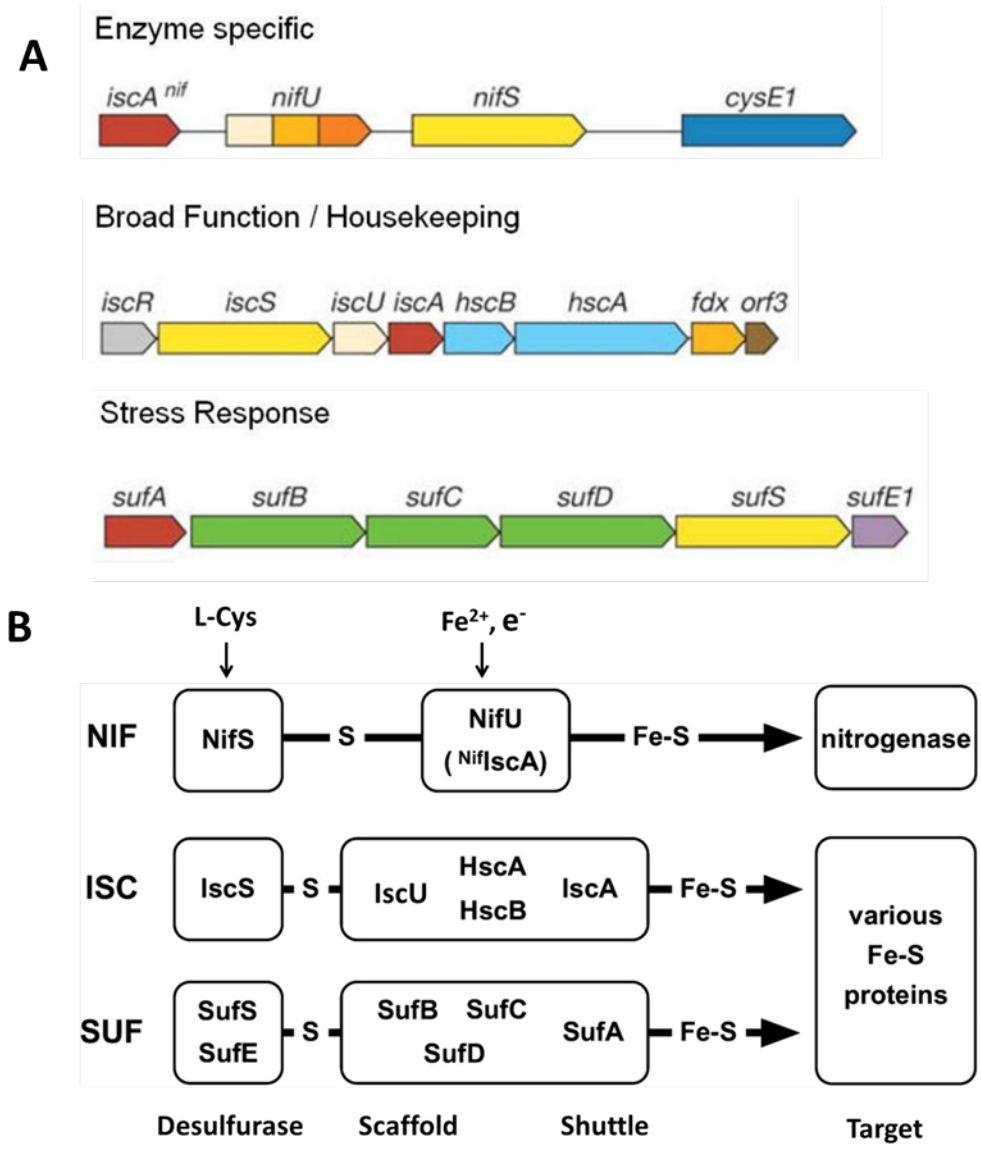

Figure 1.4 Fe-S cluster biogenesis operons (A) and pathways (B).

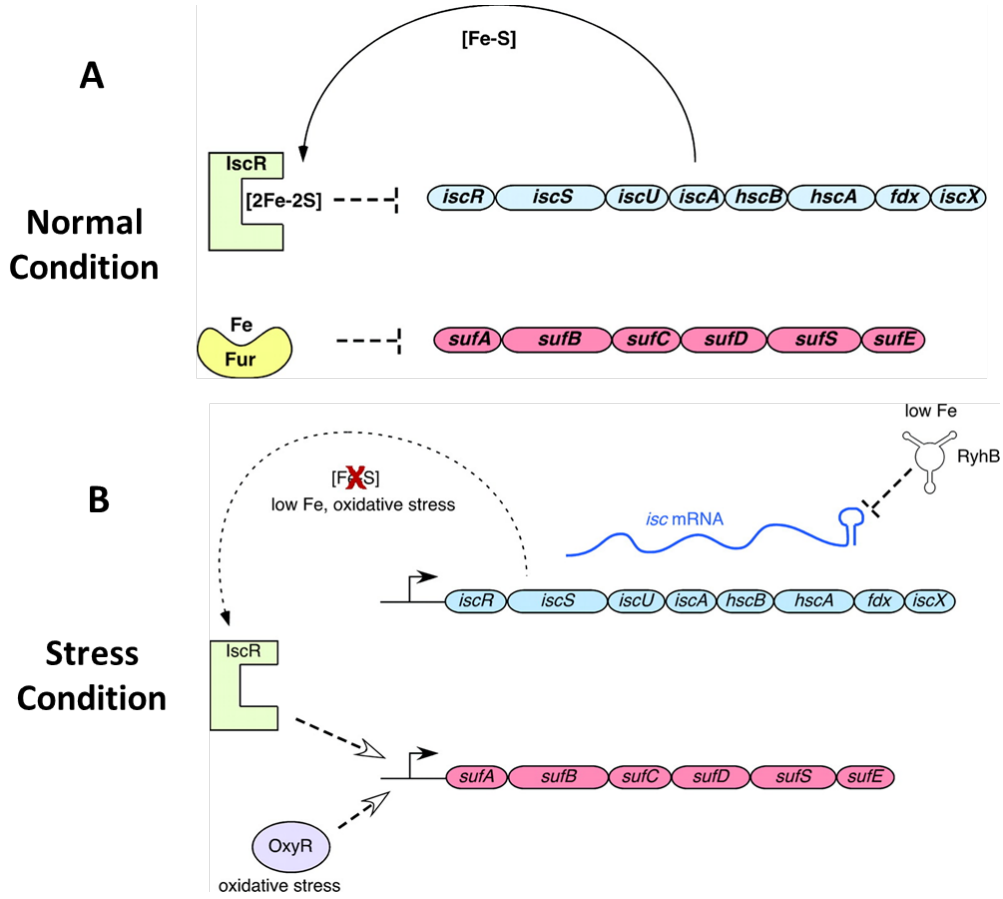

Figure 1.5 Regulation of Fe-S cluster assembly pathways in *E.coli* under normal growth conditions. Holo-IscR and apo-IscR will be present in an equilibrium that is dependent on the amount of Isc proteins available for cluster synthesis. Holo-IscR will repress *isc* transcription when there is sufficient cluster assembly capacity (i.e., when he Isc proteins are not titrated away for cluster assembly in other proteins). Under normal conditions, *suf* transcription will be low due to repression by Fe^{2+}-Fur [12].

as Fur repression is relieved. Under hydrogen peroxide stress, OxyR will also activate *suf* transcription in an integration host factor-dependent manner. Under iron starvation conditions, induction of the RyhB small RNA will lead to posttranscriptional repression of the Isc system so that Suf becomes the predominant Fe-S cluster pathway.

While the Suf and Isc pathways can both accomplish Fe-S cluster assembly in *E. coli*, there is phylogenetic divergence between the two systems. The Suf pathway contains four gene products, SufB, SufC, SufD, and SufE that have no direct homologues in the Isc system. Similarly, the Isc pathway utilizes four gene products, IscU, HscA, HscB, and Fdx that are not present in the Suf system. Both pathways contain a cysteine desulfurase enzyme (IscS and SufS) and both pathways contain a protein that may be an iron donor or Fe-S scaffold or Fe-S shuttle (IscA and SufA) [14]. The cysteine desulfurase SufS mobilizes sulfur form free cysteine via a pyridoxal phosphate-dependent mechanism. The liberated sulfur atom is then donated from SufS to an active site cysteine (Cys51) on the SufE protein. Consequently, the presence of SufE stimulates the basal activity of SufS and the two proteins together form a novel sulfur transfer system [15].

Recently it was shown that *E. coli* SufA, co-expressed with the other Suf proteins, binds a $Fe_2S_2^{2+}$ cluster in vivo that can be transferred to target Fe-S apoproteins [16]. However, recent studies have also shown that the SufB can assemble an iron-sulfur cluster in vitro. In vivo and in vitro, SufB forms a stable complex with SufC and SufD (referred to here as $SufBC_2D$) and all three proteins are necessary for in vivo Fe-S cluster assembly. Studies in our lab have shown that the $SufBC_2D$ complex can also be reconstituted in vitro with an Fe-S cluster similar to SufB alone. Since both SufA and the $SufBC_2D$ complex can assemble Fe-S clusters, this raises the question of how they

function in Suf-mediated Fe-S cluster assembly. Does SufA works as a scaffold protein or a shuttle protein for Fe-S clusters?

Cysteine Desulfurase Reaction Mechanism

In most systems studied to date, cysteine is a major physiological sulfur source for iron-sulfur clusters biosynthesis in prokaryotes and eukaryotic mitochondria and chloroplasts. A family of cysteine desulfurases is responsible for the sulfur atom mobilization, which depends on a pyridoxal 5'-phosphate (PLP) enzymatic mechanism first characterized with NifS. First, free cysteine binds to PLP and forms PLP-cysteine adduct as a Schiff base between PLP and the α-amino group of cysteine. Then a catalytic cysteine residue from the enzyme acts as a nucleophile to attack the sulfhydryl group of the substrate cysteine bound to PLP and results in formation of an enzyme-bound persulfide. This active persulfide group can then be transferred to cysteine residues in the final scaffold protein directly or via a sulfur shuttle protein using a chemical route similar to protein disulfide bond exchange (Figure 1.6) [17].

Based on sequence similarity, the cysteine desulfurases can be subdivided into two groups, group I (NifS and IscS) and group II (SufS and CsdA) (Figure 1.7). The structure of the catalytic cysteine environment for the two groups of desulfurase enzymes is different. The catalytic cysteine localizes to a shorter, more rigid loop with a more hydrophobic environment in Group II cysteine desulfurases compared to Group I enzyme [18]. This structure difference may help explain the low basal desulfurase activity of Group II enzymes compared to group I [19].

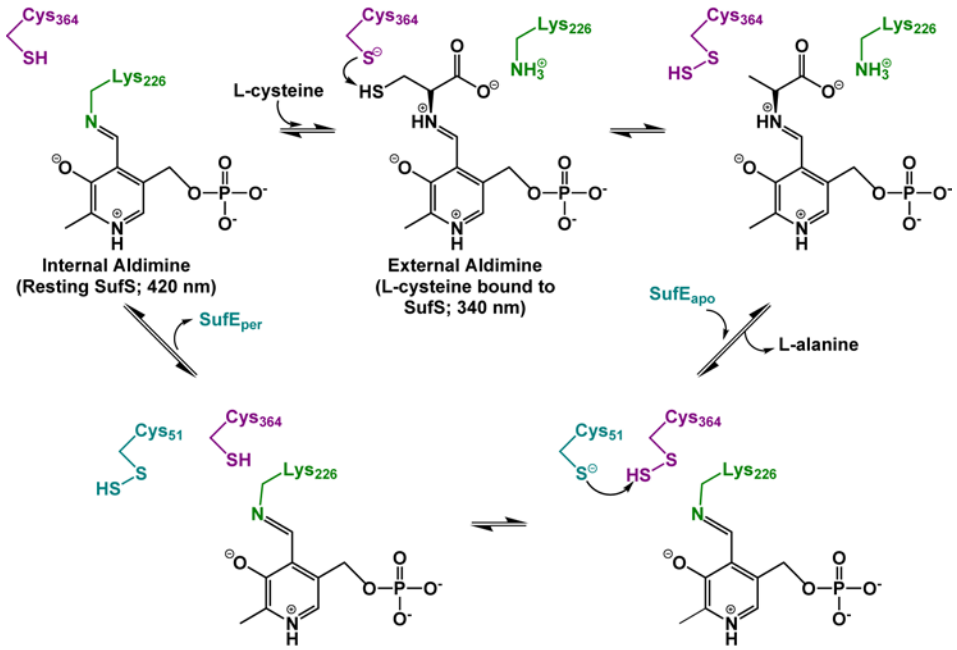

Figure 1.6 SufS cysteine desulfurase mechanism. An abbreviated reaction mechanism for SufS is shown with SufS Lys226 in green and Cys364 in purple. SufE Cys51 is in teal. PLP cofactor and substrate cysteine are in black. Multiple reaction steps and transient intermediates have been omitted for clarity. For further details see reference [17].

Functional Divergence of SufS And IscS in E. coli

The structure of SufS in *E. coli* was first characterized by Fujii [20] and indicated that Cys364 was in good position to interact with modeled substrate (L-selenocysteine) in the active site. Then the structure of external aldimine of *E. coli* SufS [18] was analyzed using L-propargylglycine as a L-selenocysteine analog that does not turn over. Based on the structure they proposed the reaction mechanism of SufS with L-cysteine is different from that with L-selenocysteine. At the same year 2002, the crystal structures of SufS in persulfide, perselenide, and seleocysteine-bound intermediate forms were reported [21]. The structures of native SufS and different SufS intermediates are consistent with the PLP-dependent mechanism described before. The roles of several amino acid residues in the catalytic reaction of SufS have been proposed based on all the solved structures.

Based on all the resolved structures of SufS, the shortness and decreased flexibility of the loop containing the catalytic Cys364 likely explains the catalytic inefficiency of Group II desulfurase enzymes compared to Group I enzymes, which have a more flexible active site loop that is 11 amino acids longer (Figure 1.7). The hypothesis is that the sluggishness of attack by the nucleophilic cysteine residue is the primary cause of this inefficiency. However, accessory proteins activate SufS activity in a specific and concerted manner to a level compared to Group I enzymes. For SufS in *E. coli*, the Gram-negative model organism and *Erwinia chrysanthemi*, a Gram-negative plant pathogen, the accessory protein is SufE. For SufS in *Bacillus subtilis*, the Gram-positive model organism, it is SufU. The genes of the accessory proteins are always localized adjacent to *sufS* in the genome.

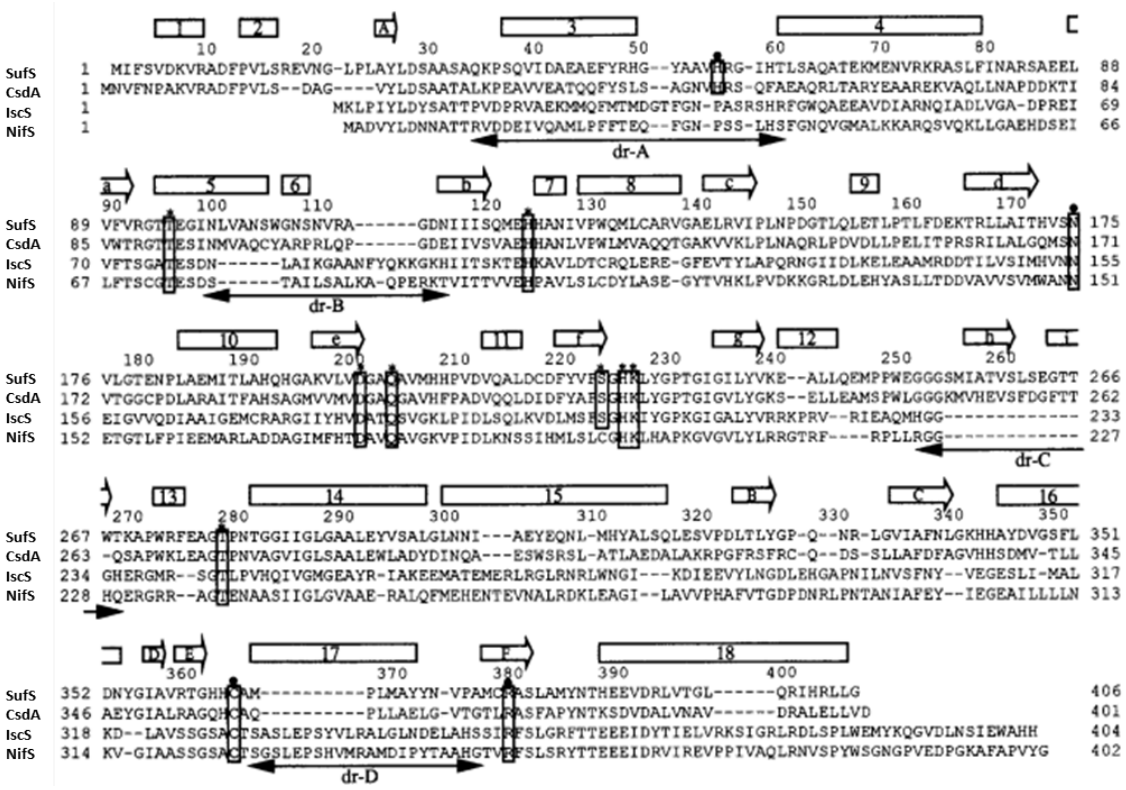

Figure 1.7 Sequence alignments of several NifS family proteins. The numbering of the sequences is based on that of SufS. The secondary structure elements of SufS are denoted by rectangles with numbers for α- and 3_{10}-helices and arrows with letters for β-strands. The amino acid residues in boxes capped with * or ● interact with PLP or possibly with the substrate, respectively. The lines with arrows denote the regions (dr-A, dr-B, dr-C, and dr-D) whose sequences are different between groups I and II [22].

In the first study, SufS and SufE interact in a complex and association with SufE was found to increase the desulfurase activity of SufS from *Erwinia chrysanthemi* by about 50-fold. The highest specific activity was obtained upon addition of one equivalent of SufE. Preliminary steady-state kinetic results indicated that SufS from *E. chrysanthemi*, alone or in complex with SufE, roughly had a Michaelis-Menten behavior using cysteine as a substrate. Binding of SufE to SufS had no effect on the K_m value for cysteine (500 μM) but a large one on the V_{max} value 0.9 units/mg compared to 0.019 units/mg. SufE had no effect on SufS selenocysteine lyase activity. Our lab subsequently demonstrated transfer of the sulfur from the SufS to SufE via a SufS bound persulfide intermediate and suggested that the acceleration of persulfide cleavage by SufE is primarily responsible for the observed activation. The possible conformational change of SufS due to SufE association causing a better substrate cysteine binding is also a possibility.

Based on the genome scanning, most Gram-positive bacteria, including *Bacillus subtilis*, do not contain a locus encoding either SufE or CsdE. Instead Gram-positives often contain the gene encoding the proposed Fe-S cluster scaffold SufU located adjacent to a Group II cysteine desulfurase gene *sufS*. SufS is essential for viability of *Bacillus subtilis*. In the desulfurase assay, using DTT as a reductant to recycle the catalytic cysteine on SufS, it resulted in a rapid formation of alanine due to the first turn over of SufS but followed by a slower alanine formation when SufS needed to be recycled. It indicated here the persulfide cleavage on the catalytic cysteine was the rate-limiting step. The mechanism of SufU enhancement may due to the acceleration of persulfide cleavage to recycle the catalytic cysteine on SufS. With their careful kinetics assay, Dos Santos

and co-workers demonstrated that SufU works as a substrate in the catalytic ping-pong mechanism of the SufU:cysteine sulfurtransferase reaction of SufS.

The *suf* pathway in *E. coli*, Gram-negative bacteria, is the best studied. The *sufABCDSE* operon of *E.coli* is induced by oxidative stress and iron deprivation. Mihara [20] first identified *sufS* as a gene encoding an *E. coli* counterpart of mammalian selenocysteine lyase due to its high specific activity for L-selenocysteine (5.5 units/mg) compared to that for L-cysteine (0.019 units/mg). Later the same group also reported that SufS protein from *E. coli* is not a Michaelis-Menten enzyme when using cysteine as a substrate. Then our lab [23] reported that SufE can stimulate the cysteine desulfurase activity of the SufS enzyme up to 8-fold and accepts sulfane sulfur from SufS. This sulfur transfer process from SufS to SufE is sheltered from the environment based on its resistance to added reductants and on the analysis of available crystal structures of the proteins. SufE has no effect on SufS selenocysteine lyase activity, and the active site Cys364 of SufS is not required for selenocysteine lyase activity. The in vivo relevance of SufS selenocysteine lyase activity remains to be elucidated. We also found that the SufB, SufC, and SufD proteins associate in a stable complex and that, in the presence of SufE, the $SufBC_2D$ complex further stimulates SufS activity up to 32-fold. The cysteine desulfurase SufS donates sulfur to the sulfur transfer protein SufE and then SufE in turn interacts with the SufB protein for sulfur transfer to SufB. The interaction occurs only if SufC is present. The sulfur incorporated into SufB was proposed for iron-sulfur cluster assembly. Based on protein interaction and sulfur trapping with mass spectrometry, the present proposed route in *E. coli* is SufS liberates sulfur atom from cysteine with a persulfide intermediate on catalytic cysteine C364 of SufS. SufS then transfers persulfide

to SufE, and finally SufE transfers persulfide to $SufBC_2D$ for cluster assembly. The exact cysteine receiving sulfur in SufB is unclear. SufBC is the minimal complex for further enhancement of SufSE activity. The mechanism for the enhancement likely involves release of persulfide from SufE which can then serve as a substrate for the next round of SufS activity. This sulfur transfer route from SufS to $SufBC_2D$ via SufE may be important for limiting sulfide release during oxidative stress conditions *in vivo*.

In vivo studies indicated that the Suf pathway is preferentially activated under oxidative stress. However, the reason why it works better than the Isc pathway has not been carefully characterized. Recent in vivo study indicated submicromolar (as little as 1 μM) H_2O_2 can deactivate the Isc machinery so that Suf is required for both repairing Fe-S enzymes and activating nascent Fe–S enzymes in general [24]. The IscS and IscA components of the Isc system are H_2O_2-resistant, suggesting that oxidants disrupt Isc by other ways like oxidizing clusters as they are assembled on or transferred from the IscU scaffold. Fe-S cluster biogenesis is sensitive to oxygen due to the proclivity of iron, sulfide, and protein sulfhydryl groups to be modified by oxygen or reactive oxygen species. Since transfer of sulfur from a cysteine desulfurase enzyme to other proteins occurs via as a highly reactive S-sulfanyl cysteine moiety, the sulfanyl cysteine species could be sensitive to reduction or oxidation if exposed to the environment. Due to the reactivity of both the persulfide intermediate and active site sulfhydryl groups on the enzymes, oxidative stress may block the sulfur donation step of Fe-S cluster biogenesis. The sulfur trafficking by the Suf pathway may be more resistant to disruption than the Isc system. We characterized the kinetic interactions between *E. coli* SufS and SufE during the desulfurase reaction cycle in order to compare the oxidative stress resistance of the

SufS-SufE sulfur transfer pathway to that of the *E. coli* IscS-IscU system. The results indicated that SufS-SufE is more active than IscS-IscU at physiological concentrations of L-cysteine and that SufS-SufE activity is more resistant to H_2O_2 exposure than IscS-IscU. Surprisingly SufE shows substrate inhibition of SufS at physiological L-cysteine concentrations.

Biomedical Relevance

The *sufABCDSE* operon is activated in bacteria to build essential Fe-S clusters during exposure to oxidative stress and iron starvation. The *suf* genes are conserved in 70% of sequenced bacterial genomes such as *Mycobacterium tuberculosis* [25], the causative agent of the disease tuberculosis. The *suf* operon is activated in pathogenic bacteria during infection. And furthermore, the Suf system appears to be the only Fe-S cluster assembly pathway. Suf is also present as a stress-response pathway in *Shigella*, the organism responsible for bacillary dysentery. Studies also show that bacteria need the *suf* system to survive under disrupted iron homeostasis. Due to lack of direct Suf homologues in humans, biochemical characterization of the components of the Suf pathway will allow us to disrupt this pathway using novel antibiotics with minimal side effects.

Chapter 2

The *E.coli* SufS-SufE Sulfur Transfer System is more Resistant to Oxidative Stress than IscS-IscU[1]

ABSTRACT

During oxidative stress in *E. coli*, the SufABCDSE stress response pathway mediates iron-sulfur (Fe-S) cluster biogenesis rather than the Isc pathway. To determine why the Suf pathway is favored under stress conditions, the stress response SufS-SufE-SufBC_2D sulfur transfer pathway and the basal housekeeping IscS-IscU pathway were directly compared. We found that SufS-SufE-SufBC_2D activity is significantly higher than IscS-IscU at physiological cysteine concentrations and after exposure to H_2O_2. Mass spectrometry analysis demonstrated that IscS-IscU is more susceptible than SufS-SufE to oxidative modification by H_2O_2. These important results provide biochemical insight into the stress resistance of the Suf pathway

INTRODUCTION

Iron-sulfur (Fe-S) clusters in metalloproteins carry out myriad cellular functions [26, 27]. Fe-S cluster biogenesis requires proteins that donate sulfur and iron, pre-assemble clusters, and traffic Fe-S clusters to target metalloproteins [28-30]. Fe-S cluster biogenesis is sensitive to oxygen due to the proclivity of iron, sulfide, and protein sulfhydryl groups to

[11] Dai, Y., and Outten, F. W. (2012) The E. coli SufS-SufE sulfur transfer system is more resistant to oxidative stress than IscS-IscU, *FEBS letters 586*, 4016-4022.

be modified by oxygen or reactive oxygen species [31]. In *Escherichia coli,* the Isc system carries out Fe-S cluster assembly under normal conditions while the Suf pathway is required for Fe-S cluster biogenesis under oxidative stress conditions [32-35].

Both Isc and Suf use superficially similar mechanisms to mobilize sulfur for Fe-S cluster assembly. The homodimeric IscS and SufS cysteine desulfurase enzymes catalyze the pyridoxal-phosphate (PLP)-dependent removal of sulfur from L-cysteine substrate resulting in a protein-bound persulfide (R-S-SH) intermediate. This persulfide S^0 species (also referred to as sulfane sulfur) is reduced and incorporated into the Fe-S cluster as sulfide (S^{2-}) during assembly on a scaffold protein (IscU or the $SufBC_2D$ complex) [23, 36-45]. Due to the reactivity of both the persulfide intermediate and active site sulfhydryl groups on the enzymes [46, 47], oxidative stress may block the sulfur donation step of Fe-S cluster biogenesis. Genetic evidence has shown that the Isc system is not efficient at Fe-S cluster assembly under oxidative stress, raising the question of whether sulfur trafficking by the Suf pathway may be more resistant to disruption than the Isc system [24].

IscU and SufE are structural (but not sequence) homologues that each interact with their cognate cysteine desulfurase enzymes to accept S^0 via a thiol exchange mechanism [23, 42, 44, 48]. While IscU is a bona fide scaffold protein where the full Fe-S cluster can be assembled, SufE uses a single active site cysteine residue (C51) for accepting S^0 and does not bind a nascent Fe-S cluster [23]. SufE then further traffics the S^0 to SufB within the $SufBC_2D$ scaffold complex where the nascent cluster is assembled [45]. SufE enhances the cysteine desulfurase activity of SufS, although the exact mechanism of enhancement is unclear. $SufBC_2D$ further increases SufE-dependent enhancement of SufS via an

unknown mechanism [23]. In contrast, IscU was recently shown to not enhance the desulfurase activity of IscS [49].

To determine if sulfur trafficking by the Suf pathway is more resistant to oxidative stress than the Isc pathway, we directly compared the oxidative stress resistance of the SufS-SufE sulfur transfer pathway to that of the *E. coli* IscS-IscU system. We found that SufE showed the potential substrate we observe at lower L-cysteine levels. Substrate inhibition by SufE could be a mechanism to limit SufS activity when cellular L-cysteine pools drop below a critical threshold. We discovered that SufS-SufE is more active than IscS-IscU at physiological concentrations of L-cysteine. And we observed a pronounced activity difference between the Isc and Suf sulfur trafficking proteins when they were exposed to H_2O_2 during the cysteine desulfurase reaction cycle. SufS-SufE activity is more resistant to H_2O_2 exposure than IscS-IscU. Furthermore, IscS and IscU are more sensitive to oxidative modification by H_2O_2 than SufS and SufE. The functional ramifications of these results for defining the relative roles of Isc and Suf are discussed.

MATERIALS AND METHODS

Strains and Plasmids

SufS, SufE, IscS, and IscU were expressed in BL21(DE3) and SufABCDSE were expressed in TOP10 (Invitrogen). The pGSO164 plasmid carrying the *sufABCDSE* operon was described previously [23]. Other vector construction is described in Table 2.1.

Cells overexpressing SufS, SufE, and IscS were in Lennox Broth (LB). Cells overexpressing IscU were gown in LB plus 60 μM $FeCl_3$ and 8.3 μM $ZnSO_4$ to stabilize IscU protein folding [50]. Ampicillin was used at 100 mg per liter. All chemicals were obtained from Sigma unless otherwise indicated.

Table 2.1 Primer Sequences for plasmid construction of pET21a_SufS, pET21a_SufE, pET21a_IscS, and pET21a_IscU.[1]

Protein	Primer Sequence[2]
SufS	5'-GAGGGGATCCATGATTTTTTCCGTCGACAA-3'
	5'-TGCCCTCGAGTTATCCCAGCAAACGGTGAA-3'
SufE	5'-AGGCCATATGGCTTTATTGCCGGATAA-3'
	5'- TCCTGGATCCTTAGCTAAGTGCAGCGGCTT-3'
IscS	5'- TAGACATATGAAATTACCGATTTATCTCG-3'
	5'- CCGAGGATCCTTAATGATGAGCCCATTCGA-3'
IscU	5'-ATTTCATATGGCTTACAGCGAAAAAGT-3'
	5'- ACCTGGATCCTTATTTTGCTTCACGTTTGC-3'

[1] Details for construction of expression plasmids: MG1655 chromosomal DNA was the template for PCR. SufE fragment was digested with NdeI and BamHI, and ligated into the corresponding sites of pET-21a (Invitrogen) to generate pET-21a_SufE. SufS fragment was digested with BamHI and XhoI, and cloned into the corresponding sites of pET-21a to generate pET-21a_SufS. IscU fragment was digested with NdeI and BamHI, cloned into the corresponding sites of pET-21a to generate pET-21a_IscU. IscS fragment was digested with NdeI and BamHI, cloned into the corresponding sites of pET-21a to generate pET-21a_IscS. The nucleotide sequences of all of the plasmid inserts were confirmed by DNA sequencing.

[2] Underlined sequences contain non-native restriction sites utilized for cloning.

Protein Expression and Purification

The $SufBC_2D$ complex was purified as described previously [51]. *E. coli* BL21(DE3) containing the pET-21a_SufS, pET-21a_ SufE, pET-21a_IscS, or pET-21a_IscU expression vector was grown in LB at 37°C and induced by 500 μM isopropyl-1-thio-β-D-galactopyranoside (IPTG) when the cultures reached an OD_{600} of 0.4 - 0.6. Induction was for 3 h at 37°C for SufS, SufE, and IscS while IscU was induced at 17°C overnight. Cells containing pGSO164 were grown in LB at 37°C and induced with 0.2% L-arabinose for 3 h [23]. Harvested cells were lysed in 25 mM Tris, pH 7.5, 100 mM NaCl, 5 mM DTT, 1 mM phenylmethylsulfonyl fluoride, and 1× EDTA-free protease inhibitor tablet via sonication. Following centrifugation at 20,000 × g for 30 min, lysate was filtered before loading on columns. SufS and IscS were purified using Q-sepharose, Phenyl FF, and Superdex 200 chromatography resins in sequence. All the columns used for purification were from GE Healthcare. SufE and IscU were purified using Q-sepharose and Superdex 75 chromatography resins in sequence. The Q-sepharose column utilized a linear gradient from 25 mM Tris-HCl, pH 7.5, 10 mM βME to 25 mM Tris-HCl, pH 7.5, 1 M NaCl, 10 mM βME. The Phenyl FF column used a linear gradient of 25 mM Tris-HCl, pH 7.5, 100 mM NaCl, 1 M $(NH_4)_2SO_4$, 10 mM βME to 25 mM Tris-HCl, pH 7.5, 10 mM βME. The Superdex column was run with 25 mM Tris-HCl, pH 7.5, 150 mM NaCl, and 5 mM DTT. Purified proteins were concentrated, frozen as drops in liquid nitrogen, and stored at -80°C until further use.

Cysteine Desulfurase Activity Assays

Cysteine desulfurase activity was measured with N,N-dimethyl-p-phenylenediamine sulfate (DMPD) and $FeCl_3$ using a slightly modified published protocol [23]. Reactions were carried out aerobically in 25 mM Tris-HCl, pH 7.4, 150 mM NaCl at 27°C. Proteins were incubated with 2 mM DTT for 5 min prior to addition of L-cysteine in a total reaction volume of 800 µL. Reactions were allowed to proceed for 10 min and then were stopped by the addition of 100 µL 20 mM DMPD in 7.2 M HCl and 100 µL 30 mM $FeCl_3$ in 1.2 M HCl. The mixture was incubated for 30 min in the dark to form methylene blue. Precipitated protein was removed by 1 min centrifugation at 16,100 x g, and the methylene blue was measured at 670 nm. A Na_2S standard solution was used for calibration. $SufE_{alk}$ was prepared by first pre-incubating with 5 mM DTT for 30 min followed by removal of DTT with a 5 ml desalting column. SufE was then incubated with 5mM iodoacetamide (IAA) for 1 h in the dark and was exchanged into desulfurase assay buffer with a desalting column. Alkylated SufE was added to the standard assay (800 µL) at different concentrations (0 - 4 µM), in the presence of 0.5 µM SufS, 2 mM cysteine, and varying concentrations of untreated SufE.

For assays in the presence of H_2O_2, SufS, SufE, $SufBC_2D$, IscS, or IscU were pre-incubated with 5 mM DTT for 30 min separately followed by removal of DTT with a 5 ml desalting column under anaerobic conditions in a Coy chamber. Desulfurase reactions were initiated by adding 2 mM L-Cys together with different concentrations of H_2O_2 for 30 minutes under anaerobic conditions. Then the reaction was quenched by a heating step at 95 ºC for 5 minutes, followed by the addition of 2 mM DTT after the quenching step to reduce and release sulfide for measurement. Finally the DMPD in 7.2

M HCl and ferric chloride in 1.2 M HCl were added to develop methylene blue for 30 min. All data was analyzed using Prism software from GraphPad.

Mass Spectrometry of H_2O_2-exposed Proteins

All protein samples were prepared anaerobically. Low-level phosphorylation of the proteins was removed by treatment with the Lambda Protein Phosphatase (NEB) together with 100-fold DTT. DTT was subsequently removed with a 5 ml desalting column (GE Healthcare). SufS or IscS were used at 1 μM concentration while SufE or IscU were used at 10 μM concentration. Mixtures of proteins were incubated for 5 min prior to further additions. Proteins were incubated with 2 mM L-cysteine in the presence or absence of 400 μM H_2O_2 for 30 minutes. Addition of trichloroacetic acid (TCA) to 10% vol/vol was used to trap and precipitate the proteins. TCA pellets were resuspended in 25 mM Tris-HCl, pH 7.4, 150 mM NaCl and treated with 100-fold iodoacetamide (IAA) in the dark for 30 min. Samples were precipitated with 10% TCA again and pellets were washed with additional 10% TCA.

Lyophilized samples were centrifuged and then dissolved in RapiGest™ (Waters). Proteomics grade trypsin was added at a protein: enzyme ratio of 1:100 and samples were digested at 37°C overnight. After cleaving the acid labile detergent for 30 minutes via the Waters protocol, 15 μL of each sample was transferred to an auto sampler vial and analyzed on an LTQ XL mass spectrometer coupled with an Orbitrap Elite HPLC. A 120 minute reverse phase gradient from 5% acetonitrile to 50% acetonitrile was utilized. The mass spectrometer was programmed for data dependent acquisition (DDA) with 1 MS scan followed by MS/MS on the 10 most abundant ions.

RESULTS

Kinetic Analysis of SufS Activity in the Presence of SufE.

Native SufS, SufE, $SufBC_2D$, IscS, and IscU proteins were purified to homogeneity and PLP cofactor occupancy was greater than 90% for IscS and SufS (Figure 2.1).

Using 2 mM L-cysteine with 2 mM DTT, SufS liberated 2.6 nmol of S^{2-} $min^{-1}mg^{-1}$, which is 20 times lower than IscS (51.7 nmol of S^{2-} $min^{-1}mg^{-1}$) (Figure 2.2). Previously, activities of 19 nmol of S^{2-} $min^{-1}mg^{-1}$ for SufS and 380 nmol of S^{2-} $min^{-1}mg^{-1}$ for IscS were measured using 12 mM cysteine and 50 mM DTT [39]. Under the same conditions used in the previous study, we observed activities of 7.9 nmol of S^{2-} $min^{-1}mg^{-1}$ for SufS and 312.8 nmol of S^{2-} $min^{-1}mg^{-1}$ for IscS. Addition of 4 molar equivalents of SufE increases SufS activity to 41.9 nmol of S^{2-} $min^{-1}mg^{-1}$ so that it is comparable to IscS (Figure 2.2).

Further addition of 4 molar equivalents of the $SufBC_2D$ complex to SufS and SufE further enhanced SufS activity to 172.6 nmol of S^{2-} $min^{-1}mg^{-1}$, making SufS a more efficient sulfur mobilization enzyme than IscS under these conditions (Figure 2.2). In agreement with recently published reports, we found that IscU, the sulfur receptor for IscS, did not enhance IscS activity under these conditions (Figure 2.2) [49].

SufS removes sulfur from L-cysteine and forms persulfide (S^0) on the active site residue C364. The persulfide intermediate of *E. coli* SufS directly transfers the sulfur atom to residue C51 of SufE and SufS activity is enhanced specifically by SufE [23, 44]. To further probe the SufS-SufE reaction, we performed kinetic analyses of *E. coli* SufS while varying both components, L-cysteine and SufE, using the methylene blue assay to quantify sulfide production [23]. This in vitro reaction requires a non-physiological reductant (such as DTT) to release persulfide from SufS and SufE by reducing persulfide

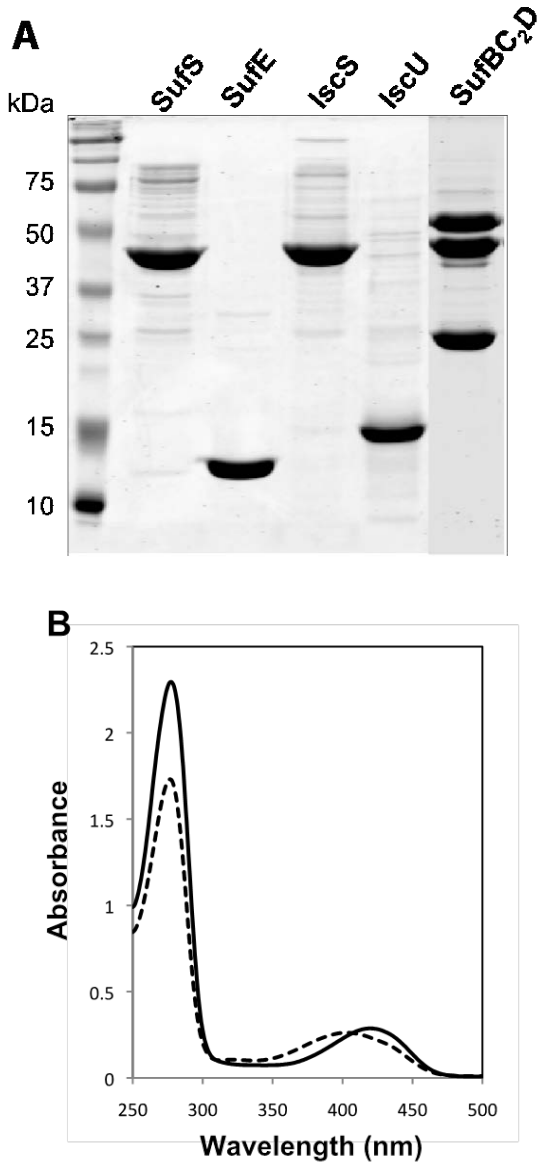

Figure 2.1 Protein purification and UV spectra of Suf and Isc proteins. (A) Purified SufS, SufE, IscS, IscU, and $SufBC_2D$ proteins. 8 μg samples except 15 μg for $SufBC_2D$ were separated on a 12% SDS-PAGE reducing gel. (B) SufS (solid line) and IscS (dash line) (2.0 mg/ml protein in 25 mM Tris-HCl, pH 7.5, 100 mM NaCl) UV-Visible absorption spectra. PLP cofactor on SufS and IscS gives a 420 nm and 400 nm peak respectively for each spectrum.

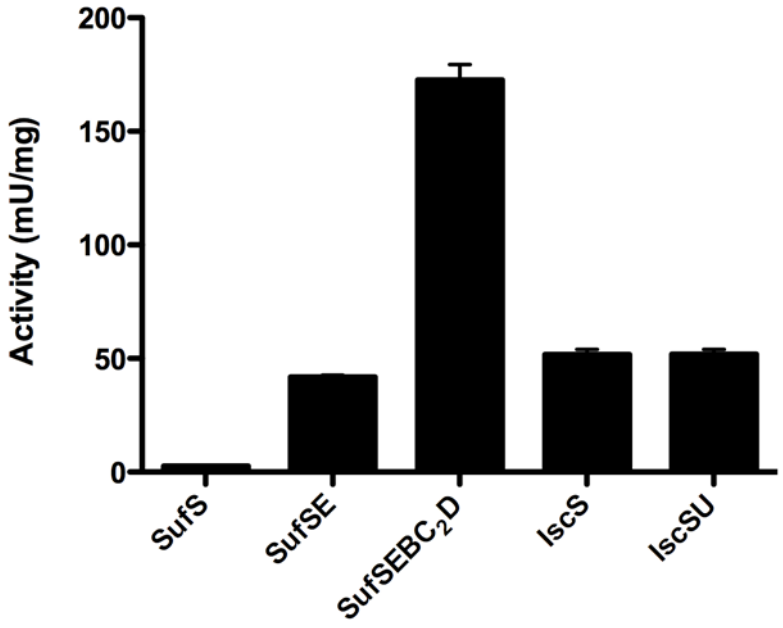

Figure 2.2 SufS and IscS desulfurase activity. The assay contained 0.5 μM SufS or IscS, 2 mM cysteine, 2 mM DTT and with different combinations of 2 μM SufE, 2 μM $SufBC_2D$, or 2 μM IscU. A unit of activity is defined as one micromole of sulfide formation by the desulfurase enzyme per minute. Activity is shown as mU per mg of SufS or IscS.

(S^0) to sulfide (S^{2-}) thereby allowing the sulfide to react with DMPD. The concentration of cysteine was varied from 0 to 500 μM in the presence of 4 μM SufE (Figure 2.3 A) while the concentration of SufE was varied from 0 to 15 μM SufE at a fixed 2 mM concentration of L-cysteine (Figure 2.3 B).

Under these conditions, SufS showed Michaelis-Menten enzyme kinetics for L-cysteine and SufE as its two substrates. The kinetic parameters are listed in Table 2.2. Previous studies of the *Erwinia chrysanthemi* SufS-SufE reported that the SufS-SufE K_m for L-cysteine was 500 μM and the V_{max} = 900 mU/mg, which are both higher than the values measured for *E. coli* SufS-SufE (Table 2.2) suggesting that the *E. coli* system has a higher affinity for the L-cysteine substrate but is a somewhat slower system [43].

We also found that SufE where C51 has been covalently blocked with iodoacetamide ($SufE_{alk}$) was able to inhibit SufS activity in the presence of unalkylated SufE with a K_i of 0.19 μM (Figure 2.4). This inhibition occurred regardless of the presence of the $SufBC_2D$ complex.

SufS Displays non-Michaelis-Menten Kinetics at Low but Physiological Cysteine Concentrations

SufS activity deviated from Michaelis-Menten enzyme kinetics when it was measured as a function of different concentrations of SufE but over a wider range of fixed L-cysteine levels (10 μM to 20 mM) (Figure 2.5 A). At L-cysteine concentrations below 300 μM, increasing the concentration of SufE actually decreased sulfide formation by SufS (Figure 2.5 A). As long as the L-cysteine concentration remained at 500 μM or higher the inhibition by SufE was not observed and SufS showed Michaelis-Menten kinetics (compare Figure 2.3 B and Figure 2.5 A). Intracellular L-cysteine concentrations

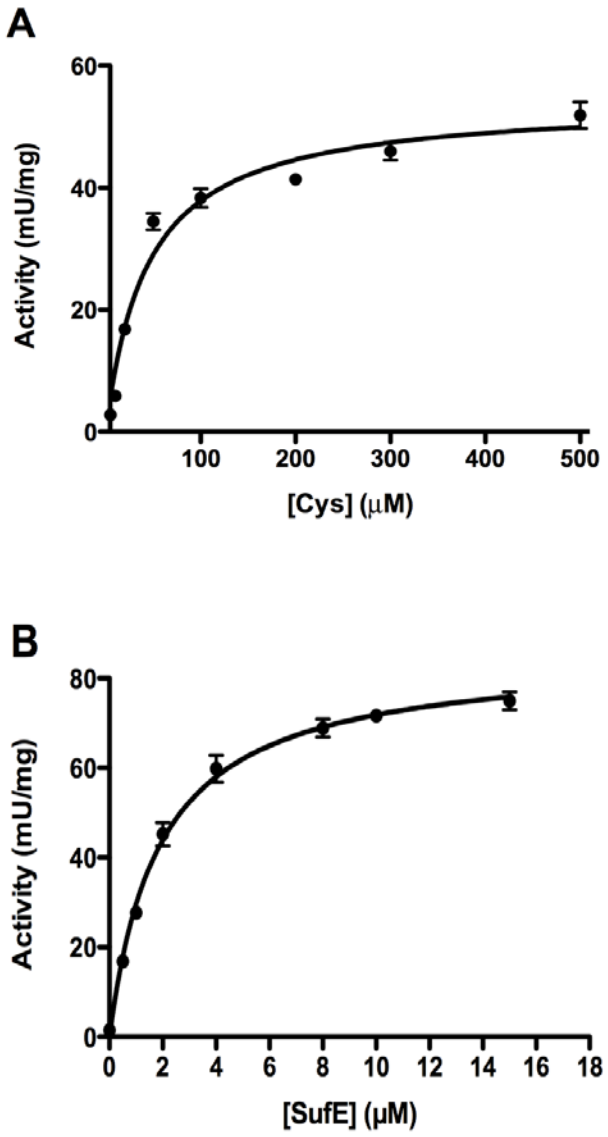

Figure 2.3 Kinetic analysis of SufS activity in response to varied substrate concentrations. The reactions contained (A) 0.5 μM SufS, 4 μM SufE, 2 mM DTT and 10 – 500 μM L-cysteine or (B) 0.5 μM SufS, 0 - 15 μM SufE, 2 mM DTT, and 2 mM L-cysteine. The lines are the best fits to the Michaelis – Menten equation obtained using GraphPad Prism.

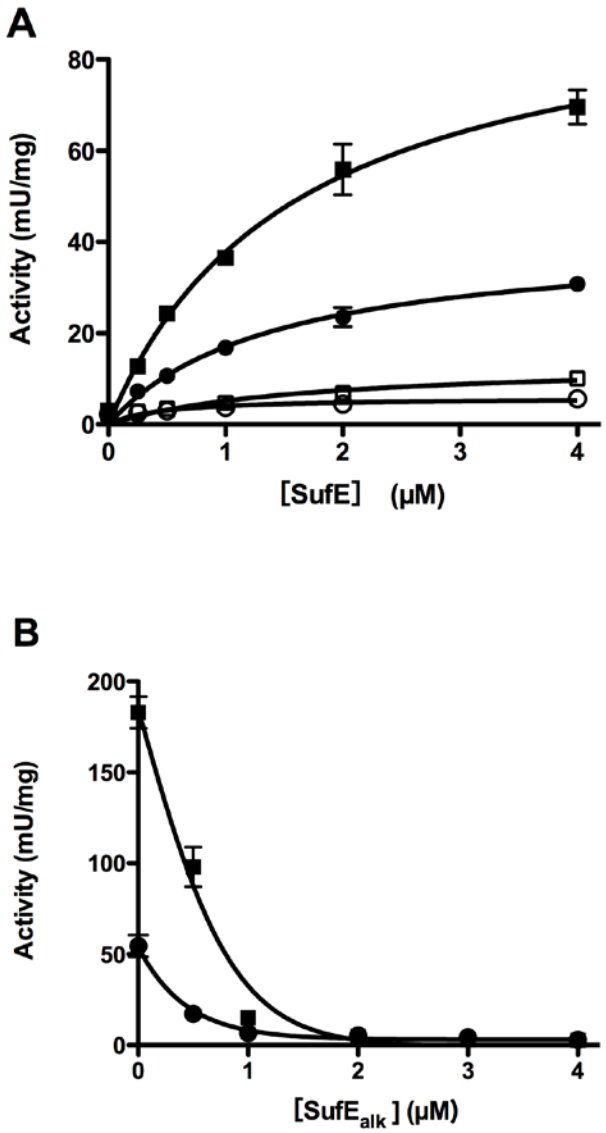

Figure 2.4 Inhibitory effects of $SufE_{alk}$ on the sulfur transfer reaction of SufS. (A) The reactions contain 0.5 μM SufS, 2 mM DTT, and 2 mM L-cysteine with 0 – 4 μM SufE and fixed levels of 0 μM (■), 0.25 μM (●), 1 μM (□) or 2 μM (○) SufEalk. The lines were fit with mixed model inhibition equation using GraphPad Prism. (B) The reactions contain 0.5 μM SufS, 2 μM SufE, with (■) or without (●) 2 μM SufBC2D, 2 mM L-cysteine, and 2 mM DTT and 0 – 4 μM $SufE_{alk}$.

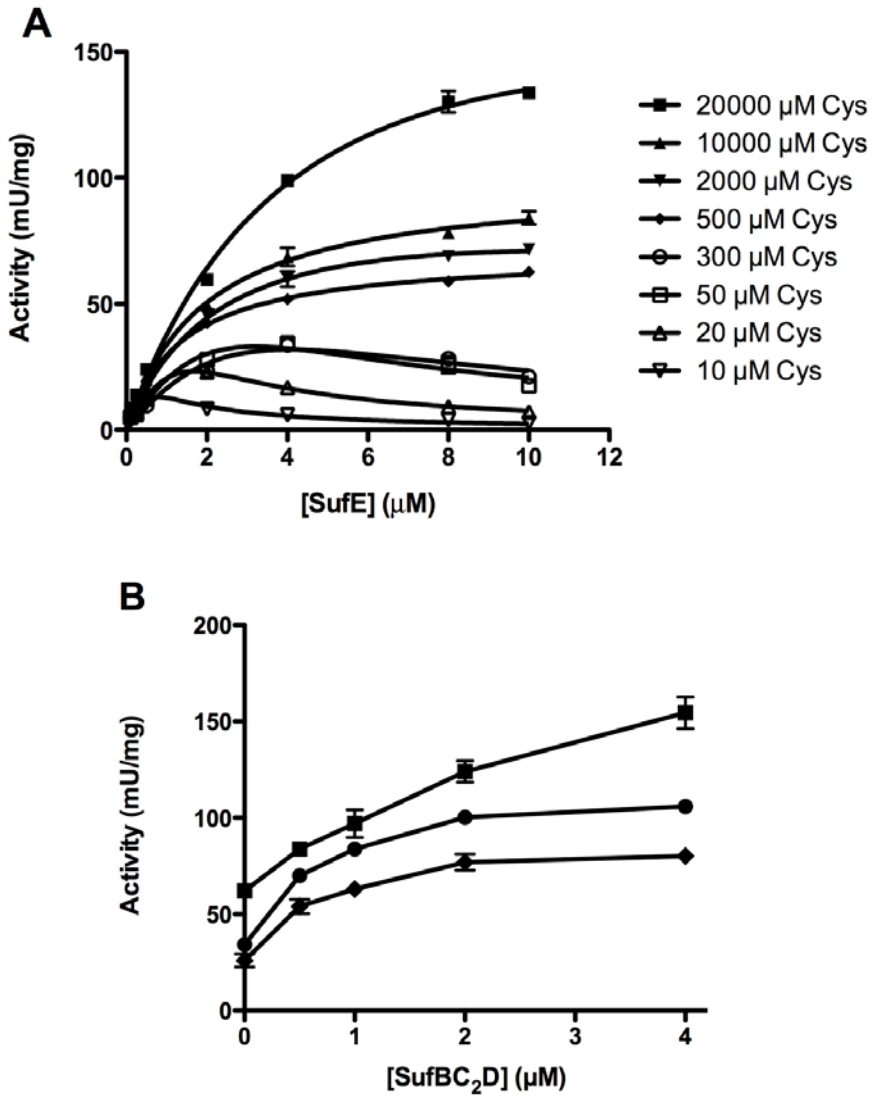
A
Activity (mU/mg)
150
100
50
0
0
2
4
6
8
10
12
[SufE] (μM)
20000 μM Cys
10000 μM Cys
2000 μM Cys
500 μM Cys
300 μM Cys
50 μM Cys
20 μM Cys
10 μM Cys
B
Activity (mU/mg)
200
150
100
50
0
0
1
2
3
4
[SufBC2D] (μM)

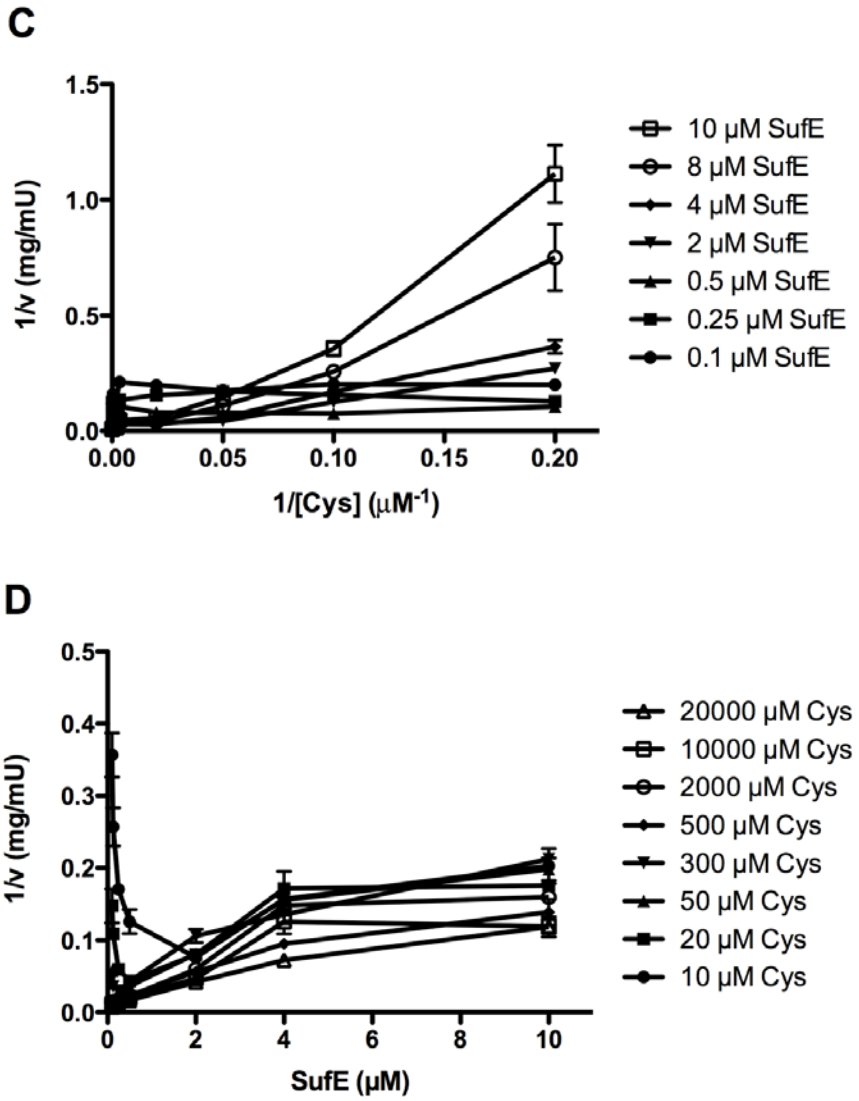

Figure 2.5 Substrate inhibition of SufS by SufE at lower concentrations of L-cysteine. (A) The reactions contain 0.5 μM SufS, 0 – 10 μM SufE, 2 mM DTT, and 10 – 20,000 μM L-cysteine (see embedded legend). (B) The reactions contain 0.5 μM SufS, 50 μM Cysteine, 2 mM DTT, 4 μM (●) or 8 μM (♦) SufE with increasing concentrations of $SufBC_2D$ (0 – 4 μM). A control reaction with 2 mM Cysteine, 2 mM DTT, 0.5 μM SufS, and 8 μM SufE with increasing concentrations of $SufBC_2D$ (0 – 4 μM) is also shown (■). Double reciprocal plots of kinetic data. Activity of 0.5 μM SufS, 2 mM DTT, and (C) varied 10 – 20,000 μM L-cysteine at several fixed concentrations of SufE or (D) varied 0.1 – 10 μM SufE at several fixed concentrations of L-cysteine. See embedded legend for symbol explanations.

Table 2.2 Kinetic parameters of the SufS cysteine desulfurase.

	Cysteine dependent[a]	SufE dependent[b]
K_m (μM)	43.5 ± 5.8	1.9 ± 0.1
V_{max} (mU/mg)	54.3 ± 1.9	85.4 ± 1.8
R^2	0.95	0.99

[a]Reaction conditions were: 0.5 μM SufS, 4 μM SufE, 2 mM DTT and 5 – 500 μM L-cysteine.
[b]Reaction conditions were: 0.5 μM SufS, 0 - 15 μM SufE, 2 mM DTT, and 2 mM L-cysteine.

in *E. coli* are variable depending on growth conditions but can often be in the range of 100 – 200 μM [52], which is below the mM levels often used for in vitro cysteine desulfurase enzyme assays, so the deviation of SufS-SufE from Michaelis-Menten behavior under these conditions may be physiologically relevant.

To test whether inhibition by SufE affects $SufBC_2D$ enhancement of SufS at lower cysteine concentrations, we assayed $SufBC_2D$ enhancement at 50 μM cysteine where SufE showed inhibition of SufS (Figure 2.5 B). For comparison $SufBC_2D$ enhancement at 2 mM L-cysteine (where SufE inhibition does not occur) is also shown in Figure 2B. The enhancement normally provided by the $SufBC_2D$ complex diminished as the fixed concentration of SufE increased, in stark contrast to the $SufBC_2D$-dependent enhancement seen at higher L-cysteine levels (Figure 2.5 B). These results indicate that $SufBC_2D$ cannot reverse the SufE inhibition of SufS that is seen at low cysteine concentrations.

The double reciprocal transformations of the kinetic data clearly show the SufS deviation from Michaelis-Menten behavior at lower cysteine concentrations (Figure 2.5 C and D). At low fixed SufE concentrations, parallel lines are observed when initial velocity as a function of L-cysteine is plotted (Figure 2.5 C). As the fixed concentration of SufE becomes inhibiting (2 μM SufE and above), the slopes of the reciprocal plots increase and the lines begin to cross at high L-cysteine concentrations (approaching the $1/v$ axis) as the SufE concentration approaches the substrate inhibition K_i (Figure 2.5 C). Similarly, when L-cysteine is fixed at concentrations below 500 μM and initial velocity is plotted as a function of SufE, we observed that as SufE concentration increases (approaching the $1/v$ axis), the initial velocity sharply decreases (turns sharply upward)

(Figure 2.5 D). The activity plot and double reciprocal plots are qualitatively similar to those of *O*-acetylserine sulfhydrylase, a PLP-dependent enzyme that reacts via a ping-pong mechanism with substrate inhibition [53]. We attempted to fit our data with the appropriate rate equation for this type of substrate inhibition [53]. Unfortunately the quality of the fit was insufficient to instill confidence in the values for the substrate inhibition constant and other kinetic constants. This leaves open the question of whether SufE inhibition is due to substrate inhibition. Previously it was shown that *E. coli* SufS itself (even in the absence of SufE) deviates from Michaelis-Menten kinetics, which may explain the difficulty in fitting the rate equation described for other enzymes [39].

The SufS-SufE system is More Active at Physiological Cysteine Concentrations than IscS and IscS-IscU.

Next we directly compared the efficiency of the SufS-SufE sulfurtransferase system to that of the *E. coli* IscS and IscS-IscU proteins under the same conditions. The desulfurase activities of SufS-SufE, IscS alone, and IscS-IscU were measured at different concentrations of L-cysteine. A 1:3 molar ratio of SufS to SufE or IscS to IscU was used throughout. At a 1:3 molar ratio of SufS (0.5 μM) to SufE (1.5 μM), SufE does not show measurable inhibition of SufS activity over the range of L-cysteine concentrations used (30 μM – 10 mM). For ease of comparison, the activity of SufS-SufE at each L-cysteine concentration was divided by the activity of IscS alone or IscS-IscU measured under the same conditions and these activity ratios were plotted as a function of L-cysteine (Figure 2.6). For the activity ratios generated by these calculations, values greater than 1 indicate that SufS-SufE have a higher activity than IscS or IscS-IscU at those specific L-cysteine concentrations (Figure 2.6). This comparison reveals that the SufS-SufE system has

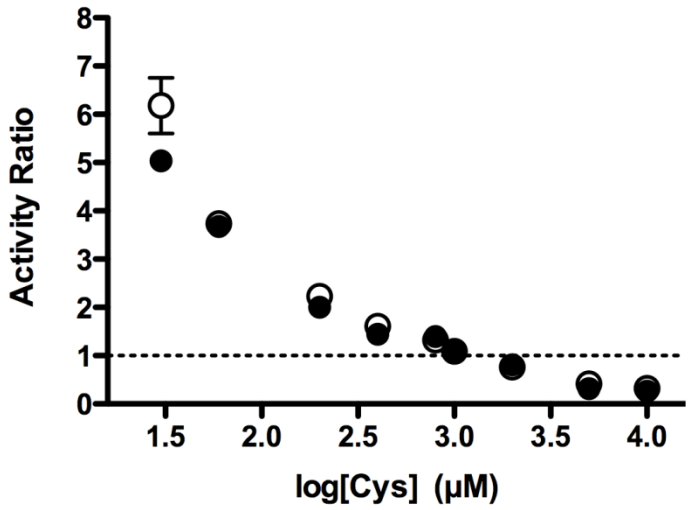

Figure 2.6 Direct activity comparison of the SufS-SufE and IscS-IscU sulfur transfer systems. SufS-SufE activity was divided by IscS activity (closed circles ●) or the IscS-IscU activity (open circles ○) and the ratios were plotted as a function of the L-cysteine concentration in the reaction. The reactions contain 0.5 μM SufS or IscS, 1.5 μM SufE or IscU, and 0.03 – 10 mM L-cysteine and DTT.

higher cysteine desulfurase activity than IscS or the IscS-IscU system at physiological L-cysteine concentrations (up to 200 μM). At 30 μM L-cysteine SufS-SufE activity was 6-fold higher than IscS or the IscS-IscU system and remained at least 2-fold higher until the L-cysteine concentration exceeded 200 μM. Only at high L-cysteine concentrations above 1 mM did IscS or the IscS-IscU system begin to exceed SufS-SufE activity. These results also showed no activity difference between IscS alone compared to the IscS-IscU mixture over the range of L-cysteine tested (Figure 2.6).

IscS-IscU Activity is More Sensitive to H_2O_2 Exposure than SufS-SufE.

The Suf pathway is activated to build Fe-S clusters during oxidative stress in *E. coli* and deletion of the *suf* operon causes disruption of Fe-S cluster biosynthesis by oxidative stress [32-34, 54, 55]. In contrast, the Isc system is unable to carry out Fe-S cluster assembly in vivo upon exposure to reactive oxygen species like H_2O_2 [24]. Active site cysteine residues and persulfide intermediates in sulfur trafficking may react with oxidants like H_2O_2 depending on their exact pKa values [46, 47]. To test if the SufS-SufE or IscS-IscU sulfur trafficking pathways are maintained under oxidative stress, we compared their relative in vitro H_2O_2 sensitivity. It is difficult to test for H_2O_2 sensitivity in the present of DTT due to the propensity for DTT itself to react with and consume H_2O_2 and the ability of DTT to reverse some H_2O_2-mediated thiol oxidation products, such as sulfenic acid [56, 57]. Therefore the desulfurase reactions were carried out in the presence of H_2O_2 but in the absence of DTT under anaerobic conditions (Figure 2.7). Since the SufE and IscU sulfur acceptors may not be as efficiently recycled in the absence of DTT (see above), they were used in a 10:1 excess over SufS and IscS. The concentration of L-cysteine was increased to 2 mM to ensure adequate activity could be measured in the presence of H_2O_2.

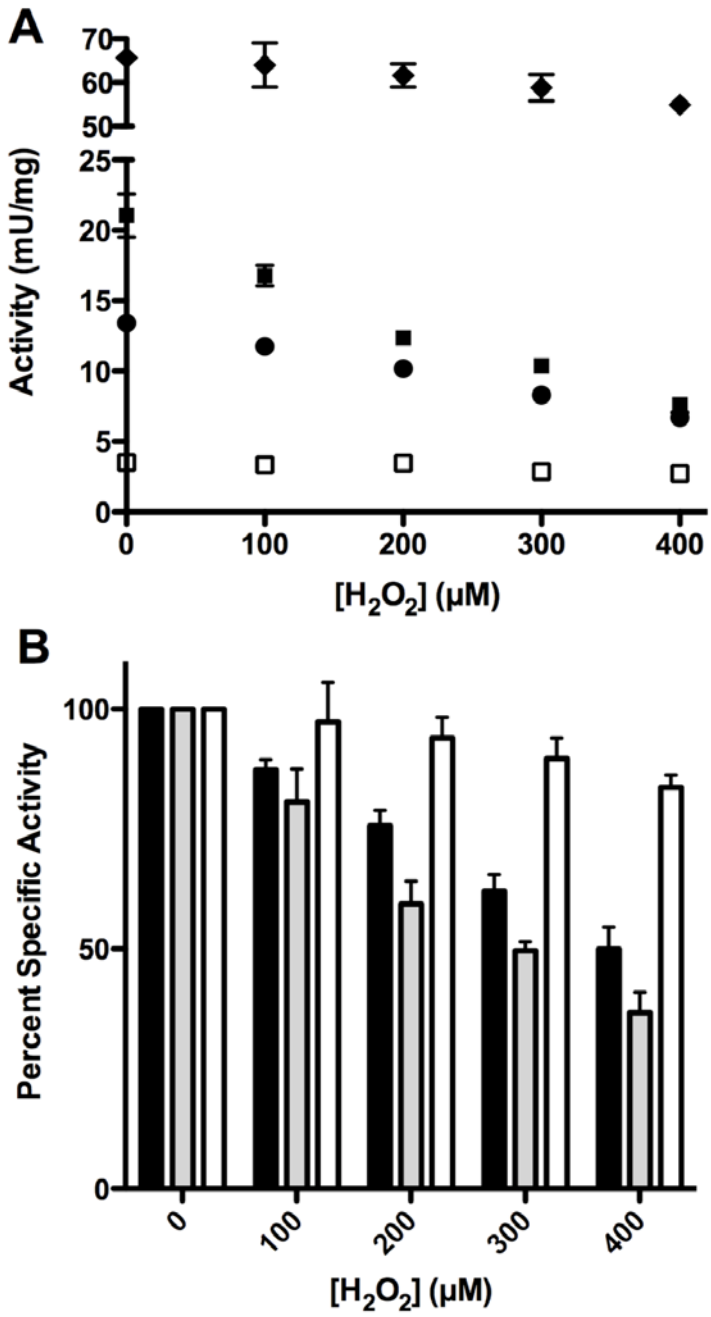

Figure 2.7 The sensitivity of SufS-SufE and IscS-IscU to H_2O_2. 1 μM SufS or IscS and (where indicated) 10 μM SufE or IscU were mixed for 5 min. 2 mM L-cysteine was added followed by 0 – 400 μM H_2O_2 to initiate the reaction. After 30 minutes the reaction was quenched by heating at 95 ºC for 5 minutes, followed by the addition of 2 mM DTT to reduce and release sulfide for measurement as described in Supplementary Materials Methods. All steps were carried out anaerobically. (A) Desulfurase activity of SufS (□), IscS (●), IscS-IscU (■) and SufS-SufE (♦). (B) Percent activity of IscS (black bar), IscS-IscU (light grey bar), and SufS-SufE (white bar) compared to their activity without H_2O_2.

Interestingly, in the absence of DTT, excess IscU was now able to enhance IscS desulfurase activity by 1.5 fold (Figure 2.7 A). This result suggests that if DTT is present it will normally outcompete IscU to release persulfide from IscS and explains why IscU enhancement is not usually observed in the unmodified assay where DTT is present.

Using this modified assay, we found that as the H_2O_2 concentration increased from 0 to 400 μM, sulfide production by IscS and IscS-IscU decreased by 50% or more (Figure 2.7 B). In contrast, sulfide production by SufS-SufE only decreased by about 10 – 15%. The percent decrease in IscS-IscU activity was greater than the percent decrease in the activity of IscS alone, suggesting that IscU enhancement of IscS is largely abolished in response to H_2O_2, possibly due to oxidative damage to IscU (Figure 2.7 B). Furthermore, total sulfide production by SufS-SufE was always from 3 – 9 fold higher than IscS or IscS-IscU throughout the entire range of H_2O_2 concentrations used (Figure 2.7 A). Together these results demonstrate that SufS-SufE sulfide production is more resistant to oxidative stress exposure than sulfide production by IscS or IscS-IscU.

Oxidation of IscS-IscU and SufS-SufE Residues after H_2O_2 exposure.

The decrease in IscS and IscS-IscU activity in response to H_2O_2 suggests that important active site residues or reaction intermediates are damaged by oxidative stress. To map the sites of oxidation in the Isc and Suf sulfur transfer proteins, anaerobic cysteine desulfurase reactions were carried out in the presence of H_2O_2 as described above (in the absence of DTT) except that the reactions were quenched and trapped by the addition of tricholoroacetic acid (TCA) rather than by heating. TCA-trapped samples were alkylated, trypsinized, and analyzed by LC-MS without any further reduction steps as described in Supplementary Materials. The individual IscU and SufE multiple

oxidative modifications to active site Cys residues C328 from IscS, C51 from SufE, and Cys 364 from SufS as well as conserved C63 and C106 in IscU were confirmed by MS/MS analysis of those peptides. The different oxidative modifications detected for the active site Cys residues or their reaction intermediates are summarized in Table 2.3. Using this protocol, stable sulfenic acid modifications were not observed but the more stable sulfinic and sulfonic acid oxidation products were detected. The m/z peak areas for each modified peptide were separately quantified (Table 2.3). For ease of comparison, the signal intensity for the oxidized forms of each specific Cys-containing peptide were pooled and divided by the total signal intensity for all forms of that Cys-containing peptide (Figure 2.8 A). These values can be used for relative comparisons between samples.

For IscS treated with 400 μM H_2O_2, peptides with oxidative modification to the active site C328 accounted for 68% of the total signal intensity (Figure 2.8 A), in rough agreement with the decrease in IscS activity observed under the same conditions (Figure 2.7 A). IscS C328 was more protected when IscU was added since the oxidized forms of C328 only represented 16% of the total signal intensity in that sample. In contrast, the total oxidation of IscU C63 and C106 by 400 μM H_2O_2 was fairly similar, regardless of the presence of IscS (Figure 2.8 A). These results suggest that IscS alone is sensitive to H_2O_2 during the desulfurase reaction cycle. While IscU seems to help prevent direct oxidation of IscS C328, probably by binding to and protecting IscS, IscU itself is oxidized by H_2O_2. Oxidized IscU can no longer enhance IscS activity and may also decrease IscS activity by acting as an inhibitor that competes with undamaged IscU for access to IscS.

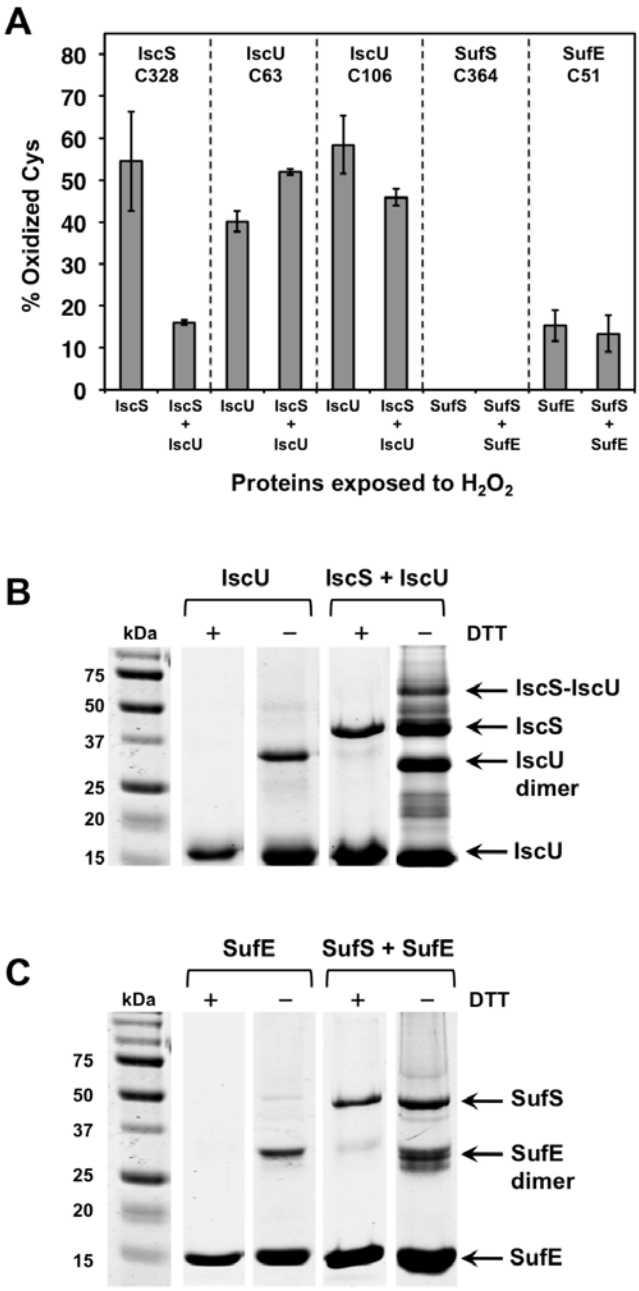

Figure 2.8 Reducing and non-reducing 12% SDS-PAGE gel separation of H_2O_2 treated proteins. The proteins were treated the same way as the samples for mass spectrometry analysis. Proteins were 10% TCA precipitated and dissolved in 1 X SDS loading buffer with and without DTT. And then heat the samples in 95 °C for 10 min before loading on the gel. (B) IscU and IscSU gel separation. (C) SufE and SufSE gel separation.

Table 2.3 Oxidative modifications detected on Cys residues after exposure to 400 μM H_2O_2 during the cysteine desulfurase reaction.

Mass shift[a]	Occupancy Percent (%)			
	SufS	SufE	SufS + SufE	
(+ Da)	C364	C51	SufS C364	SufE C51
0	100	79.0±11.1	100	23.6±3.2
32[b]	0	6.5±4.2	0	0.7±1.1
48	0	7.9±5.3	0	4.8±4.2
64[c]	0	5.7±4.2	0	63.0±8.6
80	0	0.9±1.1	0	7.9±7.8

Mass shift[a]	Occupancy Percent (%)					
	IscS	IscU		IscS + IscU		
(+ Da)	C328	C63	C106	IscS C328	IscU C63	IscU C106
0	32.3±15.5	58.2±7.6	55.4±15.6	84.0±0.6	45.8±1.6	38.7±3.3
32[b]	14.5±4.9	29.2±6.6	21.0±7.7	16.0±0.6	31.9±0.7	18.5±3.0
48	10.7±6.6	7.9±1.6	16.1±10.2	0	7.7±0.8	8.8±2.4
64[c]	13.2±5.1	1.6±0.8	2.9±1.9	0	2.2±0.2	1.4±0.1
80	29.4±30.4	3.1±1.0	4.5±7.8	0	12.4±0.9	32.5±2.6

[a]Assignment of modifications were based on the mass shift (Da) of Cys peptides as follows:

+ 0 R-SH
+ 32[b] R-SO_2H
+ 48 R-SO_3H
+ 64[c] R-S-SO_2H / R-S-S-SH

+ 80 R-S-SO_3H

[b]Based on the reactivity of a single persulfide (R-S-S^-) we think it is unlikely that this species would be stable under our conditions and would either be further sulfurated to S_3 (+64) or would be oxidized to sulfonic acid, R-S-SO_3H (+80) by H_2O_2. Also, the signal intensity for this peak did not decrease upon reduction of the sample, as would be expected if R-S-SH were present. Therefore the +32 species is most likely R-SO_2H.

[c]Since SufE has a high degree of this modification in the presence of SufS and SufE has previously been confirmed to bind polysulfide species, this +64 species is most likely R-S-S-SH. This assignment is also in consistent with the high activity of SufS-SufE during exposure to 400 μM H_2O_2. R-S-S-SH would be semi-stable to oxidation since the termini of polysulfide chains become less reactive as chain length extends beyond S_{2-3} due to charge delocalization along the sulfur chain. This assignment was applied to all Cys residues containing this modification.

In contrast to IscS, oxidized forms of the peptides containing the SufS active site C364 were not detected after H_2O_2 exposure under these conditions, indicating that residue has intrinsic resistance to oxidative damage (Figure 2.8 A). Peptides with oxidative modification to the SufE active site C51 were observed but only accounted for 21 % of total signal in the absence of SufS and 13% in the presence of SufS. The generally lower levels of Cys oxidation in the SufS and SufE proteins correlate with their higher activity in the presence of H_2O_2 (Figure 2.7 A).

Disulfide bond formation is another potential consequence of H_2O_2 oxidation of Cys thiolates. We also analyzed each oxidized sample qualitatively for the formation of mixed disulfides. After 400 μM H_2O_2 treatment, TCA-trapped samples were resuspended and separated by SDS-PAGE under both reducing (+DTT) and non-reducing (-DTT) conditions (Figure 2.8 B and C). Regardless of H_2O_2 treatment, no high molecular weight species were detected for SufS and IscS alone and each protein migrated at its monomer molecular weight irrespective of DTT addition. However, both SufE and IscU form disulfide bonded homodimers that are clearly delineated in the non-reducing gel (Figure 2.8 B and C). Quantification of the intensity of the gel bands indicates that the relative level of SufE homodimer is fairly constant at about 18% of the total protein regardless of the addition of H_2O_2 (Figure 2.8 C). In contrast, the relative amount of IscU homodimer increases from 12.5% to 27.9% of total IscU protein upon exposure to H_2O_2. In the samples containing both IscS and IscU, the IscU homodimer increased to 38.5% of total IscU protein but we also observed the appearance of a new higher molecular weight species that runs at the expected size for a disulfide bonded IscS-IscU heterodimer[58]. A disulfide bonded SufS-SufE heterodimer was not observed under our experimental

conditions although such a species has been seen for ^{35}S-labeled SufS-SufE analyzed on a non-reducing gel [23]. Based on these results it appears that upon exposure to H_2O_2, both IscU and the IscS-IscU complex have a greater propensity to form covalently linked dimers compared to SufE and the SufS-SufE complex, providing an additional mechanism by which IscS activity may be inhibited by H_2O_2 exposure.

DISCUSSION

Substrate Inhibition of SufS by SufE May be a Physiological Adaptation.

Using label transfer assays and surface plasmon resonance (SPR) measurements we previously showed that SufS-SufE interact in the absence of L-cysteine with a K_D of 0.36 μM [45]. Furthermore, previous yeast two-hybrid experiments indicate that the SufS C364S mutant, which cannot form a persulfide intermediate, interacts as well with SufE as the wild type SufS [15]. These published studies confirm that SufE interacts strongly with SufS regardless of SufS persulfide state, which is consistent with the potential substrate inhibition we observe at lower L-cysteine levels. Substrate inhibition by SufE could be a mechanism to limit SufS activity when cellular L-cysteine pools drop below a critical threshold. Measurable inhibition by SufE begins to occur if L-cysteine levels drop below 500 μM while the ratio of SufE: SufS simultaneously increases beyond 4:1. Depending on the exact in vivo ratios of SufE: SufS, which have not currently been measured, substrate inhibition may occur in vivo. Further experiments are necessary to fully explore this enzymatic behavior and its physiological relevance.

SufS-SufE Provide a More Robust Sulfur Transfer System than the Isc Pathway

We found that SufS-SufE has higher cysteine desulfurase activity than IscS or IscS-IscU at physiological L-cysteine concentrations (200 μM and below), especially if

the SufE:SufS ratio is maintained at 3:1 or lower. The higher activity of SufS-SufE at lower cysteine concentrations may be physiologically important for its oxidative stress resistance. Cysteine biosynthetic genes are upregulated under oxidative stress possibly to replenish free cysteine used for glutathione biosynthesis or replacement of oxidized protein thiols [59, 60]. There is also evidence that L-cysteine is actively exported to the periplasm during oxidative stress to protect that sub-cellular compartment [61]. Since SufS-SufE has a higher desulfurase activity than IscS-IscU at lower cysteine concentrations the Suf system may be better able to maintain Fe-S cluster biosynthesis under conditions where L-cysteine availability decreases.

We observed a pronounced activity difference between the Isc and Suf sulfur trafficking proteins when they were exposed to H_2O_2 during the cysteine desulfurase reaction cycle. Under these conditions, IscS and IscS-IscU activity was inhibited while SufS-SufE activity was largely resistant to the H_2O_2 stress. MS analysis of these samples shows that during enzyme turnover the active site Cys residues of IscS and IscU are sensitive to oxidation, forming dead-end sulfinic and sulfonic acid species as well as mixed disulfide heterocomplexes. In contrast, active site C364 of SufS remained unmodified throughout the stress. In addition, MS analysis revealed that the highly reactive S^0 persulfide intermediates on IscS, IscU, and SufE, could also react with H_2O_2 to form cysteine-*S*-sulfinate and cysteine-*S*-sulfonate derivatives (Table 2.3). This is not too surprising given that persulfides tend to have lower pKa values than thiols, making them an "activated" form of sulfur that could readily react with oxidants. Indeed in some organisms a cysteinyl persulfide is the substrate for enzymatic sulfur-oxidation rather than elemental sulfur (S_8) and is oxidized to a cysteine-*S*-sulfonate derivative as part of

the reaction cycle [62-64]. The relative stress resistance of the SufS-SufE system indicates that the active site Cys thiolates and persulfide intermediates for this sulfur transfer pathway are at least partially protected from reactive oxygen species compared to IscS-IscU.

In summary, the results above show that the SufS-SufE and SufS-SufE-SufBC_2D sulfur transfer partners maintain higher desulfurase activity upon exposure to oxidative stress than the analogous IscS and IscS-IscU systems. The robust activity of SufS-SufE at physiological cysteine concentrations, coupled with the resistance of SufS-SufE activity to oxidative stress, indicate that the *E. coli* Suf pathway is well-suited to carry out Fe-S cluster biogenesis when it is induced under stress conditions.

Chapter 3

Escherichia coli SufE Sulfur Transfer Protein Modulates the SufS Cysteine Desulfurase through Allosteric Conformational Dynamics[2]

ABSTRACT

Iron-sulfur (Fe-S) clusters are critical metallocofactors required for cell function. Fe-S cluster biogenesis is carried out by assembly machinery consisting of multiple proteins. Fe-S cluster biogenesis proteins work together to mobilize sulfide and iron, form the nascent cluster, traffic the cluster to target metalloproteins, and regulate the assembly machinery in response to cellular Fe-S cluster demand. A complex series of protein-protein interactions is required for the assembly machinery to function properly. Despite considerable progress in obtaining static three-dimensional structures of the assembly proteins, little is known about transient protein-protein interactions during cluster assembly or the role of protein dynamics in the cluster assembly process. The *Escherichia coli* cysteine desulfurase SufS and its accessory protein SufE work together to mobilize persulfide from L-cysteine, which is then donated to the SufB Fe-S cluster scaffold. Here we use amide hydrogen/deuterium exchange mass spectrometry (HDX–MS) to characterize SufS-SufE interactions and protein dynamics in solution. HDX–MS analysis shows that SufE binds near the SufS active site to accept persulfide from

[2] Singh, H., Dai, Y., Outten, F. W., and Busenlehner, L. S. Escherichia coli SufE Sulfur Transfer Protein Modulates the SufS Cysteine Desulfurase through Allosteric Conformational Dynamics, *The Journal of biological chemistry 288*, 36189-36200.

Cys364. Furthermore, SufE binding initiates allosteric changes in other parts of the SufS structure that likely affect SufS catalysis and alter SufS monomer-monomer interactions. SufE enhances the initial L-cysteine substrate binding to SufS and formation of the external aldimine with pyridoxal phosphate required for early steps in SufS catalysis. Together, these results provide a new picture of the SufS-SufE sulfur transferase pathway and suggest a more active role for SufE in promoting the SufS cysteine desulfurase reaction for Fe-S cluster assembly

INTRODUCTION

Iron-sulfur (Fe-S) clusters are small, inorganic cofactors in metalloproteins that are electron carriers in redox reactions, regulatory sensors, and catalysts [6]. Since both iron and sulfide ions are toxic, Fe-S clusters do not assemble spontaneously *in vivo*. Instead, a series of proteins are required to synthesize Fe-S clusters in a carefully controlled process that is regulated by iron bioavailability and Fe-S cluster demand. While these proteins may vary among organisms, the functional steps for cluster biogenesis are well-conserved. These steps include mobilization of sulfide, formation of the nascent Fe-S cluster, and incorporation of the cluster into target proteins [65]. In bacteria, the three common bacterial Fe-S cluster biogenesis systems are Nif (nitrogen fixation), Isc (iron sulfur cluster assembly), and Suf (sulfur formation) [66].

In many Gammaproteobacteria such as *Escherichia coli*, Fe-S cluster biogenesis is carried out by the Isc system under normal cellular conditions [67]. However, if the cell experiences oxidative stress or iron starvation, the Suf system is the major biogenesis pathway [68]. The *sufABCDSE* operon encodes six proteins SufA, SufB, SufC, SufD, SufS, and SufE. Dimeric SufS is an 88.8 kDa pyridoxal 5′-phosphate (PLP) containing cysteine

desulfurase that mobilizes sulfur from L-cysteine substrate, resulting in an enzyme-bound persulfide intermediate at Cys364 in the active site (Figure 1.6) [20, 68]. Persulfides readily react with oxidants, so the active site of SufS is more buried compared to housekeeping cysteine desulfurases like IscS [17]. The monomeric 15.8 kDa SufE co-substrate protein interacts with the SufS dimer to stimulate cysteine desulfurase activity and accepts sulfane sulfur through a persulfide transfer reaction [23, 44]. This sulfur transfer reaction, which proceeds via a ping-pong mechanism, may be important for limiting sulfide release under oxidative stress conditions [69, 70]. SufE transfers the persulfide to SufB of the $SufBC_2D$ complex, which is a scaffold complex that assembles Fe_4S_4 clusters [45, 51, 71]. Once nascent Fe-S clusters are formed, SufA may transfer the clusters to apo Fe-S proteins [51].

After SufS mobilizes sulfur from L-cysteine, a covalent persulfide intermediate with Cys364 is formed in the active site (Figure 1.6). In apo-SufS, Cys364 resides in a small loop and the Sγ lies relatively far (7.5 Å) from the C4′ atom of PLP; therefore, loop movement should be required for desulfurase activity [21, 72]. The slowest step in the desulfurase activity corresponds to the nucleophilic attack of the Cys364 thiolate ion on the substrate cysteine-PLP ketimine adduct (Figure 1.6) [73]. In the presence of SufE, SufS cysteine desulfurase activity is increased by an order of magnitude [23, 44]. The invariant Cys51 of SufE acts as a co-substrate for SufS and accepts the sulfur from Cys364 of SufS, thereby enhancing the catalytic rate [23, 43, 70]. It is also possible that interaction with SufE may elicit changes in structural dynamics within the active site that facilitate the desulfuration reaction [68]. Since the thiol group of Cys51 of SufE is buried in a solvent inaccessible hydrophobic region, a conformational change is also likely to accompany the

interaction with SufS [48]. Thus, coupled conformational changes may accompany the SufS-SufE interaction.

To fully understand the mechanistic details of the cysteine desulfurase activity of SufS and subsequent transfer of sulfur from SufS to SufE, the interaction interface and catalytically-relevant changes in protein conformational dynamics were characterized by amide hydrogen/deuterium exchange mass spectrometry (HDX-MS) (Figure 3.1) [74].

A variety of factors influence amide hydrogen exchange rates, but their dependence on hydrogen bonding, solvent accessibility, and environment make HDX a useful reporter of conformational changes that coincide with SufS-SufE complex formation [74]. In general, the extent of deuterium incorporation within the first few seconds of exchange indicates regions that are highly dynamic and solvent accessible (*e.g.*, loops). Amides that are buried in the protein interior or involved in hydrogen bonding (*e.g.,* α-helices and β-sheets) exchange at slower rates (minutes to days) because exchange is dependent on unfolding/folding equilibrium or breathing motions [74, 75]. The protection of amides within a protein-protein interface leads to a decrease in deuterium incorporation in the backbone and can be localized through pepsin digestion of the proteins and analysis of the peptides by mass spectrometry [76]. Peptides outside the region of interaction may also have altered solvent deuterium incorporation due to coupled or allosteric conformational changes, so complete evaluation of the HDX solvent accessibility and kinetics is required to obtain a full picture of the SufS-SufE interaction in different intermediate states. HDX deuterium trapping also was employed as an alternative method to confirm regions of interaction.

These studies revealed that SufE binds near the active site entrance of SufS and also influences backbone dynamics in the active site, particularly near PLP and Cys364.

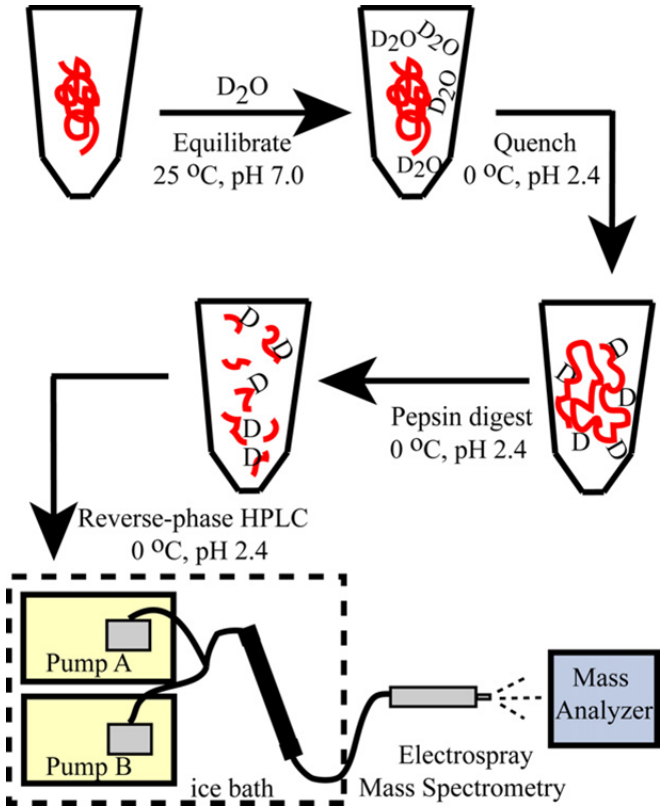

Figure 3.1 Method overview of H/D exchange mass spectrometry. A native protein (pH 7.0, 25 ˚C) is incubated with D_2O to initiate exchange of amide hydrogens. After incubation, the exchange is quenched by lowering the pH to 2.4 and temperature to 0 ˚C. Pepsin is added and the resulting peptides are injected onto a reverse-phase column and separated by HPLC connected in-line to a mass spectrometer [74].

Under conditions where sulfur transfer is stalled at Cys364 of the persulfide intermediate of SufS, the SufE interaction leads to dynamic changes in the dimer interface that could influence the reactivity of the other SufS active site. The results suggest SufE plays an active role in stimulating the SufS cysteine desulfurase reaction through modulation of conformational dynamics, which enhances L-cysteine substrate binding to SufS and the formation of the external aldimine with PLP. The mechanistic implications for Fe–S cluster assembly by the Suf system are discussed.

We collaborated with Dr. Laura S. Busenlehner's lab in University of Alabama on this project. I provided SufS and SufE proteins to Dr. Harsimran Singh who did HDX-MS analysis. I also performed cysteine binding assays and the ITC experiments for protein interaction study.

MATERIALS AND METHODS

Protein Expression and Purification

Escherichia coli $SufS_{apo}$ and $SufE_{apo}$ were independently expressed and purified as described previously [69]. All SufS preparations contained the cofactor PLP. The term "apo" refers to SufS or SufE proteins that do not contain a persulfide sulfur covalently attached to the active site Cys residue.

SufS and SufE were expressed in BL21(DE3). Cells overexpressing SufS and SufE were in Lennox Broth (LB). *E. coli* BL21(DE3) containing the pET-21a_SufS and pET-21a_ SufE expression vector was grown in LB at 37°C and induced by 500 μM isopropyl-1-thio-β-D-galactopyranoside (IPTG) when the cultures reached an OD_{600} of 0.4 - 0.6. Induction was for 3 h at 37°C for SufS and SufE. Harvested cells were lysed in 25 mM Tris, pH 7.5, 100 mM NaCl, 5 mM DTT, 1 mM phenylmethylsulfonyl fluoride,

and 1× EDTA-free protease inhibitor tablet via sonication. Following centrifugation at 20,000 × g for 30 min, lysate was filtered before loading on columns. SufS was purified using Q-sepharose, Phenyl FF, and Superdex 200 chromatography resins in sequence. All the columns used for purification were from GE Healthcare. SufE was purified using Q-sepharose and Superdex 75 chromatography resins in sequence. The Q-sepharose column utilized a linear gradient from 25 mM Tris-HCl, pH 7.5, 10 mM βME to 25 mM Tris-HCl, pH 7.5, 1 M NaCl, 10 mM βME. The Phenyl FF column used a linear gradient of 25 mM Tris-HCl, pH 7.5, 100 mM NaCl, 1 M $(NH_4)_2SO_4$, 10 mM βME to 25 mM Tris-HCl, pH 7.5, 10 mM βME. The Superdex column was run with 25 mM Tris-HCl, pH 7.5, 150 mM NaCl, and 5 mM DTT. Purified proteins were concentrated, frozen as drops in liquid nitrogen, and stored at -80°C until further use.

Formation of the Persulfide SufS Intermediate ($SufS_{per}$)

The 1.5 mM $SufS_{apo}$ stock in 25 mM Tris-HCl, 150 mM NaCl, 10 mM 2-mercaptoethanol, pH 7.4 was buffer exchanged into Buffer A (25 mM Tris-HCl, 150 mM NaCl, pH 7.4) in an anaerobic Vacuum Atmospheres glove box. Twenty-five microliters of 900 μM $SufS_{apo}$ was incubated with 5 μl of 200 mM cysteine for 30 min then desalted using spin columns (Thermo Scientific). Desalted $SufS_{per}$ was aliquoted, sealed under nitrogen atmosphere, and immediately taken for HDX experiments.

Carbamidomethylation of $SufE_{apo}$ ($SufE_{alk}$)

A 1.5 mM $SufE_{apo}$ stock in 25 mM Tris-HCl, 150 mM NaCl, 10 mM 2-mercaptoethanol, pH 7.4 was buffer exchanged into Buffer A in an anaerobic glove

box. Twenty-five microliters of 900 μM $SufE_{apo}$ was incubated in the dark with 5 μl of 500 mM iodoacetamide for 30 min then desalted using spin columns. The number of free thiols before and after alkylation was determined by a 5,5'-dithio-bis(2-nitrobenzoic) acid assay [77]. $SufE_{alk}$ retained ~10% of free thiol and tandem MS/MS sequencing did not identify non-alkylated peptides containing Cys51, as described below.

Identification of Pepsin-Generated Peptides

$SufS_{apo}$, $SufS_{per}$, $SufE_{apo}$ and $SufE_{alk}$ were separately digested with pepsin and the subsequent peptides were sequenced using MS/MS collision induced dissociation [78]. Twenty five microliters of 10 μM protein was incubated with 25 μl of "quench" buffer (0.1 M potassium phosphate, pH 2.3) followed by 2 μl of 5 mg/ml porcine pepsin in 10 mM potassium phosphate, pH 7 for 5 min on ice. The generated peptides were loaded onto a Phenomenex 50 × 2 mm microbore C18 HPLC column pre-equilibrated with solvent A (HPLC grade 98% H_2O, 2% acetonitrile, 0.4% formic acid). The digested peptides were eluted over 26 minutes at 0.1 ml/min on an Agilent 1100 HPLC using a linear gradient of 0–50% HPLC grade solvent B (98% acetonitrile, 2% H_2O, 0.4% formic acid). Peptides were sequenced using a Brüker HCTUltra PTM Discovery mass spectrometer in positive ion mode by data dependent MS/MS. Peptide identification was performed with PEAKS Client 6. The $SufS_{apo}$ and $SufE_{apo}$ pepsin peptide digest maps generated from peptide identification are shown in (Figure 3.2).

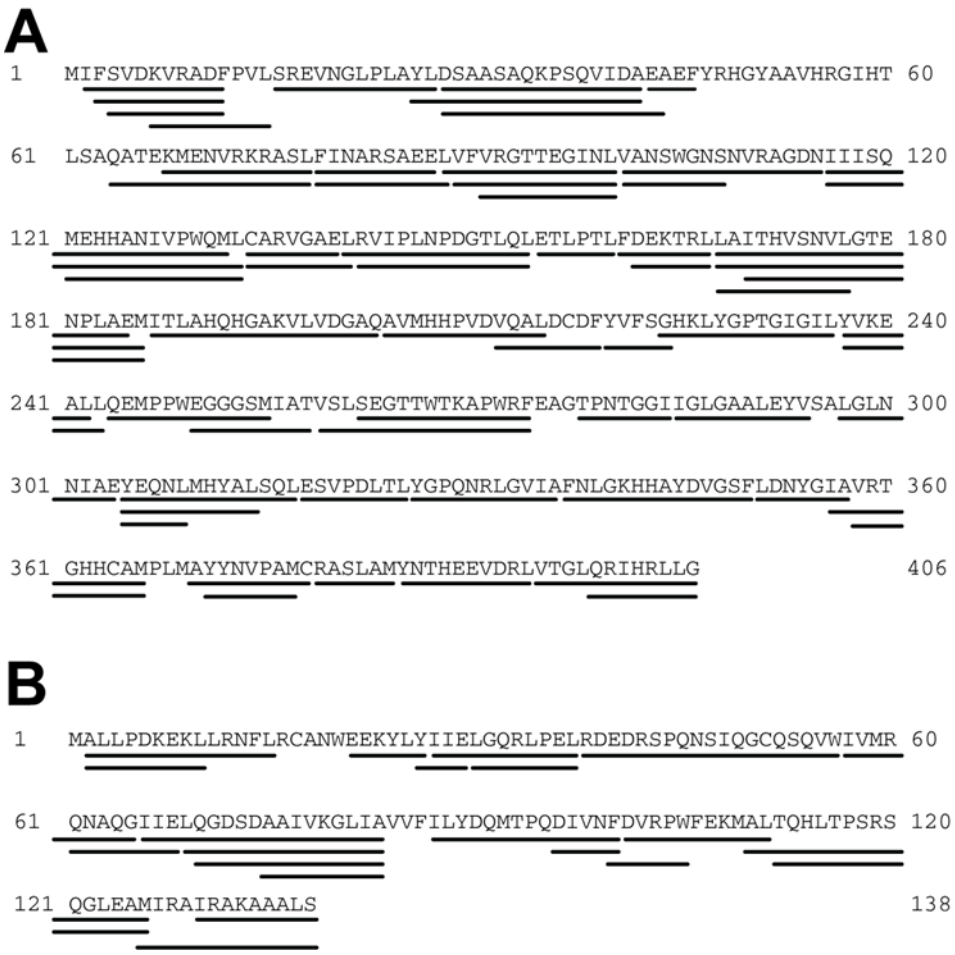

Figure 3.2 Pepsin-digest peptide maps of SufS and SufE. Peptides generated from pepsin digestion of (A) $SufS_{apo}$ and (B) $SufE_{apo}$ was subjected to collision induced dissociation. The MS/MS data were analyzed by Peaks Client 6. The sequence coverage of SufS (406 residues) and SufE (138 residues) are 96% and 94%, respectively.

H/D Exchange Mass Spectrometry (HDX–MS)

Separate HDX-MS experiments were performed with 125 μM stocks of $SufS_{apo}$, $SufE_{apo}$, and the 1:1 $SufS_{apo}$-$SufE_{apo}$ complex in Buffer A with 5 mM DTT, pH 7.4. The $SufS_{apo}$-$SufE_{apo}$ complex was generated by combining equal volumes of 250 μM $SufS_{apo}$ and 250 μM $SufE_{apo}$. The HDX reaction was initiated by addition of 23 μl of 99.9 % at. D_2O to 2 μl of 125 μM protein [78]. Samples were incubated at 25 °C for 15 s to 1 h, after which the reaction was quenched with 25 μl quench buffer and transferred to ice. The sample was immediately digested on ice using 2 μl of 5 mg/ml pepsin for 5 min. The digested peptides were separated over 15 min at 0.1 ml/min using a 0–50 % gradient of solvent B. All samples for HDX were prepared individually and ran on the same day.

The appropriate HDX control samples corresponding to the natural isotope distribution pattern for various peptides ($m_{0\%}$) and the amount of deuterium back-exchange from fully-deuterated peptides ($m_{100\%}$) were also performed. For the $m_{0\%}$ control, 2 μl of 125 μM protein was incubated with 23 μl of water at 25 °C, followed by quenching and pepsin digestion as described above. For the $m_{100\%}$ control, 2 μl of 125 μM protein was incubated with 12-fold excess of D_2O at 37 °C for 16 hours then quenched and digested as above. The spectra from each HDX-MS sample were analyzed using HDExaminer (Sierra Analytics). Each experiment was repeated in triplicate and averaged. The percentage of deuterium incorporated for each peptide was plotted as a function of log time using KaleidaGraph (Synergy Software) and the resulting plot was fit to the sum of first order rate expressions using Equation 1

$$D = N - \sum_{i=1}^{n} A_i \cdot e^{-k_i t} \quad (1)$$

where N is the total number of exchangeable hydrogens and A_i is the number of amide protons that exchange at the rate k_i for the exchange time t [74].

Amide H/D Exchange Deuterium Trapping

HDX trapping experiments were performed at protein concentrations well above the measured dissociation constant for the $SufS_{apo}$-$SufE_{apo}$ complex [45] to ensure the complex does not dissociate during exchange. The incubation times for on-exchange and back-exchange of deuterium were experimentally optimized for this system. Stock solutions of $SufS_{apo}$ and $SufE_{apo}$ (1.5 mM) were prepared in Buffer A with 5 mM DTT. For the 1:1 $SufS_{apo}$-$SufE_{apo}$ complex, 2 µl of 1.5 mM $SufS_{apo}$ and 2 µl of 1.5 mM $SufE_{apo}$ were separately incubated with 23 µl of D_2O for 8 min at 25 °C, mixed, and then incubated for 2 min at 25 °C [79, 80]. The 25 µl reaction was back-exchanged with 250 µl of H_2O at 25 °C for 2 min and immediately quenched with 3 µl of 7.5% formic acid at 4 °C. Deuterium retention for both $SufS_{apo}$ and $SufE_{apo}$ as individual proteins after 10 min in D_2O was also measured. Two microliters of 1.5 mM $SufS_{apo}$ or $SufE_{apo}$ was incubated with 23 µl of D_2O for 8 min at 25 °C. An additional 25 µl of D_2O was added (to mimic the addition of the other protein during complex formation) and incubated at 25 °C for 2 min. Next, 250 µl of H_2O was added and incubated at 25 °C for 2 min.

To determine the extent of deuterium incorporation into each protein without back-exchange with water, 2 µl of 1.5 mM protein was incubated with 23 µl of D_2O for 8 min, followed by addition of 25 µl of D_2O for 2 min. The reaction was quenched using 250 µl of 0.15 % formic acid at 4 °C. The quenched solution was digested for 5 min on ice with 5 µl of 5 mg/ml porcine pepsin in 0.01 M potassium phosphate, pH 7.4 at 0 °C.

The $m_{0\%}$ and $m_{100\%}$ controls were prepared as before for HDX-MS time course experiments. Samples were analyzed by mass spectrometry as described. Each experiment was repeated in triplicate and averaged. The percentage of retained deuterium in the complex after back-exchange with water is based on the total amount of deuterium incorporated after 10 min in D_2O for $SufS_{apo}$ and $SufE_{apo}$ individually. HDX trapping was also performed with the $SufS_{apo}$-$SufE_{alk}$ and $SufS_{per}$-$SufE_{alk}$ complexes using the same procedure.

Cysteine Binding Assays

All assays were performed at room temperature in Buffer A. L-cysteine binding was evaluated by monitoring the immediate ΔA_{420} or ΔA_{340} elicited by the addition of increasing concentrations of L-cysteine to 25 μM $SufS_{apo}$ or 25 μM $SufS_{apo}$ with an equal amount of $SufE_{alk}$ [81]. Protein was first added to the cuvettes, and then L-cysteine was added and mixed for ~5 s prior to a wavelength scan from 200–650 nm. As L-cysteine concentrations increased, the 420 nm PLP peak intensity (internal aldimine) decreased and the new 340 nm peak intensity (external aldimine) increased. Data were analyzed with Prism software (Graphpad). $SufS_{apo}$-Cys data were best fit with the one site-specific binding with Hill slope model. $SufS_{apo}$-$SufE_{alk}$-Cys data were best fit with a one site-specific binding model.

Isothermal Titration Calorimetry （ITC）

ITC measurements were performed on a VP-ITC calorimeter (MicroCal) at 27 °C. For the $SufS_{apo}$ and $SufE_{apo}$ ITC experiment, $SufS_{apo}$ present in the cell (1.44 ml at 108

μM) was titrated with 45 6-μl injections of 1.1 mM SufE (a 10-fold molar excess over $SufS_{apo}$). The duration of each injection was 7.2 s (1.2 s/μl) with an interval of 200 s between injections. For the $SufS_{apo}$ and $SufE_{alk}$ ITC experiment, $SufS_{apo}$ present in the cell (1.44 ml at 108 μM) was titrated with 40 5-μl injections of 1.1 mM iodoacetamide-treated SufE ($SufE_{alk}$). The duration of each injection was 6 s with an interval of 360 s between injections. Titrations were performed in Buffer A. Each experiment was corrected for the endothermic heat of injection resulting from the titration of SufE/$SufE_{alk}$ into buffer. $SufS_{apo}$-$SufE_{apo}$ ITC data were analyzed with the two sequential binding sites model in MicroCal Origin using a $SufS_{apo}$ dimer concentration of 54 μM. $SufS_{apo}$-$SufE_{alk}$ ITC data was analyzed with the one site model in MicroCal Origin using a SufS monomer concentration of 108 μM.

RESULTS

$SufS_{apo}$-$SufE_{apo}$ Interaction: Solvent Accessibility and Backbone Dynamics

Previously it has been shown that *Escherichia coli* $SufS_{apo}$ interacts with $SufE_{apo}$ even in the absence of L-cysteine substrate when SufS is not active [23, 43, 69]. We employed HDX–MS to characterize the interaction between $SufS_{apo}$ and $SufE_{apo}$ to determine if these interactions are relevant to the sulfur transfer mechanism. Here we use the term "apo" only to refer to SufS or SufE proteins that without persulfide sulfur covalently attached to the active site Cys residue (Cys364 for SufS or Cys51 for SufE). In all experiments, SufS contains the PLP cofactor.

The amount of deuterium exchange into backbone amides as a function of time for $SufS_{apo}$ and $SufE_{apo}$ were compared to that for the $SufS_{apo}$-$SufE_{apo}$ complex. It is useful to

compare the D_2O accessibility of amides that exchange with a very fast rate (*i.e.*, before the 15 sec time point) to identify regions that are altered by the interaction of the two proteins [74, 76]. Decreased deuterium levels denote regions that become shielded from D_2O by the interaction [76]. There are only minor differences in solvent accessibility for $SufS_{apo}$ upon the formation of the $SufS_{apo}$-$SufE_{apo}$ complex (Figure 3.3A). This indicates that $SufE_{apo}$ does not significantly protect a large surface area of $SufS_{apo}$. For $SufE_{apo}$, only residues 66-83 have a >10% decrease in deuterium incorporation in the $SufS_{apo}$-$SufE_{apo}$ complex (Figure 3.3 B). This peptide forms one side of a structural groove into which the SufE Cys51 thiolate is oriented [48].

Changes in deuterium uptake over longer time periods (*i.e.*, beyond 15 sec) occur through shifts in protein unfolding/folding equilibria, caused by constrained protein backbone dynamics upon interaction of $SufS_{apo}$ and $SufE_{apo}$ [74, 82]. HDX–MS kinetic traces show that two regions of $SufS_{apo}$ lose conformational flexibility when in complex with $SufE_{apo}$. Kinetic traces for peptides 356-366 and 225-236 reveal a 2-fold and 4-fold decrease in the rate of deuterium incorporation, respectively, for the $SufS_{apo}$-$SufE_{apo}$ complex (Figure 3.4, A and B). Peptide 356-366 is a loop that extends from the surface of SufS to the active site channel and includes the sulfur-accepting residue Cys364 [21, 72]. In contrast, residues 225-236 are located at the bottom of the active site cavity and contain Lys226, which is covalently bound to the PLP cofactor as an internal aldimine (Figure 3.4, C and D). These results suggest that $SufE_{apo}$ binding near the surface of the active site channel (residues 356-366) leads to an allosteric change in conformational dynamics near the catalytic PLP cofactor (residues 225-236).

Changes in $SufE_{apo}$ backbone dynamics near Cys51, the sulfur acceptor, are also observed upon formation of the $SufS_{apo}$-$SufE_{apo}$ complex. Peptide 38-56, which is a surface loop containing Cys51 [48], has a ~3-fold reduced rate of deuterium incorporation in the $SufS_{apo}$-$SufE_{apo}$ complex (Figure 3.5 A and C). Another peptide in close proximity to Cys51 (residues 66-83) also has altered deuterium uptake in the complex (Figure 3. 5 B), but this is more reflective of decreased solvent accessibility since it is protected within 15 sec of D_2O incubation (Figure 3.3 B). Thus, residues within 66-83 are most likely involved in the $SufS_{apo}$ interaction, which may cause conformational changes that are propagated to the Cys51 loop (residues 38-56).

$SufS_{apo}$-$SufE_{apo}$ Interaction: Deuterium Trapping

One of the limitations with traditional HDX-MS is that some regions in the individual proteins may not incorporate a significant amount of deuterium after 15 sec of D_2O incubation. If a change in solvent accessibility does occur after complex formation, it might be too small to accurately measure because of normal deuterium loss during HPLC analysis. This was observed for $SufS_{apo}$ for which there was little change in solvent accessibility upon $SufE_{apo}$ binding (Figure 3.3 A). Therefore, a simple technique was sought to overcome this limitation.

Modified HDX deuterium trapping was used to identify deuterated amides in the $SufS_{apo}$-$SufE_{apo}$ complex that are not easily off-exchanged with water (*i.e.*, "trapped") [80, 83, 84]. By pre-incubating $SufS_{apo}$ and $SufE_{apo}$ individually with D_2O for 10 min, highly or

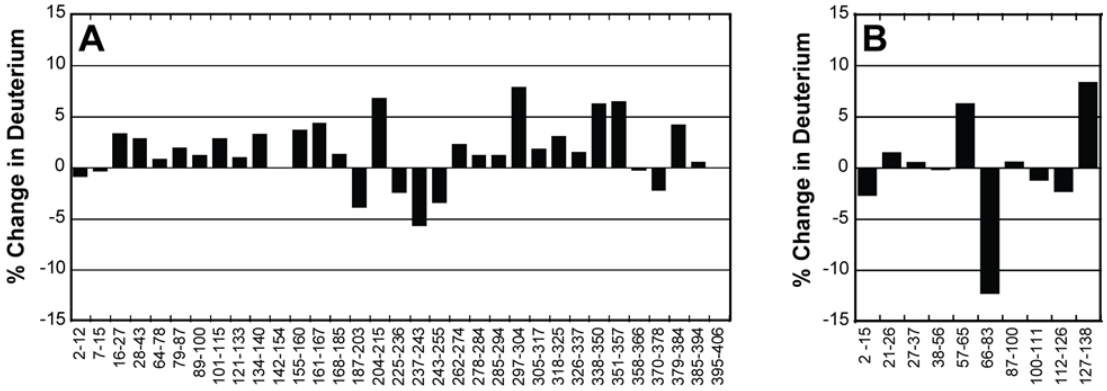

Figure 3.3 Differential changes in amide solvent accessibility upon $SufS_{apo}$-$SufE_{apo}$ complex formation. HDX reactions with free $SufS_{apo}$, $SufE_{apo}$, and the $SufS_{apo}$-$SufE_{apo}$ complex were initiated by addition of 23 µl of D_2O to 2 µl of 125 µM protein. The percentage of deuterium incorporated into peptides after 15 s of D_2O incubation for the $SufS_{apo}$-$SufE_{apo}$ complex was subtracted from that for (A) free $SufS_{apo}$ and (B) $SufE_{apo}$. Positive and negative percent change values correspond to increased and decreased accessibility to deuterium, respectively.

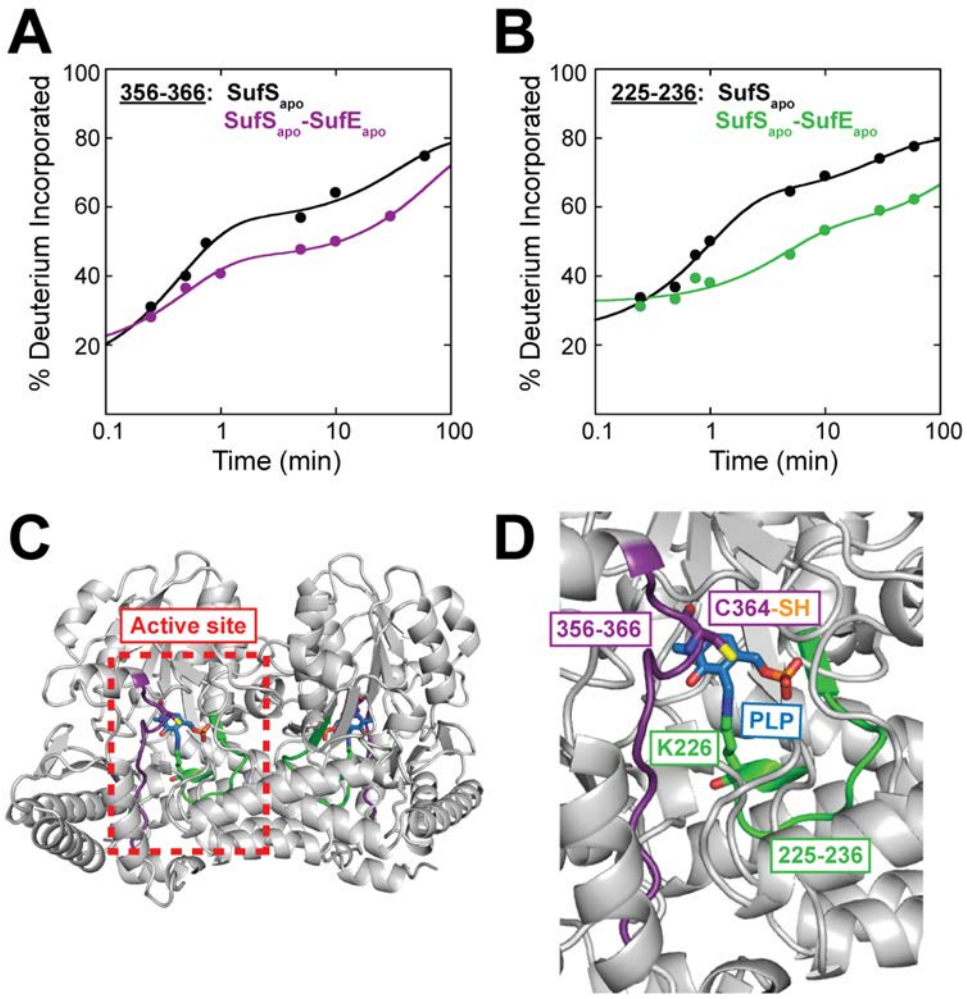

Figure 3.4 HDX-MS kinetic traces comparing deuterium incorporation as a function of time for $SufS_{apo}$ and the $SufS_{apo}$-$SufE_{apo}$ complex. HDX reactions were initiated by addition of 23 µl of D_2O to 2 µl of 125 µM $SufS_{apo}$ or $SufS_{apo}$-$SufE_{apo}$. Samples were incubated at 25 °C for 15 s to 1 h, after which the reactions were quenched and digested with pepsin for 5 min at 4 °C. SufS peptides (A) 356-366 and (B) 225-236 show decreased rates of deuterium incorporation in the $SufS_{apo}$-$SufE_{apo}$ complex. Peptides 356-366 (purple) and 225-236 (green) are represented on the (C) full and (D) zoomed in structure of $SufS_{apo}$ (PDB: 1JF9) [21]. Cys364, Lys226, and PLP (blue) are indicated in stick format. The data were fit to a sum of first-order rate expressions, which can be found in Table 3.1. The uptake plots for all peptides are found in Figure 3.10.

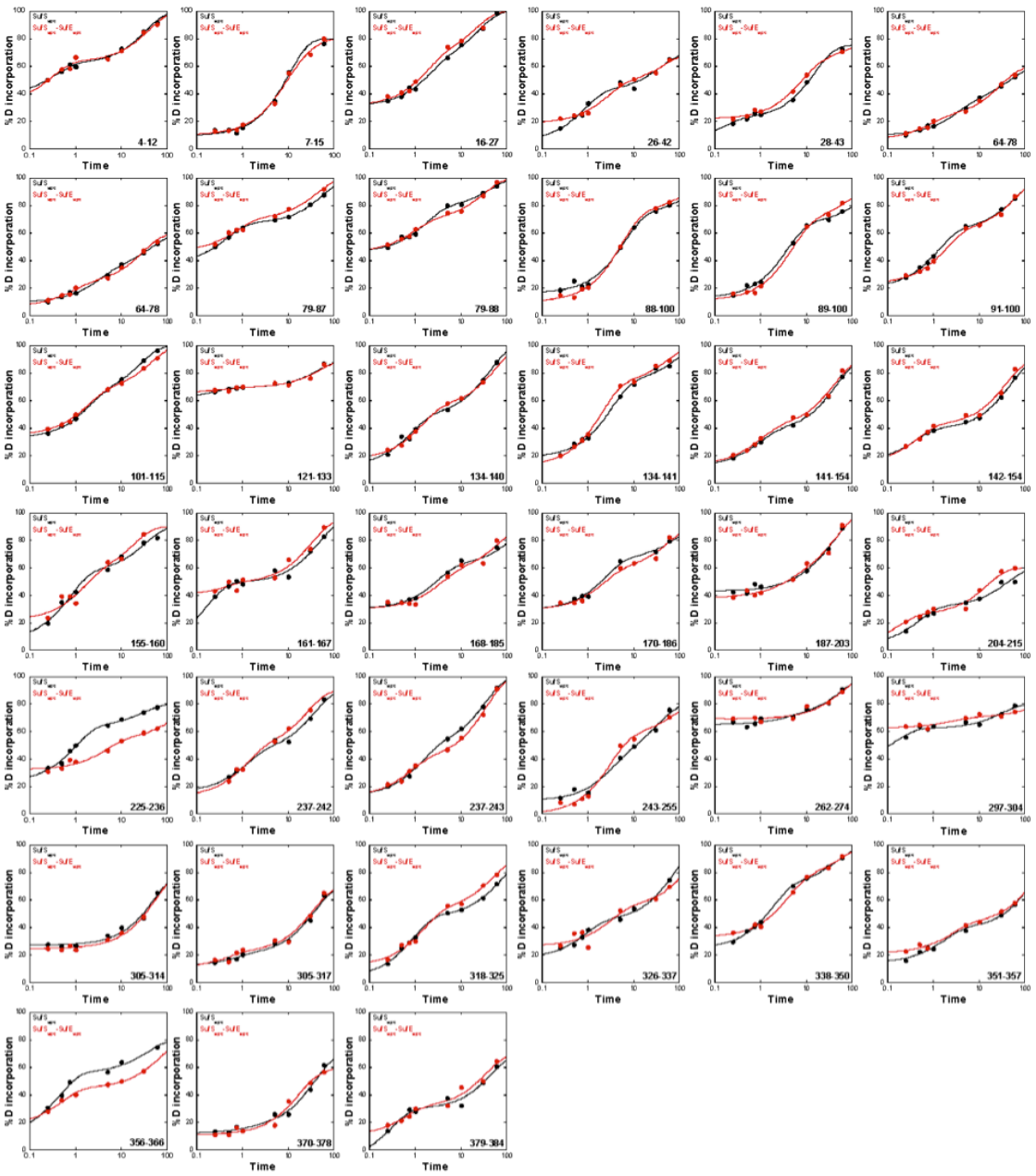

Figure 3.10 HDX-MS kinetic profiles for $SufS_{apo}$ and the $SufS_{apo}$-$SufE_{apo}$ complex. HDX-MS kinetic traces compare the percent deuterium incorporation as a function of time for $SufS_{apo}$ (black) and the $SufS_{apo}$-$SufE_{apo}$ complex (red).

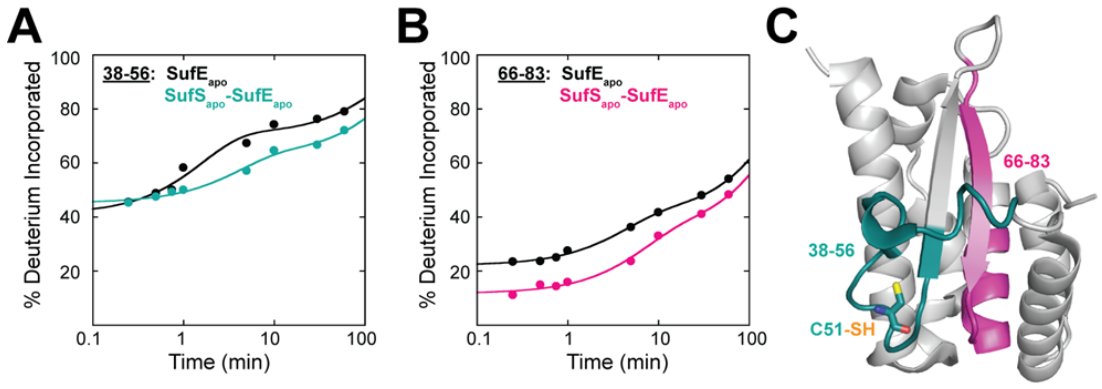

Figure 3. 5 HDX-MS kinetic traces comparing deuterium incorporation as a function of time for $SufE_{apo}$ and the $SufS_{apo}$-$SufE_{apo}$ complex. HDX reactions were initiated by addition of 23 µl of D_2O to 2 µl of 125 µM $SufE_{apo}$ or $SufS_{apo}$-$SufE_{apo}$. Samples were incubated at 25 °C for 15 s to 1 h, after which the reactions were quenched and digested with pepsin for 5 min at 4 °C. SufE peptides (A) 38-56 and (B) 66-83 show decreased rates of deuterium incorporation in the $SufS_{apo}$-$SufE_{apo}$ complex. (C) The peptides 38-56 (teal) and 66-83 (pink) along with Cys51 in stick format are depicted on the structure of $SufE_{apo}$ (PDB:1MZG) [48]. The data were fit to a sum of first-order rate expressions, which can be found in supplemental Table 3.1. The uptake plots for all peptides are found in Figure 3.11.

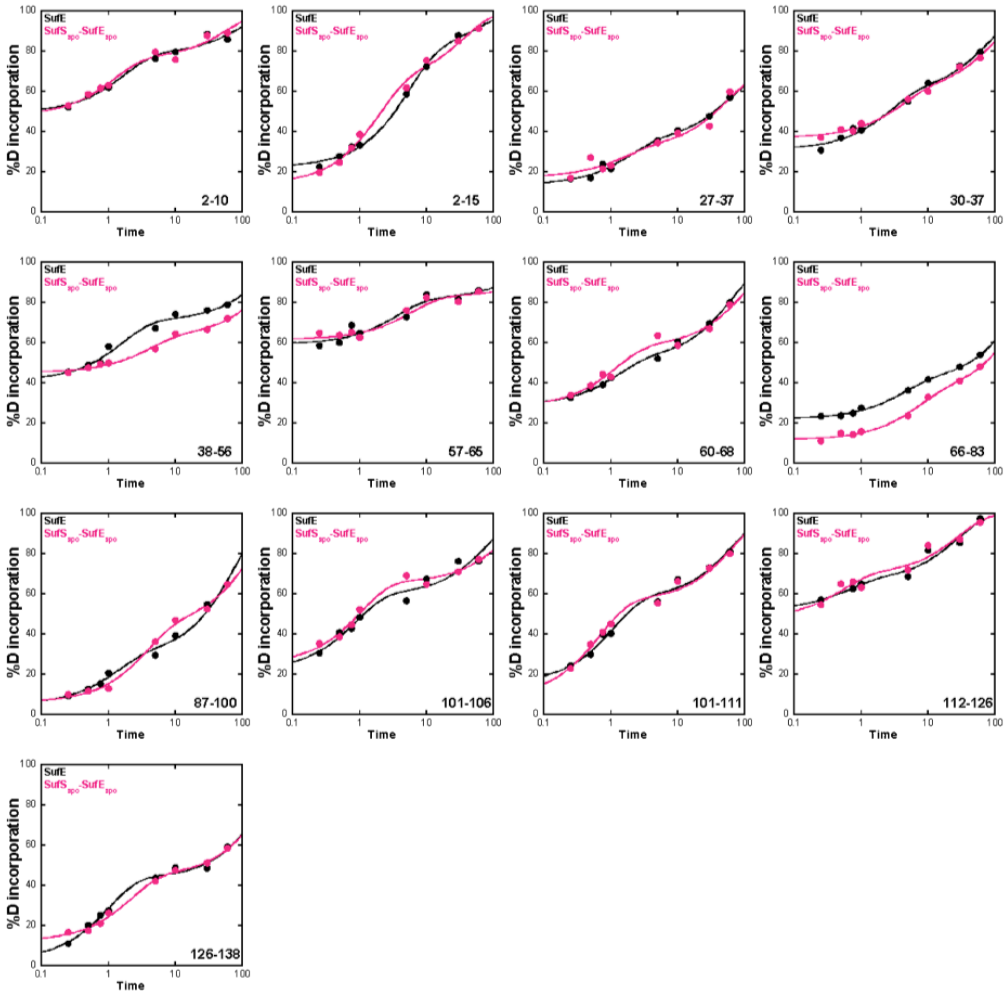

Figure 3.11 HDX-MS kinetic profiles for $SufE_{apo}$ and the $SufS_{apo}$-$SufE_{apo}$ complex. HDX-MS kinetic traces compare the percent deuterium incorporation as a function of time for $SufE_{apo}$ (black) and the $SufS_{apo}$-$SufE_{apo}$ complex (pink).

Table 3.1 HDX–MS rate constants and amplitudes for $SufS_{apo}$ (Figure 3.4) and $SufE_{apo}$ (Figure 3.5)[a]

Peptide	$\%D_{Pre\text{-}Ex}$[b]	$\%D_1$	k_1 (min^{-1}) *"Fast"*	$\%D_2$	k_2 (min^{-1}) *"Intermediate"*	$\%D_3$	k_3 (min^{-1}) *"Slow"*
SufS: 356-366							
$SufS_{apo}$	~12	45.4 (±10.3)	2.04 (±0.66)	42.2 (±2.7)	0.008 (±0.002)	–	–
$SufS_{apo}$-$SufE_{apo}$	~18	27.3 (±4.1)	1.95 (±0.48)	54.7 (±1.4)	0.008 (±0.001)	–	–
SufS: 225-236							
$SufS_{apo}$	~23	41.6 (±3.9)	0.93(±0.18)	34.7 (±1.9)	0.007 (±0.001)	–	–
$SufS_{apo}$-$SufE_{apo}$	~34	21.9 (±5.1)	0.21 (±0.12)	45.6 (±5.5)	0.003 (±0.002)	–	–
SufE: 38-56							
$SufE_{apo}$	~41	29.4 (±4.2)	0.61 (±0.26)	29.3 (±2.8)	0.006 (±0.003)	–	–
$SufS_{apo}$-$SufE_{apo}$	~45	17.6 (±2.8)	0.24 (±0.10)	37.1 (±3.0)	0.004 (±0.002)	–	–
SufE: 66-83							
$SufE_{apo}$	~23	15.7 (±1.7)	0.31 (±0.09)	22.4 (±2.0)	0.02(±0.003)	~39	$\leq 1\times10^{-4}$
$SufS_{apo}$-$SufE_{apo}$	~11	20.5 (±5.7)	0.16 (±0.07)	27.7 (±6.1)	0.01 (±0.005)	~41	$\leq 1\times10^{-4}$

[a]Parameters obtained from fitting the HDX profile curves of $SufS_{apo}$ peptides with and without $SufE_{apo}$ (from Figure 3.4) and for $SufE_{apo}$ peptides with and without $SufS_{apo}$ (from Figure 3.5) according to a single, double or triple exponential equations as described in Experimental Procedures. The rates have been loosely grouped in to fast, intermediate and slow exchange.

[b]The amount of exchange before the first time point is estimated from the fit parameters and is assigned a rate of exchange > 4 min^{-1}.

moderately solvent accessible amides will exchange. This leads to a greater percentage of deuterium incorporation, which is inherently easier to measure by MS. $SufS_{apo}$ and $SufE_{apo}$ are then mixed to form the $SufS_{apo}$-$SufE_{apo}$ complex and further diluted into H_2O to off-exchange solvent accessible amide deuterons. The percentage of deuterium retained in peptides from the $SufS_{apo}$-$SufE_{apo}$ complex after off-exchange with water was compared to the amount of deuterium retained within the individual proteins after off-exchange. The percent retention was based on the total amount of deuterium incorporated before off-exchange with water (*i.e.*, after 10 min incubation in D_2O). Amides that retain more deuterium in the complex are either involved in the interaction between $SufS_{apo}$ and $SufE_{apo}$ or are highly protected by associated conformational changes that influence stable hydrogen bonding [80]. Note that some amide deuterons at the protein-protein interface may still back-exchange for hydrogen if they are accessible to water. This method only surveys amides whose exchange rates have been significantly reduced by complex formation [80, 83].

Deuterium trapping analysis showed that $SufS_{apo}$ peptides 356-366 and 225-236 retain more deuterium in the $SufS_{apo}$-$SufE_{apo}$ complex compared to free $SufS_{apo}$ (Figure 3.6 A and B). These are the same peptides identified by the traditional HDX-MS method (Figure 3.4). The increased retention confirms that $SufE_{apo}$ binding protects deuterated $SufS_{apo}$ amides in those regions from back-exchange with water. Peptide 356-366 is at the opening of the cavity leading to the active site (Figure 3.6 C and D), so the deuterium protection could be from direct interaction with $SufE_{apo}$, which must gain access to Cys364 for sulfur transfer [23]. Since residues 225-236 are at the bottom of the active site cavity, it is unlikely that they directly interact with $SufE_{apo}$ [21]. Increased protection of this

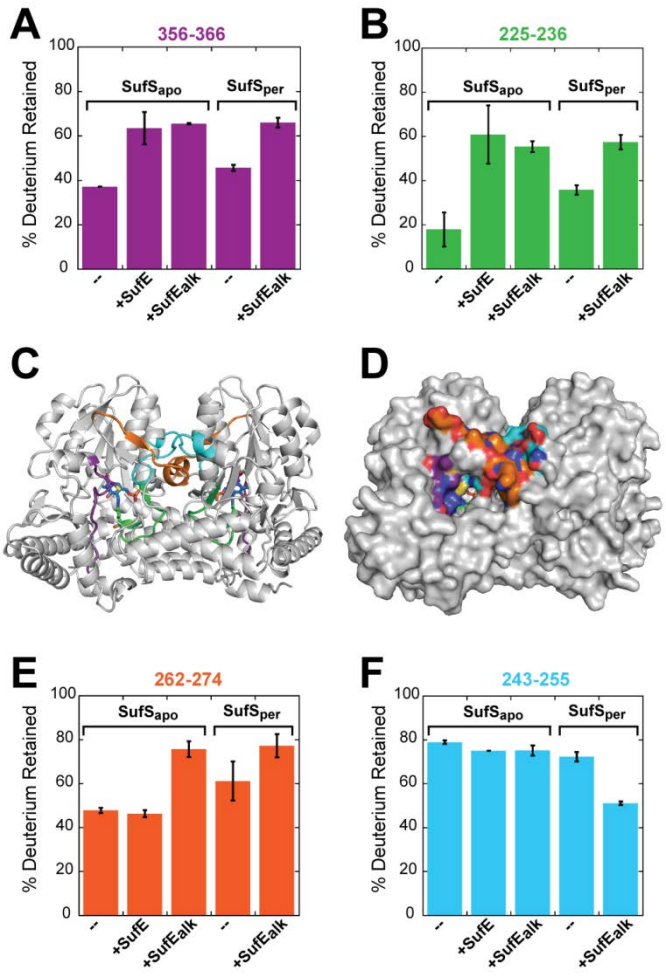

Figure 3.6 Deuterium retention by SufS in HDX trapping assays. The percentage of deuterium retained for SufS peptides was obtained for $SufS_{apo}$ with and without SufEapo or SufEalk and for $SufS_{per}$ with and without $SufE_{alk}$, as described in Experimental Procedures. Bar graphs of the results are shown for (A) peptide 356-366 (purple), (B) peptide 225-236 (green), (E) peptide 262-274 (orange), and (F) peptide 262-274 (cyan), which are highlighted on the (C) cartoon structure with Cys364 and PLP in stick format and on the (D) surface representation of SufS with nitrogen in blue and oxygen in red (PDB: 1JF9) The deuterium retention plots for all peptides are found in Figure 12 – 15. Error bars indicate standard deviation.

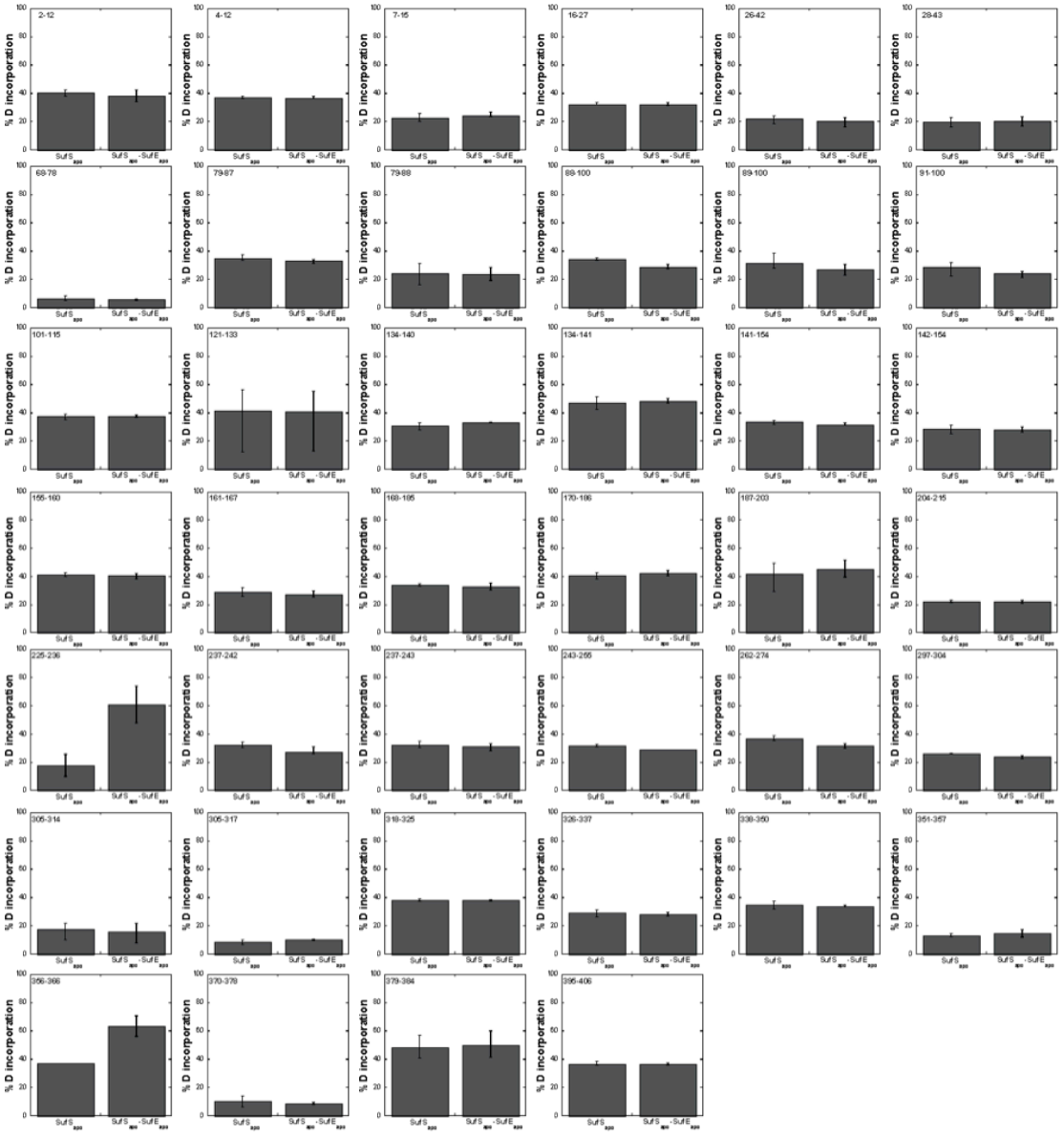

Figure 3.12 Deuterium trapping plots for $SufS_{apo}$ and the $SufS_{apo}$-$SufE_{apo}$ complex. The percentage of deuterium retained for SufS peptides was obtained for $SufS_{apo}$ with and without $SufE_{apo}$.

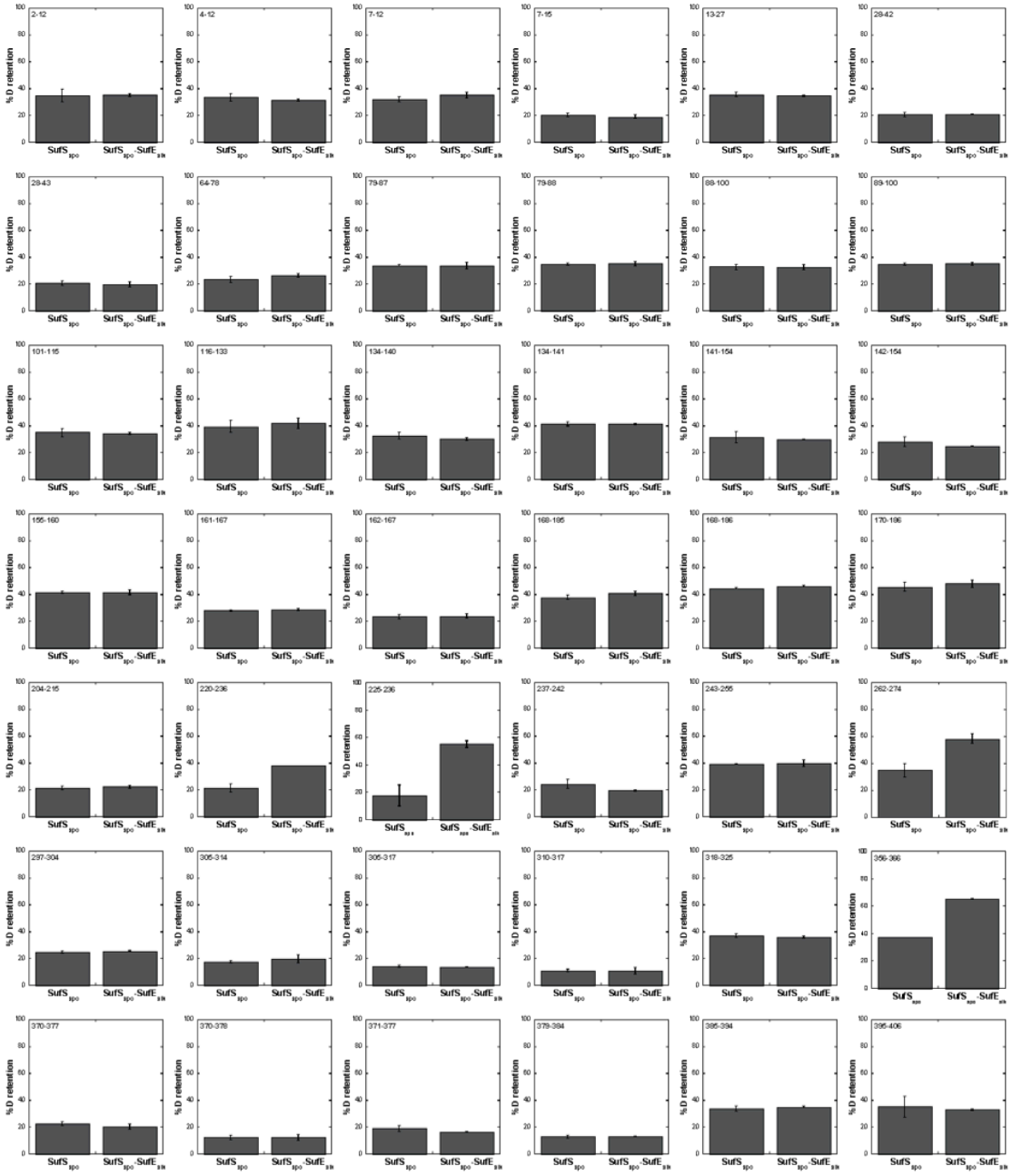

Figure 3.14 Deuterium trapping plots for $SufS_{apo}$ and the $SufS_{apo}$-$SufE_{alk}$ complex. The percentage of deuterium retained for SufS peptides was obtained for $SufS_{apo}$ with and without alkylated SufE ($SufE_{alk}$).

peptide suggests that $SufE_{apo}$ binding leads to significant allosteric changes in hydrogen bonding around the active site PLP or that SufE interacts with PLP, which is covalently bound to Lys226.

Two peptides from $SufE_{apo}$ (38-56 and 66-83) retain >10% amide deuteration in the $SufS_{apo}$-$SufE_{apo}$ complex compared to free $SufE_{apo}$ (Figure 3.7 A and B). Peptide 38-56 contains the sulfur acceptor Cys51 (Figure 3.7 C) [48]. Since these two regions form a surface around Cys51, the increased deuterium retention in the complex suggests direct interaction with $SufS_{apo}$ or a significant change in the conformation of $SufE_{apo}$ upon binding to $SufS_{apo}$. This is consistent with kinetic HDX-MS results (Figure 3. 5).

Deuterium Trapping with the SufS Persulfide Intermediate

The previous experiments determined that $SufE_{apo}$ affected $SufS_{apo}$ conformation and mapped the interacting regions of both proteins simultaneously in the absence of a Cys364 persulfide. It is known, however, that $SufE_{apo}$ binding to the persulfide intermediate form of SufS ($SufS_{per}$) stimulates SufS desulfurase activity by providing an acceptor for the persulfide species via direct sulfur transfer [23, 43, 70]. Thus, SufS could have a different conformational response to SufE that is dependent on the SufS catalytic intermediate state. To obtain a better understanding of whether the SufS-SufE interaction interface is modulated by the Cys364 persulfide, we performed deuterium trapping assays with $SufS_{per}$ in complex with SufE. In these experiments, sulfur transfer to $SufE_{apo}$ needs to be blocked to prevent turnover of the $SufS_{per}$ species. Therefore, $SufE_{apo}$ Cys51 was alkylated with iodoacetamide ($SufE_{alk}$) to specifically prohibit sulfur transfer from $SufS_{per}$ Cys364 to $SufE_{apo}$ Cys51. HDX–MS time course experiments reveal that carbamidomethylation of SufE yields increased solvent accessibility and dynamics

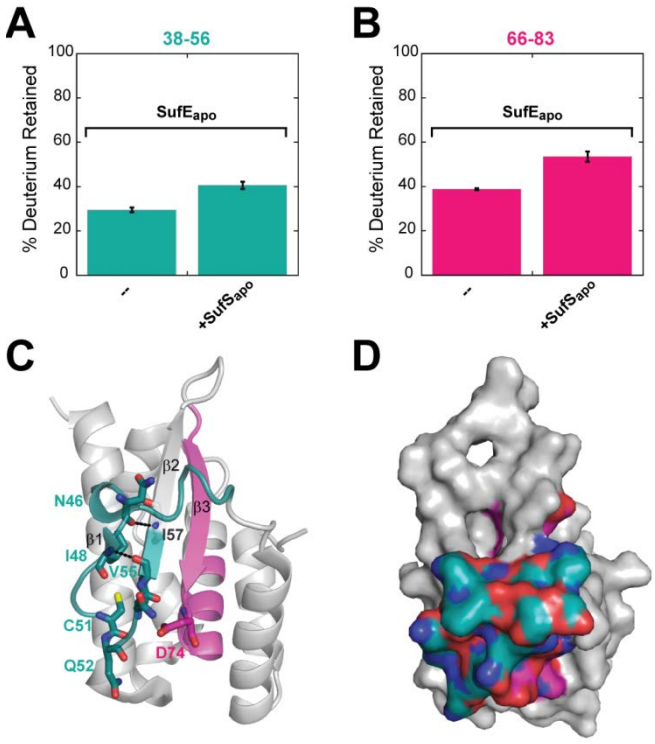

Figure 3.7 Deuterium retention by SufE in HDX trapping assays. The percentage of deuterium retained for SufE peptides was obtained for $SufE_{apo}$ with and without $SufS_{apo}$, as described in Experimental Procedures. Bar graphs of the results are shown for (A) peptide 38-56 (magenta) and (B) peptide 66-83 (teal), which are highlighted on the (C) cartoon structure with Cys51 and other surface amino acids in stick format and on the (D) surface representation of $SufE_{apo}$ with nitrogen in blue and oxygen in red (PDB: 1JF9) [21] The deuterium retention plots for all peptides are found in Figure 11 – 15. Error bars indicate standard deviation.

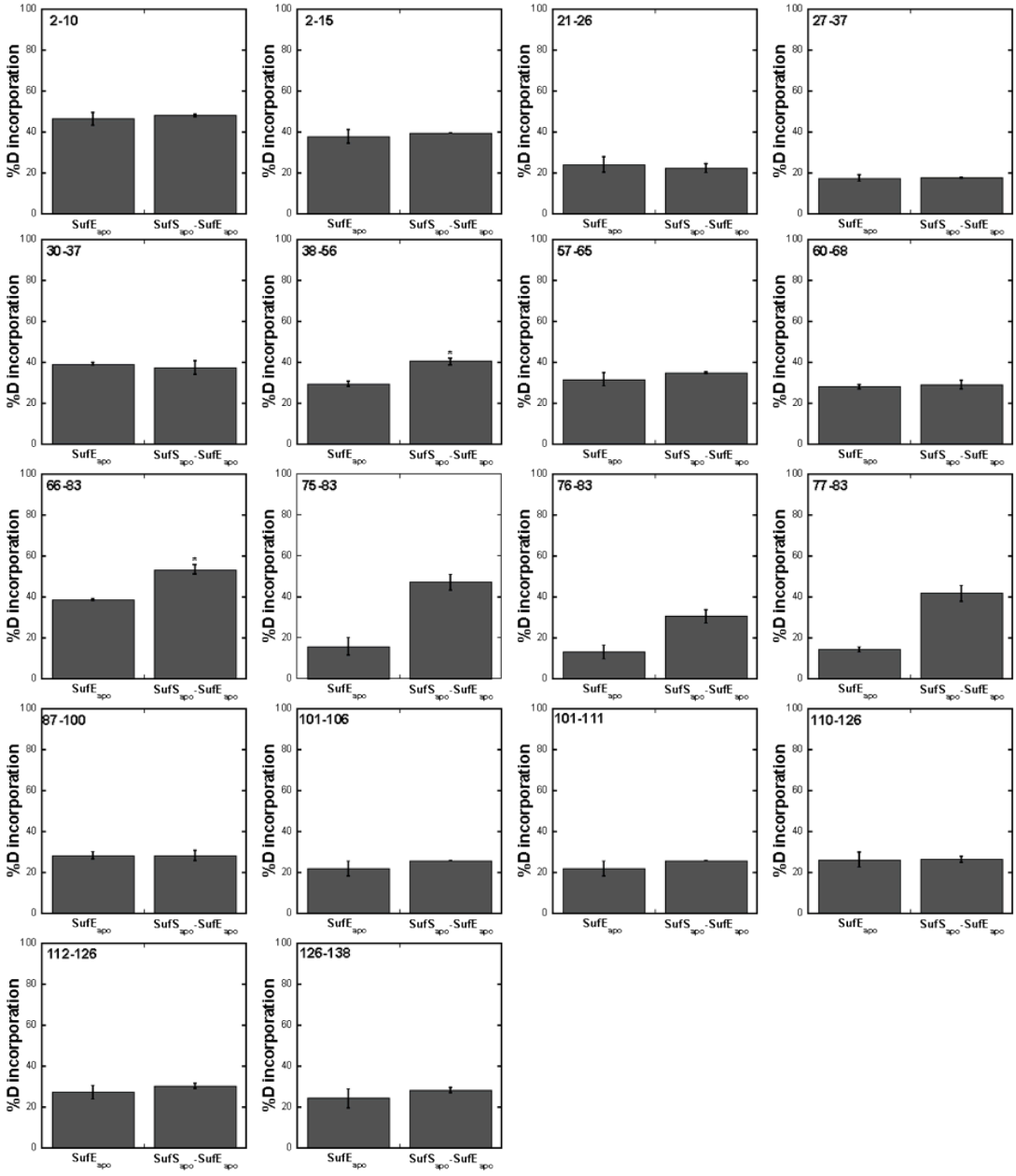

Figure 3.13 Deuterium trapping plots for $SufE_{apo}$ and the $SufS_{apo}$-$SufE_{apo}$ complex. The percentage of deuterium retained for SufE peptides was obtained for $SufE_{apo}$ with and without $SufS_{apo}$.

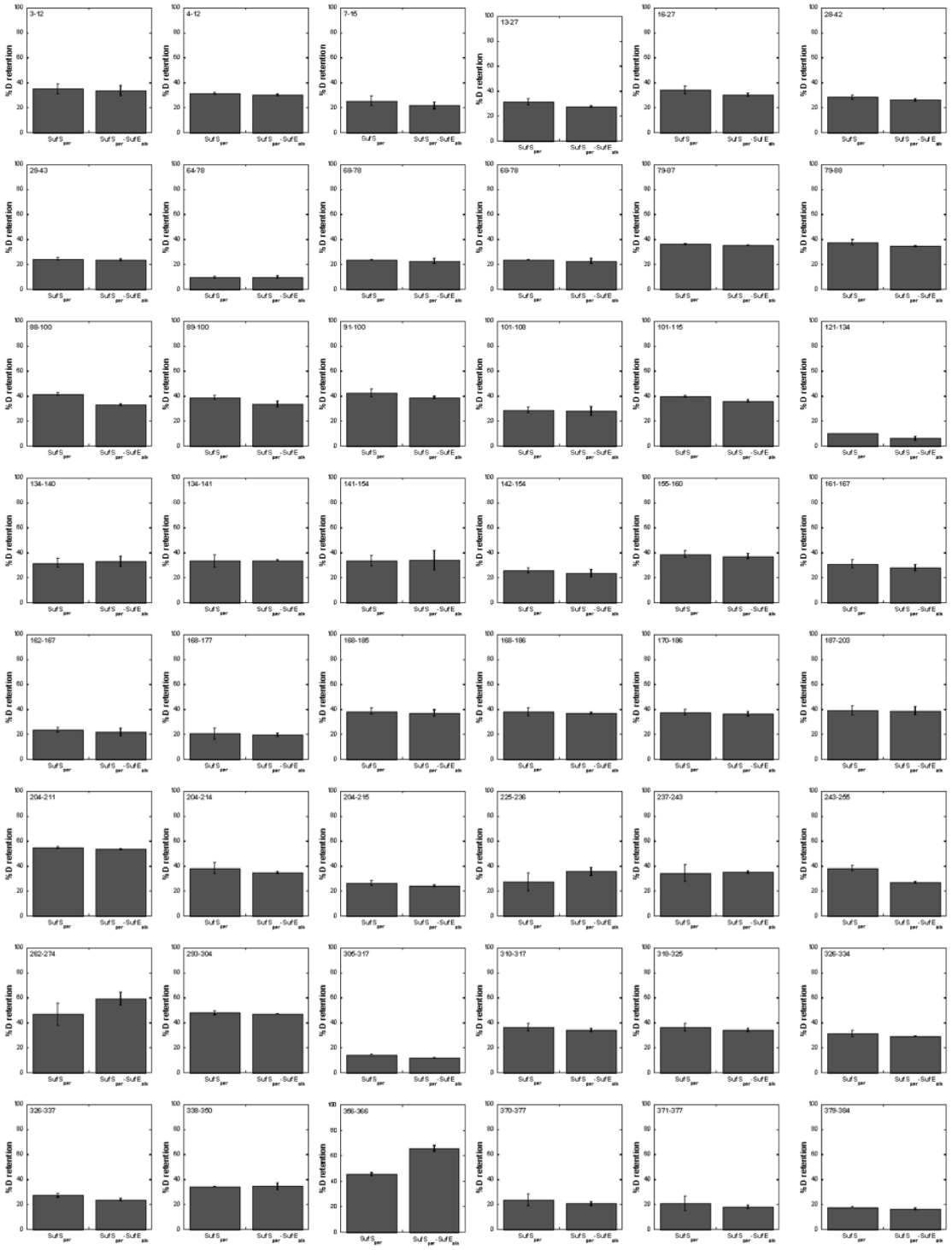

Figure 3.15 Deuterium trapping plots for $SufS_{per}$ and the $SufS_{per}$-$SufE_{alk}$ complex. The percentage of deuterium retained for SufS peptides was obtained for persulfurated SufS ($SufS_{alk}$) with and without alkylated SufE ($SufE_{alk}$).

around Cys51[4]. A loss of hydrogen bonding with increased backbone solvent accessibility suggests that alkylation of SufE triggers a conformational switch in the loop that could mimic the "sulfur accepting" state, possibly by forcing the Cys51 thiolate out of its groove and into an exposed conformation [85]. This interpretation is supported by previous studies showing that $SufE_{alk}$ is a potent inhibitor of SufS enhancement by $SufE_{apo}$ [69].

Before testing $SufE_{alk}$ binding to $SufS_{per}$, we first determined whether SufE alkylation affected the interaction with $SufS_{apo}$. Isothermal titration calorimetry (ITC) was used to compare the binding affinity of both $SufE_{apo}$ and $SufE_{alk}$ for $SufS_{apo}$. The ITC isotherm shows that $SufE_{apo}$ binding to $SufS_{apo}$ has a biphasic behavior with an initial exothermic phase at lower $SufE_{apo}$ concentrations and an endothermic phase at higher $SufE_{apo}$ concentrations (Figure 3.8 A, Table 3.2). The $SufE_{apo}$ binding data is best fit by a sequential two sites binding model with a higher affinity site ($K_{d1} \leq 3.59$ μM) and a lower affinity site ($K_{d2} \leq 312$ μM). Each $SufS_{apo}$ dimer has two active sites (one per monomer), but the ITC data suggests the two sites are not equivalent for $SufE_{apo}$ binding. Instead, the observed $SufE_{apo}$ binding behavior is consistent with a flip-flop mechanism of allosteric regulation where binding of $SufE_{apo}$ to one active site on the SufS dimer diminishes further $SufE_{apo}$ binding to the second active site. A similar mechanism has been proposed for SufS-SufU interactions in the *B. subtilis* Suf system [86]. This type of allosteric regulation may also explain the previously reported substrate inhibition behavior exhibited by SufE on SufS at low L-cysteine concentrations [69].

In stark contrast, $SufE_{alk}$ for $SufS_{apo}$ was primarily exothermic and the binding data was well fit using a one-site binding model (Figure 3.8 B, Table 3.2). The $SufE_{alk}$ K_d for

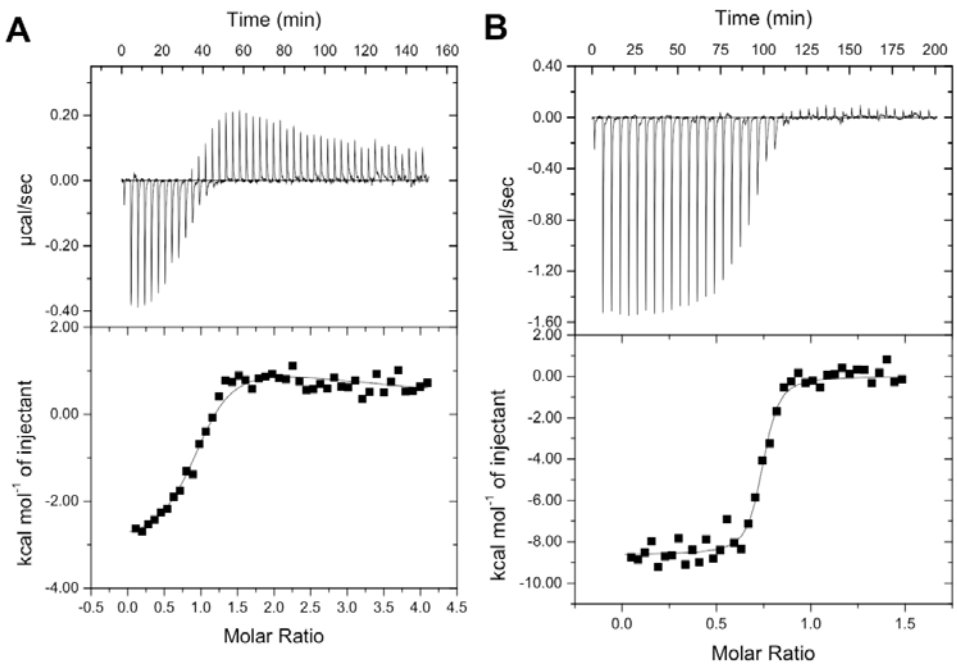

Figure 3.8 Analysis of the binding of $SufE_{apo}$ and $SufE_{alk}$ to $SufS_{apo}$ by isothermal titration calorimetry. $SufS_{apo}$ in the cell at 108 µM was titrated with a 10-fold molar excess of $SufE_{apo}$ or $SufE_{alk}$. (A) Titration of $SufE_{apo}$ into $SufS_{apo}$. The fitting of the data was derived from the integrated heats of binding plotted against the molar ratio of $SufE_{apo}$ added to $SufS_{apo}$ in the cell, after correction for the heat of dilution. The best–fit model was a two sequential binding sites model with dissociation constant of K_{d1} = 3.59 µM and K_{d2}= 312 µM. (B) Titration of $SufE_{alk}$ into $SufS_{apo}$. The best-fit model was a one binding site model with K_d 0.263 µM. The data fitted parameters are in Table 3.2.

Table 3.2 Fitting parameters from ITC analysis of binding between SufS and either $SufE_{apo}$ or $SufE_{alk}$.

SufS + $SufE_{apo}$				SufS + $SufE_{alk}$	
Two Sequential Binding Sites Model				One Site Model	
Chi^2/DOF		3.338E4		Chi^2/DOF	2.028E5
K_1	2.81E5 ± 2.5E4 M^{-1}	K_2	3.31E3 ± 5.8E2 M^{-1}	K	4.06E6 ± 1.03E6 M^{-1}
ΔH_1	-2893 ± 88.7 cal/mol	ΔH_2	1.030E4 ± 1.18E3 cal/mol	ΔH	-8519 ± 123.7 cal/mol
ΔS_1	15.3 cal/mol/deg	ΔS_2	50.4 cal/mol/deg	ΔS	1.86 cal/mol/deg
				N	0.730 ± 0.006 Sites

binding to $SufS_{apo}$ was ≤ 0.25 μM, indicating it binds $SufS_{apo}$ 10-fold more tightly than $SufE_{apo}$. The number of $SufE_{alk}$ binding sites on SufS calculated from ITC is only 0.73, suggesting that $SufE_{alk}$ binding may induce negative allosteric regulation of the second SufS monomer, albeit at a significantly lower level than that observed for $SufE_{apo}$. This result is consistent with $SufE_{alk}$ being locked into a conformation that mimics the "sulfur acceptor" state of $SufE_{apo}$, which would likely bind more tightly to SufS.

HDX trapping assays indicate that, like the $SufS_{apo}$-$SufE_{apo}$ complex, peptides 356-366 and 225-236 have increased deuterium retention in the $SufS_{apo}$-$SufE_{alk}$ complex (Figure 3.6 A and B). An additional area of protection within residues 262-274 is also observed (Figure 3.6 E). In the $SufS_{apo}$ dimer, residues 262-274 from one SufS monomer chain form a surface above and covering the active site channel of the second SufS monomer, which we refer to as the active site "lid" (Figure 3.6 C and D) [18, 21]. Increased retention of deuterium in the active site lid indicates that additional interactions are detectable at the $SufS_{apo}$-SufE interface when Cys51 of SufE is alkylated. This may contribute to the higher affinity observed for $SufS_{apo}$, as well as the ability to partially override the negative cooperativity observed for $SufE_{apo}$ binding to $SufS_{apo}$ (Figure 3.8).

Once $SufE_{alk}$ contributions to HDX deuterium trapping were determined for $SufS_{apo}$, assays with the $SufS_{per}$-$SufE_{alk}$ "stalled" sulfur transfer complex were performed. Like $SufS_{apo}$-$SufE_{apo}$ and $SufS_{apo}$-$SufE_{alk}$, protection of deuterated amides is observed for SufS peptides 356-366, 225-236, and 262-274 in the $SufS_{per}$-$SufE_{alk}$ complex (Figure 3.6 A, B, and E). Thus, these regions of SufS are protected by SufE regardless of the presence of the SufS Cys364 persulfide (and regardless of SufC Cys51 modification). Surprisingly, peptide 243-255 shows a *loss* of deuterated amide protection in the $SufS_{per}$-$SufE_{alk}$

complex (Figure 3.6 F). These residues are part of a long loop at the $SufS_{per}$ dimer interface with several interactions between the two SufS monomers (Figure 3.6 C and D) [18, 21]. HDX trapping suggests that $SufE_{alk}$ binding to $SufS_{per}$ increases the solvent accessibility at the dimer interface, leading to more back-exchange with water. Therefore, residues within the dimer interface respond to both persulfuration of SufS Cys364 and the orientation of SufE Cys51, which may coordinate active site cooperativity in the SufS dimer.

$SufE_{alk}$ alters L-cysteine binding to SufS

Since SufE binding to $SufS_{apo}$ leads to conformational changes within the SufS peptide containing the PLP ligand Lys226, it was important to test if SufE binding alters the reactivity of PLP for L-cysteine substrate (Figure 1.6). If so, this could provide additional functional insight into how SufE activates SufS. This assay required $SufE_{alk}$ to prevent sulfur transfer from SufS to SufE (*i.e.*, SufS turnover) and to allow us to exclusively examine the first step of the reaction, L-cysteine binding to SufS PLP in the presence of SufE. When L-cysteine binds to PLP it displaces the internal aldimine with Lys226 and forms an external aldimine at the same position (Figure 1.6) [18]. The initial binding of L-cysteine substrate to resting $SufS_{apo}$ was compared to the $SufS_{apo}$-$SufE_{alk}$ complex by following the formation of the external aldimine with L-cysteine, which absorbs at 340 nm, and the disappearance of the internal aldimine, which absorbs at 420 nm (Figure 3.9 A and C). Fitting of the ΔA_{420} measurements to a one site binding model shows that the K_d of SufS for L-cysteine decreases 3-fold from 61 ±1.5 μM for SufS alone to 18 ±1.6 μM for SufS with one equivalent of $SufE_{alk}$ (Figure 3.9 B and D). We should note that these values are not true dissociation constants since this assay does not

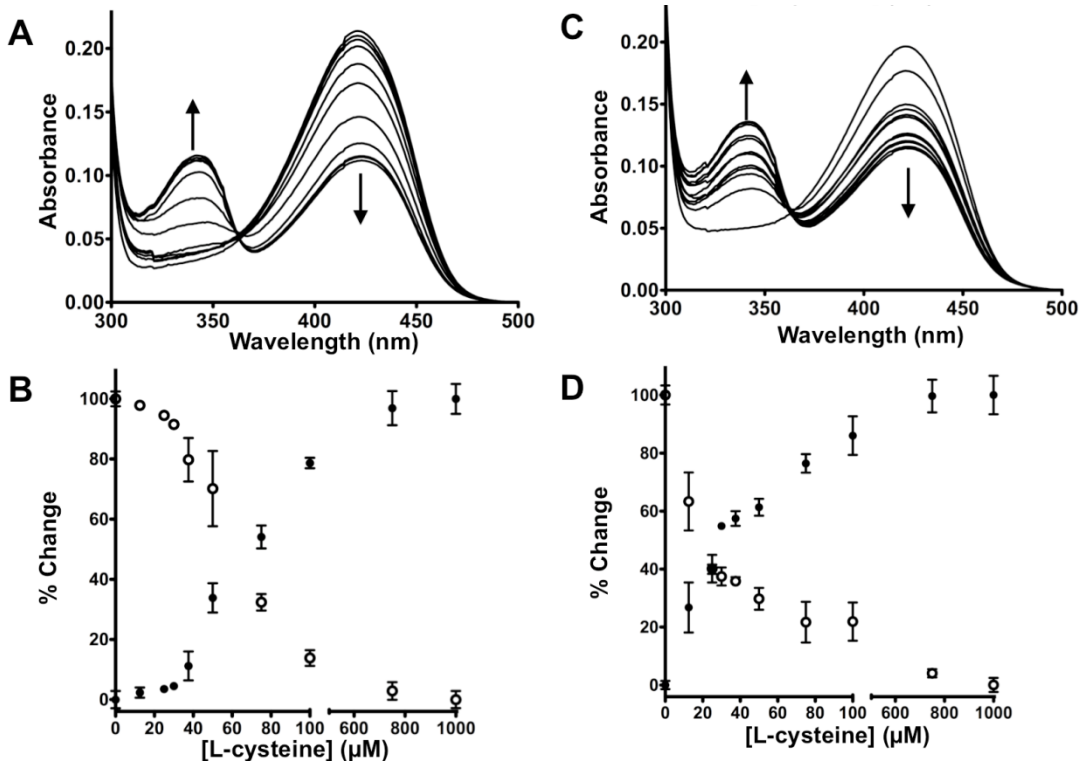

Figure 3.9 Spectroscopic and kinetic analysis of L-cysteine binding to $SufS_{apo}$. (*A*) UV-Visible absorption spectra of 25 μM $SufS_{apo}$ immediately after addition of 0 – 1 mM (0, 12.5, 25, 30, 37.5, 50, 75, 100, 250, 500, 750, 1000 μM) L-cysteine. (*B*) Percent change of ΔA_{420} (open circles) and ΔA_{340} (closed circles) after adding increasing concentrations of L-cysteine. (*C*) UV-Visible absorption spectra of 25 μM $SufS_{apo}$ with 25 μM $SufE_{alk}$ immediately after addition of 0 – 1 mM (0, 12.5, 25, 30, 37.5, 50, 75, 100, 250, 500, 750, 1000 μM) L-cysteine. (*D*) Percent change of ΔA_{420} (open circles) and ΔA_{340} (closed circles) after adding increasing concentrations of L-cysteine.

distinguish between L-cysteine binding and the rate of external aldimine formation once L-cysteine is bound. Either step or both steps might be promoted by $SufE_{alk}$ in this equilibrium assay. Regardless, the results indicate that the binding of SufE may actively remodel the $SufS_{apo}$ active site, leading to changes in deuterium incorporation by the peptides present around the active site cavity, in order to promote catalysis at the PLP site.

DISCUSSION

Conformational dynamics may be essential for the catalytic activity of many enzymes [74]. It is important to define structural and conformational changes in the vicinity of the active/binding site, but also in the surrounding regions that may have allosteric responses. This holistic view provides insight into how structural dynamics are related to catalytic and allosteric mechanisms. Many enzymes interact with other proteins as part of their function so localization of the interaction interface is of primary importance. However, if binding leads to allosteric effects, the conformational changes resulting from the interaction are also relevant. This point is illustrated by the results presented here on the interaction between the SufS cysteine desulfurase and its co-substrate SufE as part of the Suf Fe-S cluster biosynthesis system in *E. coli*. The enzyme-bound PLP cofactor in the active site of SufS forms an external aldimine with substrate L-cysteine to catalyze abstraction of sulfur by SufS Cys364, followed by sulfur transfer to Cys51 of $SufE_{apo}$ [45]. However, the structure of the *E. coli* $SufS_{apo}$-$SufE_{apo}$ complex and potential conformational changes that result from their interaction are not defined. SufE binding increases the SufS desulfurase activity, at least in part, by acting as a co-substrate for the ping-pong reaction pathway that depends on SufE Cys51 [23, 70]. In this study we used

HDX-MS, HDX deuterium trapping, and biochemical assays to better define the role protein dynamics plays in possible SufE allosteric activation of SufS catalytic activity.

Characterization of the $SufS_{apo}$-$SufE_{apo}$ Interaction

HDX-MS and deuterium trapping experiments indicated that $SufE_{apo}$ residues within 38-56 and/or 66-83 interact with $SufS_{apo}$ and undergo a conformational change upon complex formation (Figure 3. 5). $SufE_{apo}$ peptide 38-56 contains the sulfur acceptor Cys51 as part of the loop connecting the β_1 and β_2 strands (Figure 3.7 C) [48]. In the static structure of SufE, the thiolate side chain of Cys51 is in a solvent-inaccessible, hydrophobic pocket partially formed from residues within 66-83 (Figure 3.7 D). A conformational change in both regions could expose the Cys51 thiolate for sulfur transfer upon docking with SufS [48]. Our $SufE_{apo}$ HDX data show that the Cys51 loop is moderately solvent accessible and that binding to $SufS_{apo}$ decreased its backbone dynamics. A recent crystallographic structure of a complex between two *E. coli* proteins related to SufS and SufE, CsdA and CsdE, is consistent with the conformational change and dynamic stabilization we observed for the Cys51 loop [85]. In the $CsdA_{apo}$-$CsdE_{apo}$ co-structure, the CsdE Cys61 loop region underwent an ~11 Å shift upon interaction with CsdA. Based on the $CsdA_{apo}$-$CsdE_{apo}$ co-structure [85], HDX trapping assays, and sequence alignments, there are many $SufE_{apo}$ surface residues that could form stabilizing side chain and backbone hydrogen bonds that constrain dynamics within residues 38-56 and 66-83 including Gln52, Gln54 and Asp74.

Despite the change in $CsdE_{apo}$ conformation, there were no noticeable structural changes to the $CsdA_{apo}$ cysteine desulfurase backbone in the $CsdA_{apo}$-$CsdE_{apo}$ complex [85].

This is in contrast to our HDX-MS studies with $SufS_{apo}$ that showed altered deuterium uptake for two active site peptides, residues 225-236 and 356-366, in the presence of $SufE_{apo}$ (Figure 3.4 A and B). HDX trapping experiments further confirmed that deuterated amides within these regions are highly solvent protected in the presence of $SufE_{apo}$ and $SufE_{alk}$ (Figure 3.6 A and B). The location of peptide 356-566 near the surface suggests that some residues may be directly involved in the interaction with SufE [72]. The $CsdA_{apo}$ structure in complex with $CsdE_{apo}$ is partially consistent with our HDX experiments and showed that CsdA residues Gln356 (SufS His362) and Gln360 (SufS Met366) directly interact with CsdE [85]. It is possible that some of the interactions within this region provide specificity for SufS/SufE to limit cross-reactivity with CsdA/CsdE [87].

Based on the $CsdA_{apo}$-$CsdE_{apo}$ co-structure, it was proposed that residues within 343-354 ($helix_{16}$), 355-378 (the "Cys364" loop), and 393-406 ($helix_{18}$) of $SufS_{apo}$ form hydrogen bonds and van der Waals interactions with $SufE_{apo}$ [85]. Our HDX trapping data agree that SufS residues within 356-366 (the Cys364 loop) are involved in the interaction with SufE (Figure 3.6 A). If residues from $SufS_{apo}$ helices 16 and 18 contribute to the $SufS_{apo}$-$SufE_{apo}$ interface, they are not reflected in backbone amide solvent accessibility upon binding (Figure 3.3). Given the variety of binding modes between cysteine desulfurases and sulfur acceptors such as CsdA-CsdE, IscS-IscU, and IscS-TusA systems, it is not unreasonable that the $SufS_{apo}$ and $SufE_{apo}$ interaction may not be completely analogous to that of the CsdA-CsdE complex [85, 88]. We propose that $SufE_{apo}$ binding at or near His362 and Met366 on the surface of $SufS_{apo}$ leads to subtle changes in hydrogen bonding or solvent accessibility of backbone amides as manifested by the limited HDX $SufE_{apo}$ "footprint" observed.

Mechanistic Insight into SufE Activation of SufS

In addition to interaction mapping, specific changes in solvent accessibility and backbone dynamics of $SufS_{apo}$ were discerned with HDX-MS kinetic experiments that were not apparent from the $CsdA_{apo}$-$CsdE_{apo}$ co-structure [85]. We demonstrated for the first time that $SufS_{apo}$ active site architecture and dynamics were linked to $SufE_{apo}$ binding, providing insight into the mechanism of activation. It is clear that the interaction with $SufE_{apo}$ does not cause large conformational changes in $SufS_{apo}$ (Figure 3.3 A). Instead, highly localized dynamic perturbations involving backbone amides within residues 225-236 (the PLP binding site) and 356-366 (the active site Cys364 loop) were observed (Figure 3.4 A and B).

Because residues 225-236 are buried in the active site cavity, the stabilizing changes in conformation observed around PLP upon $SufE_{apo}$ binding may be transmitted via the 356-366 active site loop, which we propose is involved in the $SufE_{apo}$ interaction based on HDX trapping experiments and the $CsdA_{apo}$-$CsdE_{apo}$ co-structure [85]. The strong protection of deuterated amides (Figure 3.6 B) and the decrease in backbone dynamics (Figure 3.4 B) within 225-236 suggested that $SufE_{apo}$ alters the PLP environment, which is also supported by the enhanced formation of the PLP-L-cysteine external aldimine in the presence of $SufE_{alk}$ (Figure 3.9). The PLP binding site is highly conserved for both type I and II cysteine desulfurases [17]. It is possible that $SufE_{apo}$ binding shifts the SufS equilibrium towards a conformation optimal for substrate L-cysteine binding or external aldimine formation. The results suggest that $SufE_{apo}$ subtly remodels $SufS_{apo}$ architecture in the vicinity of the internal aldimine (Lys226-PLP) to promote catalysis and may not activate SufS solely through a passive persulfide-acceptor role.

Since SufE stimulates SufS cysteine desulfurase activity during the ping-pong reaction, we also considered that the binding interactions could be modulated by the presence of the SufS Cys364 persulfide (where SufS is primed for sulfur transfer to $SufE_{apo}$) or by the conformation/orientation of SufE Cys51 thiolate. In the SufS persulfide intermediate ($SufS_{per}$) structure, the Cys364 persulfide moiety is facing the entrance to the active site cavity, presumably to orient it towards Cys51 of SufE [21]. It has been postulated that the Cys51 thiolate must reach into the active site channel to carry out a nucleophilic attack on the Cys364 persulfide for sulfur transfer [66]. It is also known that in the absence of a further sulfur acceptor (*e.g.*, SufB or a thiol reductant), Cys51 of SufE can accept multiple sulfur groups thereby forming a polymeric sulfur species [44, 70]. This indicates that both apo and persulfurated/polysulfurated SufE can bind to SufS, presumably with protrusion of the Cys51 side chain into the active site cavity, as was observed in the co-structure of CsdA-CsdE in which the CsdE Cys61 thiolate is exposed and oriented towards Cys359 of CsdA [85]. It is unclear whether SufS stabilizes this particular "sulfur accepting" conformation of SufE or vice versa.

We simulated the "sulfur accepting" SufE conformation by alkylating Cys51 ($SufE_{alk}$). HDX-MS indicated that alkylation led to increased solvent exposure in the SufE Cys51 loop peptide compared to native $SufE_{apo}$, consistent with loss of stabilizing internal hydrogen bonds and potential exposure of Cys51 from its secluded pocket[4]. We demonstrated through deuterium trapping assays that alkylation of SufE led to additional amide deuterium retention within SufS residues 262-274 for both $SufS_{apo}$ and $SufS_{per}$ (Figure 3.6 E). The additional interactions were not dependent on the state of SufS, but entirely mediated by the presumed change in SufE conformation when Cys51 is

modified. Residues 262-272 are part of a surface β-hairpin loop that forms a lid over the SufS active site (Figure 3.6 C and D). This β-hairpin structure is not found in type I PLP-dependent cysteine desulfurases and is proposed to have a specialized functional role in SufS enzymes [18]. Unlike what we observed for $SufS_{apo}$-$SufE_{alk}$, the lid region from the related type II cysteine desulfurase enzyme CsdA does not interact with CsdE or exhibit a significant conformational change in the CsdA-CsdE complex [85]. Consistent with the additional interactions observed by HDX trapping, $SufE_{alk}$ bound $SufS_{apo}$ with a higher affinity than $SufE_{apo}$ (Figure 3.8) and $SufE_{alk}$ stimulates the formation of the SufS-L-cysteine external aldimine (Figure 3.9). Thus, the shift in SufE equilibrium towards the sulfur accepting conformation of Cys51 may enhance the interaction with SufS and impact the SufS active site architecture, possibly altering PLP cofactor reactivity via changes in residues 225-236 (Figure 3.4).

Further analysis of the $SufS_{per}$-$SufE_{alk}$ complex revealed that SufE binding to the Cys364 persulfide intermediate of SufS led to increased solvent accessibility at the SufS dimer interface. Deuterium trapping assays indicate that ~75-80% of the deuterium incorporated into the backbone of peptide 243-255 is resistant to back exchange with hydrogen under our experimental conditions in the apo or persulfide forms of SufS, the $SufS_{apo}$-$SufE_{apo}$ complex, and the $SufS_{apo}$-$SufE_{alk}$ complexes (Figure 3.6 F). It is only in the $SufS_{per}$-$SufE_{alk}$ complex (*i.e.*, the stalled sulfur transfer complex) that some of these stable hydrogen bonds between the SufS monomers are broken, leading to more back-exchange with water. The changes at the SufS dimer interface suggest that formation of the stalled sulfur transfer complex with $SufE_{alk}$ may partially uncouple the $SufS_{per}$ monomers. This uncoupling, which could decrease the flip-flop regulation of

SufS, is consistent with the different binding data obtained for $SufE_{alk}$ compared to $SufE_{apo}$ (Figure 3.8 and Table 3.2).

Residues 243-255 comprise a loop connecting the entrance of the active site cavity to the dimer interface (Figure 3.6 C and D). In the SufS persulfide intermediate crystal structure, the Cys364 persulfide is oriented towards the entrance of the active site channel and is stabilized through formation of a hydrogen bond with the amide of Ser254, which is contained within peptide 243-255 [21]. However, no significant changes in deuterium retention levels were noted in deuterium trapping assays with individual $SufS_{apo}$ and $SufS_{per}$ enzymes (Figure 3.6 F). The levels of deuterium retention in this region for $SufS_{apo}$ in complexes with $SufE_{apo}$ and $SufE_{alk}$ were also similar to the $SufS_{apo}$ protein alone, indicating that SufE or $SufE_{alk}$ has little effect on hydrogen bonding at the dimer interface of $SufS_{apo}$. However, if SufS Cys364 is in the persulfide state, binding of $SufE_{alk}$ leads to a destabilization of hydrogen bonding within residues 243-255 at the dimer interface (resulting in the observed alterations in amide exchange). Functionally, this might suggest that in the absence of SufE, the SufS Cys364 persulfide is stabilized by residues within 243-255 (especially the amide hydrogen bond to Ser254). If the SufE sulfur acceptor is bound to SufS, the persulfide stabilization is diminished to facilitate nucleophilic attack by SufE Cys51 on the SufS Cys364 persulfide for direct sulfur transfer. The SufE-mediated changes in the 243-255 loop could also provide an allosteric mechanism for one SufS monomer to alter the reactivity of the other SufS monomer via a flip-flop mechanism. Unfortunately, we were unable to directly assay $SufE_{apo}$ binding to $SufS_{per}$ since this would lead to SufS turnover on the timescales of HDX and greatly complicate data analysis and interpretation.

Conclusions

The results presented here provide a clearer picture of the dynamic interactions between SufS and SufE during sulfur liberation and transfer for Fe-S cluster biogenesis by the Suf system in *E. coli*. The observed changes around the SufS PLP cofactor binding site suggest that SufE actively promotes external aldimine formation between L-cysteine and PLP. This SufE-dependent effect may also provide a mechanistic explanation for the observation that the SufS-SufE complex has a higher level of activity at lower L-cysteine levels than other Type I cysteine desulfurases like IscS [69]. An active role for SufE in stimulating the first step of the ping-pong reaction also is consistent with the fact that $SufE_{apo}$ binds well to $SufS_{apo}$, which would be unlikely if SufE were purely a passive co-substrate for the second step of the reaction. Finally, the results suggest that the sulfur accepting conformation of SufE (mimicked by $SufE_{alk}$) is able to trigger additional changes in $SufS_{per}$ that help facilitate sulfur transfer and/or provide allosteric regulation of the other SufS monomer. Further detailed mechanistic and structural studies are underway to fully test these intriguing hypotheses.

Chapter 4

Escherichia coli SufE(D74R) is a better Substrate of SufS Cysteine Desulfurase than Wild Type SufE

ABSTRACT

The SufE(D74R) (Asp74 to Arg) mutant was designed based on the putative interaction model for CsdA and CsdE [89] which indicated that Asp74 on SufE might be involved in salt bridge formation during the interaction between SufS and SufE. However, our results indicated that the mutant protein actually has stronger binding affinity for SufS than wild-type SufE. In addition, SufE(D74R) can still enhance SufS desulfurase activity and did not show saturation at higher SufE(D74R) concentrations like SufE. Our current hypothesis is that the SufE(D74R) mutant enhances the persulfide removal from SufS due to tighter protein – protein interactions coupled with a lower pK_a of its active site Cys51. This novel mutant demonstrates that SufE Asp74 is important for the SufS – SufE interaction but is not simply involved ionic interactions. The full structural and biochemical mechanism to explain how this mutation enhances the interaction with SufS requires further study.

INTRODUCTION

A complex series of protein – protein interactions is required for the Fe-S cluster assembly machinery to function properly. The *Escherichia coli* cysteine desulfurase SufS and its accessory protein SufE work together to mobilize persulfide from L-cysteine, which is then donated to the SufB Fe-S scaffold [69]. SufE functions as one substrate for SufS and is required for full activity of SufS. Previously, it has been shown that *E. coli* SufS interacts with SufE even in the absence of L-cysteine substrate when SufS is not active.

SufS is a pyridoxal 5'-phosphate (PLP)-dependent dimeric enzyme and belongs to the group II desulfurase enzyme family, which share similar structures and have low basal activity [18]. SufS has two remarkable features that distinguish it from group I desulfurases like IscS or NifS [22]. First, there are more extensive interactions between the two monomers of dimeric SufS. The most prominent example of the unusual SufS dimer interactions is the interaction between the lobe containing α-helix 17 from one SufS monomer and the β-hairpin loop connecting strands h and i in the other SufS monomer [22]. The lobe with α-helix 17 lies between β-strands E and F, extending from the small domain to the large domain in the same subunit. α-Helix 17 on the lobe in one subunit of the dimer interacts with the tip of the β-hairpin loop from the other subunit through hydrophobic interactions. The β-hairpin loop in SufS is not found in IscS or NifS, indicating the interaction between the lobe and the β -hairpin loop observed in SufS is not conserved in the other group I PLP-dependent enzymes (Figure 4.1).

The other key difference between SufS and the group I desulfurases is that the extended lobe of SufS containing the active site loop has an 11-residue deletion

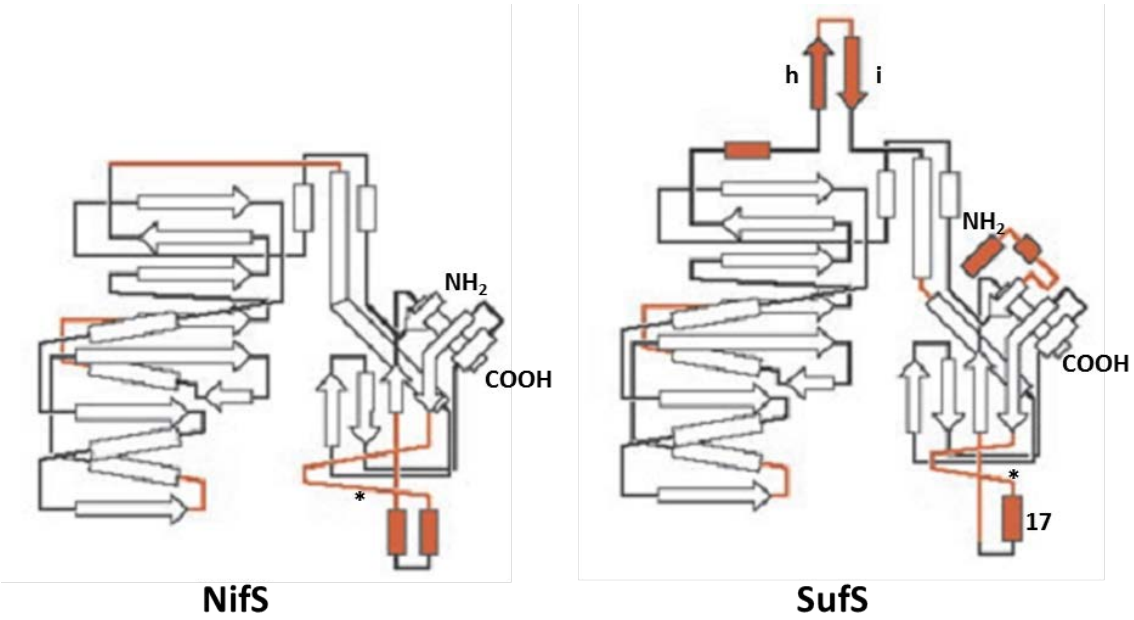

Figure 4.1 Comparison of NifS and SufS. Topology diagrams of NifS and SufS are shown in red. 17 represents α–Helix 17 h and i represent β–strands h and i respectively. * represents the location of the active site cysteine. COOH represents the C-terminal. NH_2 represents N-terminal of the protein [22].

compared with that of IscS. This shortening of this region in SufS structurally restricts the flexibility of the SufS Cys364-anchoring extended lobe (Figure 1.7). The decreased flexibility results in a more ordered structure such that the active site cysteine Cys364 in SufS is clearly visible on a loop of the extended lobe (Thr362 – Arg375). In contrast the corresponding loop (Ala327 – Leu333) of IscS is longer and disordered in most structures of IscS due to its flexibility.

Besides the structure difference between the group I and group II desulfurases, group II desulfurases appear to require a specific sulfur shuttle protein for full activity. For SufS, it is SufE. SufE is predominantly monomeric in solution and its structure shows that active site Cys51 occurs at the tip of a loop where its side-chain is buried from solvent exposure in a hydrophobic cavity (Figure 4.2).

The crystal structure of IscS – IscU and the interaction between them has been intensively studied; however the structure of the SufS – SufE complex and the structural details of how SufS SufE interact is not clear. Potential modes of interaction can be inferred from the recent co-structures of two homologous proteins CsdA (YgdJ) and CsdE (YgdK)[89]. CsdE shares 35% sequence identity with SufE and CsdA shares 45% sequence identity with SufS. The overall structure of SufE and CsdE monomers are very similar and conserved surface patches were identified in the CsdE/SufE protein family [90] (Figure 4.3). Some key charged amino acid residues were proposed to form salt bridges between CsdE and CsdA, including Glu84 in CsdE with Arg353 in CsdA and Arg129 in CsdE with Glu270 in CsdA (Figure 4.4) [89]. Salt bridge formation was proposed to bring active site Cys61 in CsdE and Cys358 in CsdA to close position for sulfur transfer. We were particularly interested in the proposed interaction between Glu84 in CsdE and

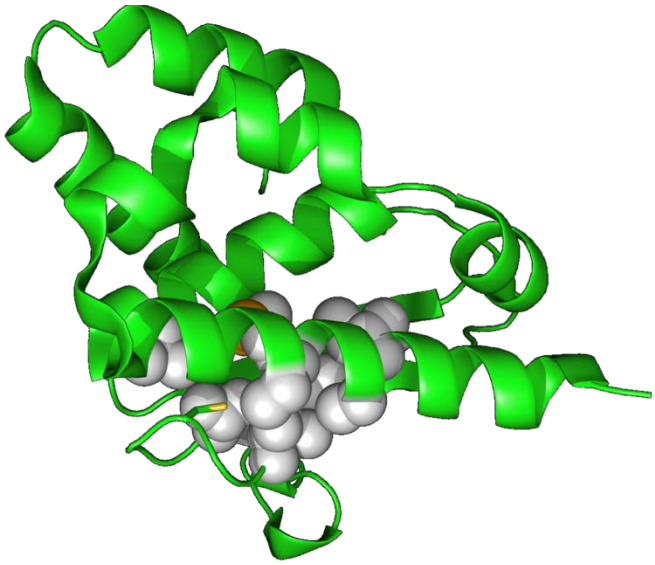

Figure 4.2 Crystal structure of SufE. Hydrophobic amino acid residues (grey spheres) surrounding SufE Cys51 (yellow stick). This picture was made by MacPymol software.

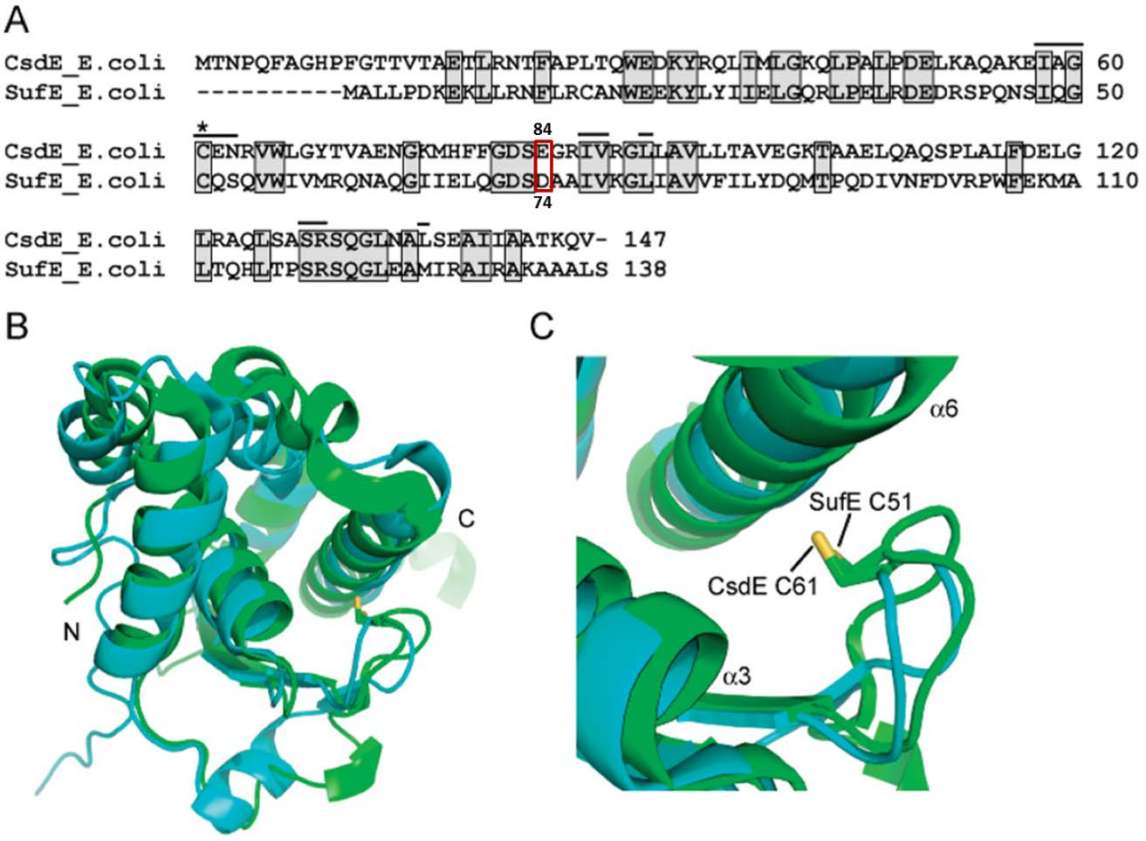

Figure 4.3 CsdE and SufE display significant sequence and structural homology. (A) Primary sequence alignment of *E. coli* CsdE and SufE made using ClustalW2. Identical residues are shaded. The bars indicate the residues that line the cavity containing the conserved persulfide-forming Cys61 (CsdE) and Cys51 (SufE) (denoted with a star). (B) Structural alignment of *E. coli* CsdE and SufE. The ribbon diagram shows CsdE in cyan and SufE in green, with the side-chains of the conserved persulfide-forming Cys61 (CsdE) and Cys51(SufE) presented in stick representation with carbon and sulfur atoms colored green and yellow, respectively. The CsdE solution structure (PDB 1NI7) 36 and the SufE crystal structure (PDB 1MZG) 37 were aligned with Mac PyMOL. The structures superimpose with a root mean-square deviation of 2.0 Angstroms for 132 backbone carbon (Cα) atoms. (C) Active site containing the conserved persulfide forming Cys61 (CsdE) and Cys51 (SufE) is formed by a loop and α-helices 3 and 6 [90].

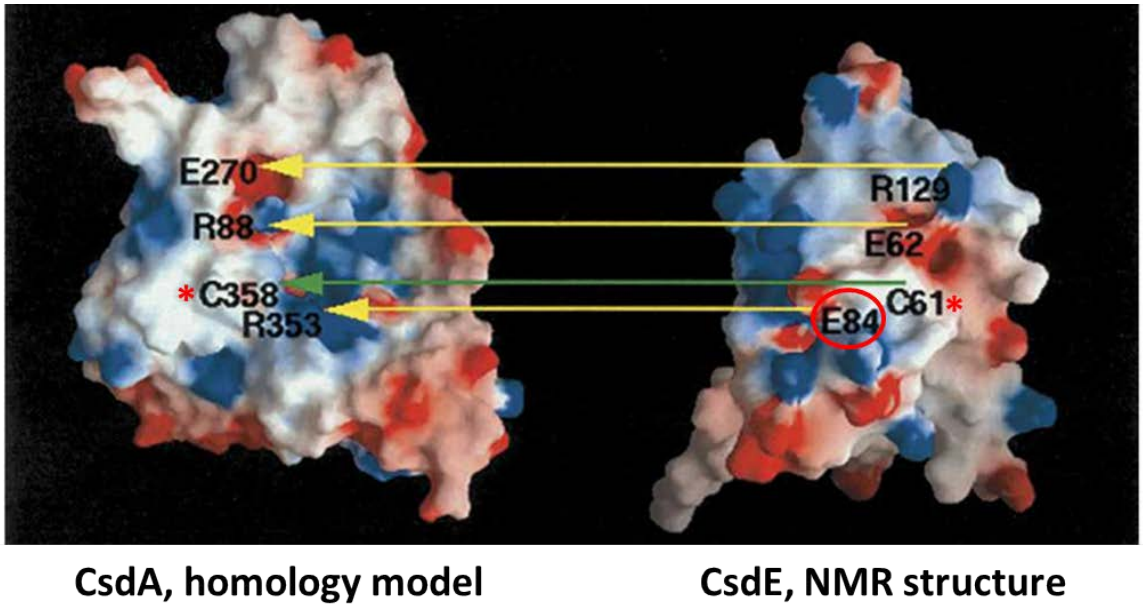

Figure 4.4 Proposed model of the interaction between CsdA and YgdK. A homology model of CsdA (shown on the left) was derived from the X-ray crystal structure of SufS (PDB ID: 1I29), with which it shares 45% sequence identity. The NMR structure of YgdK is shown on the right. The figure displays surface electrostatic potential images calculated with the program GRASP, where red and blue surfaces denote negative and positive electrostatic potentials, respectively. The surfaces of CdsA and CsdE predicted to interact are facing the viewer. The active cysteine was labeled with red *. Based on the complementarity of conserved residues, in particular the active-site cysteines, as well as the electrostatic surface potentials, it is predicted that the YgdK/CsdA complex would be obtained by rotating the CsdE structure by ~180˚ about a vertical axis and laying it on top of the CsdA model [89].

Arg353 in CsdA due to their spatial vicinity to the active site cysteine. The corresponding residues in the Suf proteins are Asp74 in SufE and Arg359 in SufS. Both amino acids are conserved between CsdE and SufE, and CsdA and SufS. To determine if these sites are important for SufS – SufE interaction, we mutated SufE Asp74 to Arg (D74R). If the salt bridge does mediate SufS – SufE interactions, reversing the charge of this amino acid should repel SufS and prevent or diminish their interaction. To our surprise we found that the SufE D74R mutation actually increased SufE enhancement of SufS activity. We hypothesize that these changes are due to structural changes in the SufE protein that flip the loop containing active site Cys51 into a "sulfur-accepting" conformation that increases the ability of SufE to mobilize SufS persulfide.

MATERIALS AND METHODS

Strains, Plasmids, and Growth Conditions

For mutagenesis of *sufE*, pET21a_sufE was used as a template[69]. The SufE(D74R) mutation was introduced by site-directed mutagenesis using the QuikChange Kit (Stratagene) with primers 5'-AGGGCGACAGCCGTGCGGCGATTGT-3' and its complementary primer 5'-ACAATCGCCGCACGGCTGTCGCCCT-3' on pET21a_sufE. The SufE (C17S-D74R) double mutation was introduced by site-directed mutagenesis using the QuikChange Kit (Stratagene) with primers 5'-TTTTACGCTCCGCCAACTGGGAAGA-3' and its complementary primer 5'-TCTTCCCAGTTGGCGGAGCGTAAAA-3' on pET21a_sufE(D74R)

Protein Expression and Purification

E. coli SufS and SufE were independently expressed and purified as described previously [69]. *E. coli* BL21(DE3) containing the pET-21a_SufE(D74R) was grown in LB with 100 μg/ml Amp^+ at 37°C overnight, diluted 100 fold to LB and induced by 500 μM isopropyl-1-thio-β-D-galactopyranoside (IPTG) when the cultures reached an OD_{600} of 0.4 - 0.6. Induction was at 18°C overnight. Cells were harvested and lysed in 25 mM Tris, pH 7.5, 100 mM NaCl, 5 mM DTT and 1 mM phenylmethylsulfonyl fluoride via sonication. Following centrifugation at 20,000 × g for 30 min, lysate was filtered before loading on columns. SufE(D74R) were purified using Q-sepharose and Superdex 75 chromatography resins in sequence. The Q-sepharose column utilized a linear gradient from 25 mM Tris-HCl, pH 7.5, 10 mM βME to 25 mM Tris-HCl, pH 7.5, 1 M NaCl, 10 mM βME. The Superdex column was run with 25 mM Tris-HCl, pH 7.5, 150 mM NaCl, and 5 mM DTT. Purified proteins were concentrated, frozen as drops in liquid nitrogen, and stored at -80°C until further use.

Cysteine Desulfurase Activity Assays.

Cysteine desulfurase activity was measured with N,N-dimethyl-p-phenylenediamine sulfate (NNDP) and $FeCl_3$ using a slightly modified published protocol [23]. Reactions were carried out aerobically in 25 mM Tris-HCl, pH 7.4, 150 mM NaCl at 27°C. Proteins were incubated with 2 mM DTT for 5 min prior to addition of L-cysteine in a total reaction volume of 800 μL. Reactions were allowed to proceed for 10 min and then were stopped by the addition of 100 μL 20 mM NNDP in 7.2 M HCl and 100 μL 30 mM $FeCl_3$ in 1.2 M HCl. The mixture was incubated for 30 min in the dark to form methylene blue.

Precipitated protein was removed by 1 min centrifugation at 16,100 x g, and the methylene blue was measured at 670 nm. A Na_2S standard solution was used for calibration.

Circular Dichroism Spectroscopic Analysis

Circular dichroism (CD) spectra were measured using a JASCO J815 spectropolarimeter (JASCO, Essex, UK) AT 20℃. SufE or SufE(D74R) were prepared at 20 μM concentration in 25 mM, pH 8.0 boric acid buffer. Far-ultraviolet (180 nm – 300 nm) spectra were collected with a cuvette of 1-cm path length.

Cysteine Binding Assays

All assays were performed at room temperature in 25 mM Tris-HCl, 150 mM NaCl, pH 7.4. L-cysteine binding was evaluated by monitoring the immediate ΔA_{420} or ΔA_{340} elicited by the addition of increasing concentrations of L-cysteine to 25 μM $SufS_{apo}$ or 25 μM $SufS_{apo}$ with an equal amount of $SufE(D74R)_{alk}$ [81]. Protein was first added to the cuvettes, then L-cysteine was added and mixed for ~5 s prior to a wavelength scan from 200–650 nm. As L-cysteine concentrations increased, the 420 nm PLP peak intensity (internal aldimine) decreased and the new 340 nm peak intensity (external aldimine) increased. Data were analyzed with Prism software (Graphpad). $SufS_{apo}$-$SufE(D74R)_{alk}$-Cys data was best fit with a one site-specific binding with Hill slope model. $SufE(D74R)_{alk}$ was prepared by first pre-incubating with 5 mM DTT for 30 min followed by removal of DTT with a 5 ml desalting column. SufE was then

incubated with 5mM iodoacetamide for 1 h in the dark and was exchanged into desulfurase assay buffer with a desalting column.

Isothermal Titration Calorimetry （ITC）

ITC measurements were performed on a VP-ITC calorimeter (MicroCal) at 27 °C. For the $SufS_{apo}$ and $SufE(D74R)_{apo}$ ITC experiment, $SufS_{apo}$ present in the cell (1.44 ml at 50 μM) was titrated with 45 x 6-μl injections of 1.1 mM SufE (a 10-fold molar excess over $SufS_{apo}$). The duration of each injection was 7.2 s (1.2 s/μl) with an interval of 200 s between injections. Titrations were performed in Buffer A. Each experiment was corrected for the endothermic heat of injection resulting from the titration of SufE(D74R) into buffer. $SufS_{apo}$-$SufE_{apo}$ ITC data were analyzed with the two sequential binding sites model in MicroCal Origin using a $SufS_{apo}$ dimer concentration of 54 μM. $SufS_{apo}$-SufE(D74R) ITC data was analyzed with the one site model in MicroCal Origin using a SufS monomer concentration of 500 μM.

PDT-Bimane for pK_a measurement of cysteine residue C51 on SufE

A nucleophile is a species that donates an electron pair to an electrophile to form a chemical bond in a reaction. pK_a for free cysteine is 8.3. Low pKa cysteine residues are redox active. For pK_a measurement of C51 in the SufE(D74R) mutant, SufE(C17S) and SufE(C17S_D74R) were incubated with 50 mM DTT for 1 hr at room temperature. The buffer was then exchanged to 25 mM potassium phosphate, pH 6.0, 50 mM NaCl, 1 mM EDTA. Protein was then diluted to 10 μM concentration in sodium citrate or phosphate buffers spanning the pH range 4 – 11. The reaction volume is 150 μl and the final

PDT-Bimane concentration is 80 μM. After rapid mixing, the absorbance at 343 nm was monitored over 120 min in a 96-well microplate. Each curve was fit to either a first or second order exponential function Henderson-Hasselbalch equation $Y= Y_0 + A*\exp(-X/t_1)$, and the rate constants were determined. The inverse of the rate constants (t_1) were plotted as a function of pH.

RESULTS

Structure and conformation of SufE(D74R) is similar to wild type SufE.

When generating point mutations that might alter protein – protein interactions, one must be sure that the mutation does not destabilize the overall secondary or tertiary structure of the protein. To determine if SufE D74R secondary structure is altered, we compared the circular dichroism (CD) spectra of SufE D74R and wild-type SufE in the far UV region (190-260 nm). The similar signals indicated that the D74R mutation did not change the secondary structure, which contains a mixture of α-helix and β-sheet elements (Figure 4.5).

We also monitored the solution conformation of SufE(D74R) by gel filtration chromatography using an analytical Superdex 75 column. SufE(D74R) elutes as a single symmetric peak at the same position as wild-type SufE, giving an apparent molecular weight of 21,323 Da compared to 21,304 Da for wild-type SufE. The theoretical MW of SufE(D74R) and SufE are 15,841 Da and 15,800 Da respectively. Based on this analysis, SufE(D74R) exists as a monomer in solution like wild-type SufE. Based on the CD and gel filtration data, we believe SufE(D74R) is correctly folded in a conformation similar to wild type SufE.

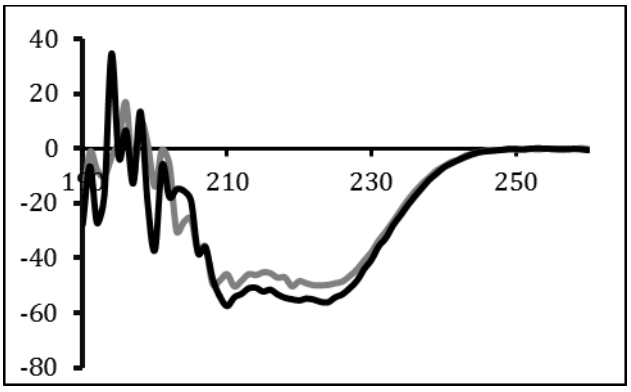

Figure 4.5 Circular dichroism spectra of wild-type SufE (black) and SufE(D74R) (grey) in the far UV region (190-260 nm). CD signal for SufE is black and for SufE(D74R) is grey.

SufE(D74R) interacts stronger and binds differently to SufS compared to SufE.

To test our initial hypothesis that the SufE D74R mutation should disrupt the interaction between SufE and SufS, isothermal titration calorimetry (ITC) was used to directly measure $SufS_{apo}$ – $SufE(D74R)_{apo}$ binding (Figure 4.6). The SufS – SufE(D74R) binding isotherm was exothermic. The SufS – SufE(D74R) binding data were well fit using a one-site binding model. This result is in direct contrast to SufS – SufE binding data, which best fits a sequential two-site binding model [91]. The results indicate that the SufS binding mode of SufE(D74R) is different from wild-type SufE. Strikingly, SufE(D74R) interacts more strongly with SufS than does wild-type SufE. The SufE(D74R) K_d for binding to SufS was ≤ 0.53 μM, which is 7 fold higher than the first high affinity binding of wild-type SufE to SufS under the same conditions (3.59 μM). The number of SufE(D74R) binding sites on SufS calculated from ITC is only 0.57. It indicates that when SufE(D74R) binds tightly to one SufS monomer, the other monomer ceases to bind SufE. This is consistent with negative cooperativity previously found between the active cysteine in each SufS monomer when interacting with $SufE_{alk}$ [91]. It is not clear how binding of the mutant SufE to one SufS monomer blocks subsequent binding to the second monomer of SufS.

Overall the binding affinity and binding mode of $SufE(D74R)_{apo}$ is more similar to results obtained in previous studies using $SufE_{alk}$, where the SufE Cys51 has been modified with iodoacetamide (but is otherwise wild-type). Previous HDX-MS and ITC results demonstrated that alkylation of active site Cys51 on SufE enhances the interaction with SufS due to increased solvent exposure of Cys51, which may more closely mimic the sulfur-accepting conformation of the Cys51 loop on wild-type SufE. HDX-MS time

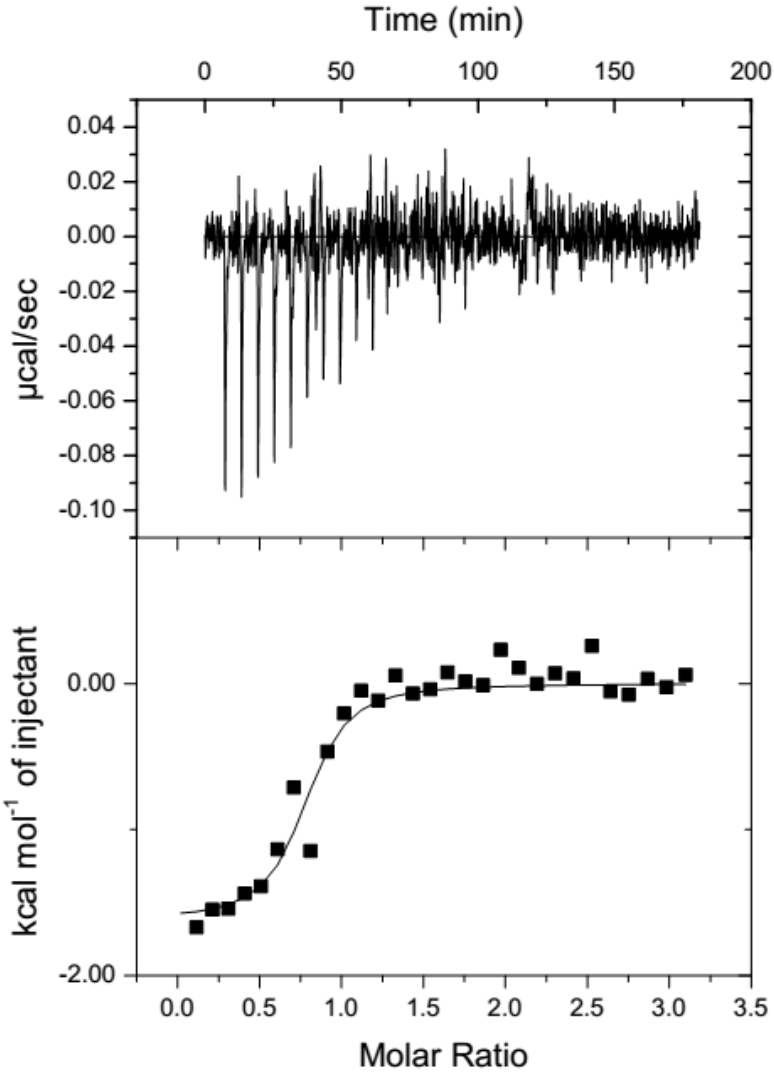

Figure 4.6 Analysis of the binding of SufE(D74R) to SufS by isothermal titration calorimetry. SufS in the cell at 50 µM was titrated with a 10-fold molar excess of SufE(D74R). The fitting of the data was derived from the integrated heats of binding plotted against the molar ratio of SufE(D74R) added to SufS in the cell, after correction for the heat of dilution. The best-fit model was a one binding site model with K_d 0.53 µM. The data fitted parameters are in Table 4. 1.

Table 4.1 Fitting parameters from ITC analysis of binding between SufS and either SufE(D74R) or $SufE_{alk}$.

SufS + SufE(D74R)		SufS + $SufE_{alk}$	
One Site Model		One Site Model	
Chi^2/DOF	1.672E4	Chi^2/DOF	2.028E5
K	1.88E6 ± 7.16=5E5 M^{-1}	K	4.06E6 ± 1.03E6 M^{-1}
ΔH	-1757 ± 99.6 cal/mol	ΔH	-8519 ± 123.7 cal/mol
ΔS	22.7 cal/mol/deg	ΔS	1.86 cal/mol/deg
N	0.565 ± 0.0236 Sites	N	0.730 ± 0.006 Sites

course experiments revealed that carbamidomethylation of SufE Cys51 results in increased solvent accessibility and dynamics around Cys51. Since our SufE(D74R) behaved similarly to $SufE_{alk}$, we propose that the D74R mutation changes the environment of Cys51 and shifts its conformation toward the sulfur-accepting status (more solvent exposed and more dynamic). One prediction of this model is that SufE(D74R) may be a better substrate for SufS than wild-type SufE during the sulfur mobilization reaction.

SufE(D74R) is a better sulfur acceptor for SufS then SufE.

To analyze whether SufE(D74R) enhances SufS activity like wild-type SufE, we performed kinetic enzyme measurement of SufS activity in the presence of different concentrations of SufE(D74R) and L-cysteine (Figure 4.7). As SufE concentration increased the SufS desulfurase activity increased until saturation. However, over a similar concentration range of SufE, SufS desulfurase activity did not saturate in the presence of SufE(D74R) and continued to increase. The divergence point of SufE(D74R) and SufE is at 8 μM where the SufE:SufS molar ration is 16:1 in the assay. When monitoring SufE(D74R) as a substrate for SufS, SufS activity did not follow Michaelis-Menten behavior. To test if SufE(D74R) alters the use of L-cysteine as a substrate, SufS activity was measured with constant SufE(D74R) (0.5 μM SufS with 4 μM SufE(D74R)) and increasing cysteine concentrations. At this concentration of SufE(D74R), the activity enhancement on SufS is similar to the enhancement of wild-type SufE. When Under these conditions the enzyme kinetics could be fit with the Michaelis-Menten equation (grey line fitting) with a moderate fitting goodness (R square

= 0.89) (Table 4.2). Using this fit, the K_m of SufS for L-cysteine in the presence of SufE(D74R) is 16.5 μM which is nearly 3-fold lower than the K_m obtained using an equal concentration of wild-type SufE (K_m of 43.5 μM). However, the data was also fit with an enzyme kinetic model that includes allosteric sigmoidal behavior. The R square for this fitting is 0.97 and it shows a positive cooperativity for the reaction (h = 3.2). Despite the better R squared value, the K_m had a large standard error using this fitting (Table 4.2). It seems that SufE(D74R) deviates from the Michaelis-Menten behavior compared to SufE, at least at higher SufE concentrations. Based on these preliminary analyses, we concluded the SufE(D74R) was a better receptor for sulfur transfer from SufS and modulated the SufS reaction to show positive cooperativity.

SufE(D74R)$_{alk}$ alters L-cysteine binding to SufS in less extent than SufE$_{alk}$.

SufE$_{apo}$ binding to SufS$_{apo}$ leads to conformational changes within the SufS peptide containing the PLP ligand Lys-226. SufE$_{alk}$ binding also alters the reactivity of PLP for L-cysteine substrate. To test if the D74R mutation alters SufE effects on SufS PLP, we generated SufE(D74R)$_{alk}$. Alkylation of SufE Cys residues prevents sulfur transfer from SufS to SufE(D74R) (*i.e.*, SufS turnover) and allows us to exclusively examine the first step of the reaction, L-cysteine binding to SufS PLP, in the presence of SufE(D74R) (Figure 4.8). When L-cysteine substrate binds to PLP it displaces the internal aldimine between PLP and SufS Lys226 and forms an external aldimine at the same position. The initial binding of L-cysteine substrate to resting SufS$_{apo}$ was compared to the SufS$_{apo}$-SufE(D74R)$_{alk}$ complex by following the formation of the external aldimine with L-cysteine, which absorbs at 340 nm, and the disappearance of the internal aldimine,

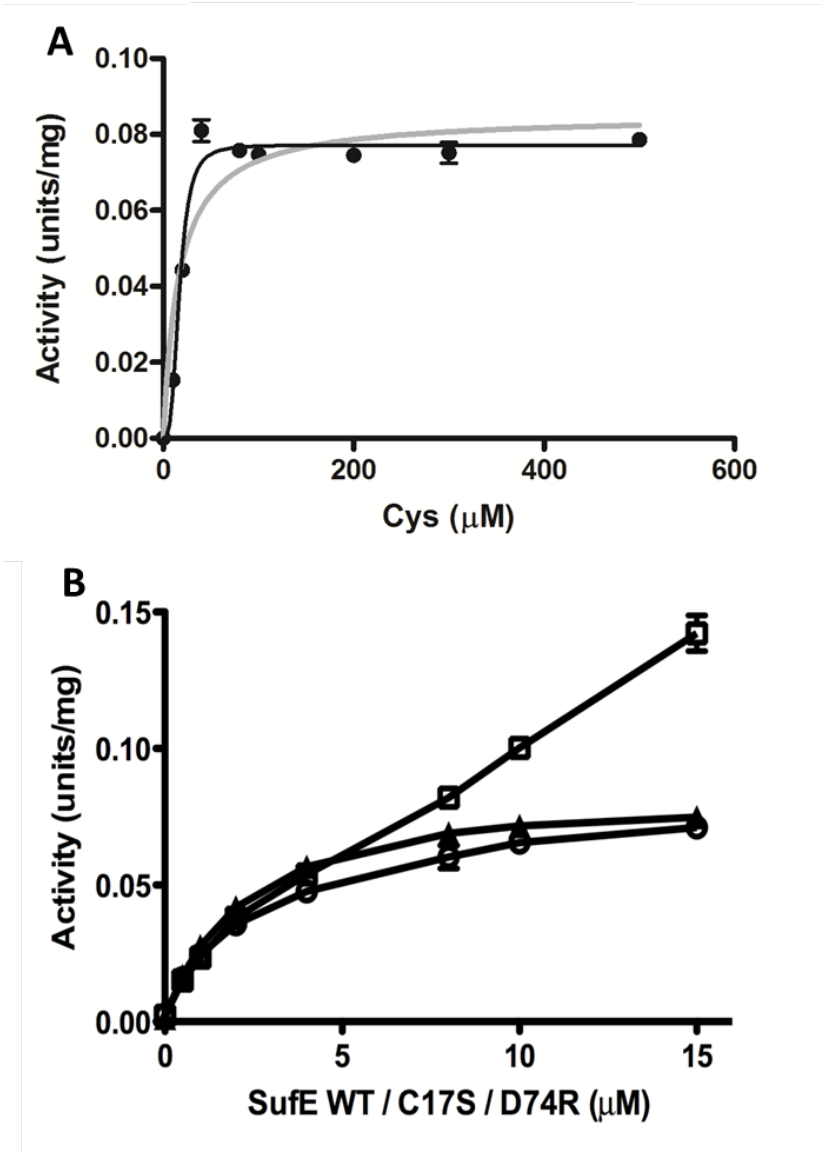

Figure 4.7 Kinetic analysis of SufS activity in response to varied substrate concentrations. (A) The reactions contained 0.5 μM SufS, 4 μM SufE(D74R), 2 mM DTT and 10 – 500 μM L-cysteine. The grey line was fitted with Michaelis-Menten equation model. And the black line was fitted with allosteric sigmoidal model. The fitting parameters are shown in Table 4.2. (B) The reactions contained 0.5 μM SufS, 0 - 15 μM SufE (▲), SufE_C17S (○) or SufE(D74R) (□), 2 mM DTT, and 2 mM L-cysteine. The line in panel A is the best fits to the Michaelis – Menten equation obtained using GraphPad Prism.

Table 4.2 Different fitting method for kinetic analysis of desulfurase activity assay containing 0.5 μM SufS, 2 μM SufE(D74R) and 0 – 500 μM L-Cys.

Michaelis-Menten		Allosteric sigmoidal	
Vmax	0.08515	Vmax	0.07716
Km	16.48	h	3.203
		Kprime	8795
95% Confidence Intervals		95% Confidence Intervals	
Vmax	0.07735 to 0.09295	Vmax	0.07471 to 0.07961
Km	8.937 to 24.03	h	2.397 to 4.009
		Kprime	0.0 to 29019
R square	0.8861	R square	0.9774

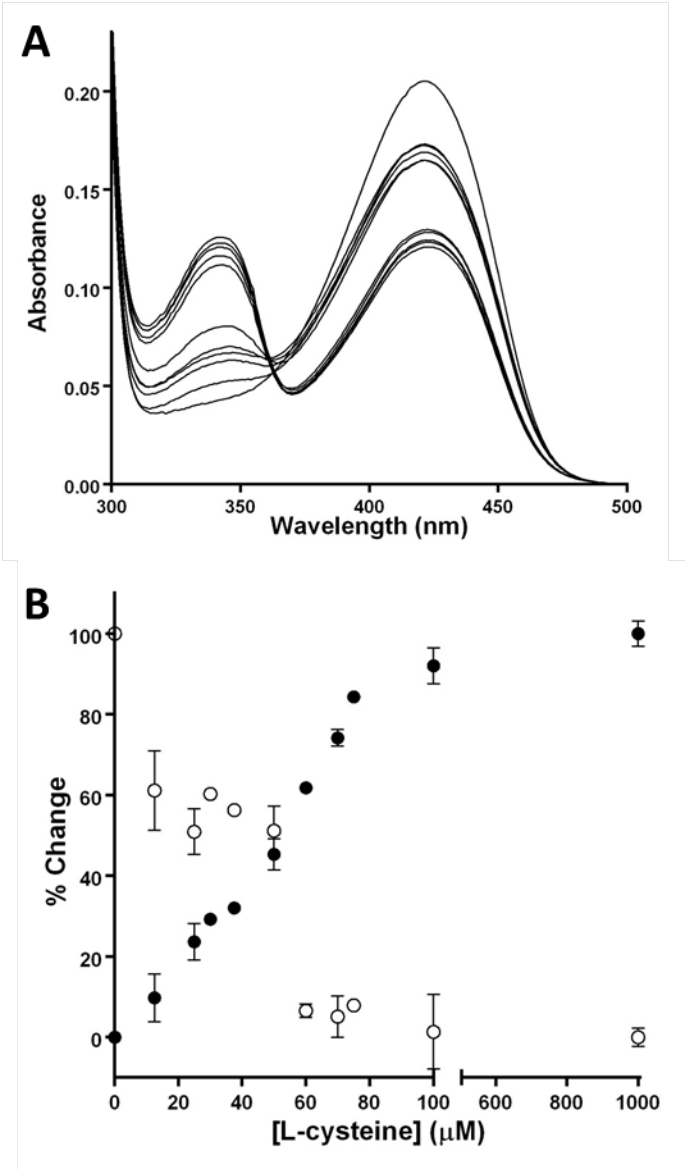

Figure 4.8 Spectroscopic and kinetic analysis of L-cysteine binding to SufS. (*A*) UV-Visible absorption spectra of 25 μM SufS with 25μM SufE(D74R) immediately after addition of 0 – 1 mM (0, 12.5, 25, 30, 37.5, 50, 75, 100, 250, 500, 750, 1000 μM) L-cysteine. (*B*) Percent change of ΔA_{420} (open circles) and ΔA_{340} (closed circles) after adding increasing concentrations of L-cysteine.

which absorbs at 420 nm. Fitting of the ΔA_{340} measurements to a one site binding model shows that the K_d of SufS for L-cysteine is 39 μM if one equivalent of SufE(D74R)$_{alk}$ is present. This apparent K_d is in between the 61 ±1.5 μM measured for SufS alone and the 18 ±1.6 μM measured for SufS with one equivalent of wild-type SufE$_{alk}$. We should note that these values are only apparent dissociation constants since this assay does not distinguish between L-cysteine binding and the rate of external aldimine formation once L-cysteine is bound. Either step or both steps might be altered by SufE(D74R)$_{alk}$ in this equilibrium assay. The results indicate that while the binding of SufE(D74R) can actively remodel the SufS$_{apo}$ active site, the effect is less pronounced than that observed with wild-type SufE$_{alk}$. However, the data showed a similar positive cooperativity fitting with the ΔA_{340} measurements for L-cysteine binding like L-Cys binding to SufS alone. This result suggests that the increased enhancement of SufS by SufE(D74R) may be due to stimulation of L-Cys binding to SufS, unlike the potential prevention of L-Cys binding for wild type SufE.

The better enhancement is may partially be due to the lower pK_a of active site Cys51 in SufE(D74R).

To test if the SufE D74R mutation alters the reactivity of the active site Cys51, we also measured the pK_a of Cys51 in SufE D74R. SufE has one other Cys residue at position 17, but this residue is not involved in SufS enhancement (Figure 4.7B). However, to prevent Cys17 from interfering with the thiol pK_a measurement, we first generated the SufE_C17S and SufE_C17S_D74R mutants. The SufE C17S mutation did not affect SufE enhancement of SufE when generated in the wild-type SufE or SufE(D74R) (Figure

4.7B). The pK_a of Cys51 in SufE_C17S_D74R is 5.7, which is more than 0.5 pH units lower than Cys51 in SufE_C17S (6.3) [90](Figure 4.9A). At the pH of 7.4 used in the desulfurase assay, Cys51 in SufE(D74R) is more prone to exist as a thiolate anion. Increased deprotonation of SufE Cys51 should facilitate the nucleophilic attack of the thiolate anion of Cys51 on the SufS Cys364 persulfide during the sulfur exchange process. However, the percent of deprotonated Cys51 for SufE_D74R is around 98.0% compared to 92.6% for SufE. The deprotonated Cys51 percentage between the mutant and wild type is not big different. However, since the enhancement behavior of SufE(D74R) only diviates from wild-type SufE at higher concentration when ratio of SufE(D74R) to SufS is larger than 10, the 5.4% deprotonated Cys51 difference may still contributes part of reason for the better enhancement of SufE(D74R). The lower pK_a of Cys51 in SufE_C17S_D74R could also make it easier for DTT to cleave the Cys51 persulfide in the desulfurase assay, thereby allowing the SufE(D74R) mutant to turn over faster than wild-type SufE after it has taken the persulfide from SufS. Faster turnover of the SufE Cys51 persulfide could indirectly lead to greater enhancement of SufS activity. To compare how the mutant and wild-type SufE respond to DTT, we kept the SufE and L-cysteine concentrations constant while varying the DTT concentration (Figure 4.9B). We can see that the SufS enhancement by SufE(D74R) and wild type SufE both increase in response to increasing DTT and that the curves are parallel to each other. This result suggests that the lower pK_a of Cys51 in SufE(D74R) does not make the mutant SufE more sensitive to reduction by DTT.

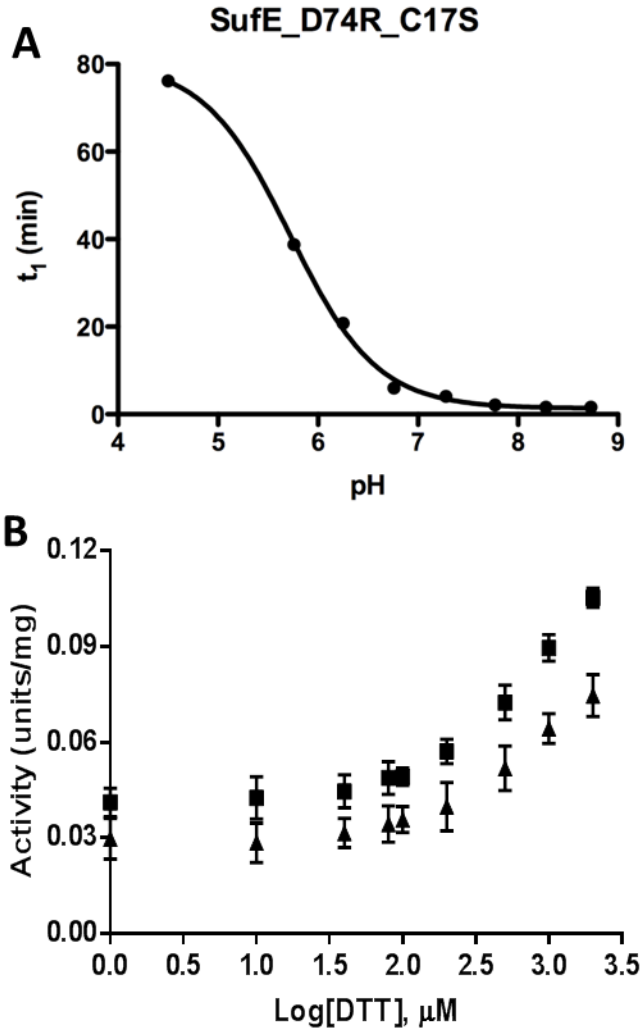

Figure 4.9 pK_a determination of active site Cys 51 in SufE(D74R) and activity comparison between SufE and SufE(D74R) at different DTT concentration. (A) pK_a determination of sulfhydryls with PDT-bimane. Reaction of SufE_D74R_C17S with PDT-bimane was monitored at 343 nm at pH values ranging from 4.5 to 9. The increase at 343 nm results from the release of pyridyl-2-thione from PDT-bimane. Each curve was fit to either a first or second order exponential function, and the rate constants were determined. Inverse of the rate constants (t1) were plotted as a function of pH. The results are fit to the Henderson-Hasselbalch equation $Y= Y_0 + A*\exp(-X/t_1)$. From these curve fits sulfhydryl pKa values of 5.7 were determined for SufE_D74R_C17S. (B) Activity comparison between SufE and SufE(D74R) at different DTT concentration. The reaction contained 0.5 µM SufS, 2µM SufE (▲) or SufE(D74R) (■), 2 mM L-cys and different concentration DTT (0 – 2000 µM).

DISCUSSION

Structure change of SufE(D74R) compared to wild type SufE.

Asp74 resides on a small loop which provides a possibility to accommodate a larger amino acid (Arg) without disturbing the main secondary structure. The CD spectrum of this mutant and wild-type SufE showed that the secondary structures of these two proteins are quite similar. However, Asp74 is involved in the hydrogen bonding with SufE Gln54. Mutation of this amino acid may prevent this hydrogen bond formation and impose a minor conformational change on SufE that is not clearly observed by CD. Our HDX-MS data indicated that two peptides on wild-type SufE (peptide 38-56 and peptide 66-83) are involved in the interaction with SufS [92]. Peptide 38-56 is a surface loop containing Cys51. Peptide 66-83 forms one side of a structural groove into which the SufE Cys51 thiolate is orientated. Residues within SufE 66-83 are most likely involved in the SufS interaction, which may cause conformational changes that are propagated to the Cys51 loop. We can see that Asp74 is located in the peptide 66-83 and the Gln54 is located at the Cys51 loop. The Asp74Arg mutation may modulate the Cys51 loop and affect the SufS interaction. Interestingly, the residue corresponding to Gln54 on SufE is Arg64 on CsdE, which does not form a hydrogen bond with CsdE Glu84 in resting CsdE but is instead predicted to form a hydrogen bond with Thr369 on CsdA in the CsdA – CsdE co-crystal structure[85]. The direct involvement of Gln54 is not found in SufS – SufE interaction derived from HDX-MS analysis[92]. The crystal structure analysis of SufE(D74R) will help us understand how this single mutation affects the overall structure and Cys51 environment of SufE. HDX-MS analysis also will help us understand the interactions between SufS – SufE(D74R) compared to SufS – SufE.

Asp74 is not involved ionic interaction between SufE and SufS.

We designed the SufE(D74R) mutant based on the putative CsdA – CsdE interaction model [89] since this residue is conserved between SufE (Asp74) and CsdE (Glu84). However, our results indicated that Asp74 is not involved in ionic interactions between SufE and SufS (Figure 4.6). Our findings are consistent with the recently published CsdA – CsdE co-crystal structure, in which Glu84 is not involved the interaction with CsdA. More surprisingly, the interaction between SufE(D74R) and SufS is 7 times stronger than the interaction between wild-type SufE and SufS. At present, we are not sure if the mutated Arg residue is directly involved in the interaction or if the mutation induced a conformational change in SufE that helps its interaction with SufS. A crystal structure of SufE(D74R) and solution HDX-MS analysis will help us answer these questions. One more interesting finding is the ITC curve of $SufE(D74R)_{apo}$ – $SufS_{apo}$ binding is more similar to $SufE_{alk}$ – $SufS_{apo}$, as both are mainly exothermic and best fitted with a one binding site model [92]. However, the binding sites N is only 0.565 for $SufE(D74R)_{apo}$, which is smaller than the 0.73 sites for $SufE_{alk}$. It seems that this mutant interacted with SufS and uncoupled the monomer-monomer interaction of SufS to prevent SufE binding to the second monomer. Our hypothesis is that the D74R mutation may modulate SufE conformation to mimic the sulfur-accepting state of SufE, which then would likely binding more tightly to SufS.

SufE(D74R) can bypass the saturation point in the desulfurase reaction when using SufE as a co-substrate for SufS.

The kinetic analysis of SufS-SufE(D74R)-Cys system indicated that SufE(D74R) can

bypass the saturation point in the desulfurase reaction (Figure 4.7B). Binding of L-cysteine to SufS in the presence of the mutant SufE retained the positive cooperativity behavior seen for SufS alone. The ΔA_{340} Cys binding curve showed sigmoidal behavior. The mutation did lower the pK_a of active site Cys51 (Figure 4.9A). However, the resulting increase in deprotonated Cys51 in the mutant seems fairly minor, suggesting that the effect on the pK_a of Cys51 was not the main reason for bypassing the saturation point of SufE(D74R). The mechanism of how this mutant can better enhance SufS activity at higher concentrations needs further study. One possibility is that once SufE(D74R) receives sulfur from SufS, it can leave SufS more easily than SufE at higher SufE(D74R) or SufE concentration. To test this hypothesis, we need to do the surface plasmon resonance (SPR) experiment to test the on and off rate for SufE(D74) binding to SufS and compare the rates with wild-type SufE binding. SufE(D74R) binding may also modulate SufS structure, which may be clarified by HDX-MS analysis to study this possibility. Overall, we found an interesting SufE mutant, SufE(D74R) that may help us better understand the sulfur mobilization system of the Suf pathway in *E. col.*

Chapter 5

The SufBC$_2$D Fe-S Scaffold Complex Interacts with SufA for Fe-S Cluster Transfer[3]

ABSTRACT

Iron-sulfur clusters are key iron cofactors in biological pathways ranging from nitrogen fixation to respiration. Due to the toxicity of ferrous iron and sulfide to the cell, *in vivo* Fe-S cluster assembly is carried out by multi-protein biosynthetic pathways. Fe-S cluster assembly proteins traffic iron and sulfide, assemble nascent Fe-S clusters, and correctly transfer Fe-S clusters to the appropriate target metalloproteins *in vivo*. The gram-negative bacterium *E. coli* contains a stress-responsive Fe-S cluster assembly system, the SufABCDSE pathway that functions under iron starvation and oxidative stress conditions that compromise Fe-S homeostasis. Using a combination of protein-protein interaction and *in vitro* Fe-S cluster assembly assays, we have characterized the relative roles of the SufBC$_2$D complex and the SufA protein during Suf Fe-S cluster biosynthesis. These studies reveal that SufA interacts with SufBC$_2$D in order to accept Fe-S clusters formed de novo on the SufBC$_2$D complex. Our results represent the first biochemical evidence that the SufBC$_2$D complex within the Suf pathway functions as a novel Fe-S scaffold system to assemble nascent clusters and transfer them to the SufA Fe-S shuttle.

[3] Chahal, H. K., Dai, Y., Saini, A., Ayala-Castro, C., and Outten, F. W. (2009) The SufBCD Fe-S scaffold complex interacts with SufA for Fe-S cluster transfer, *Biochemistry 48*, 10644-10653.

INTRODUCTION

Protein-bound iron-sulfur (Fe-S) clusters are one of the most common enzyme prosthetic groups and play important roles in fundamental life processes such as electron transfer reactions, substrate binding and catalysis, transcriptional regulation, and sensing of reactive oxygen and nitrogen species [93, 94]. *In vivo* formation of Fe-S clusters involves multiple components working in concert. Three primary Fe-S assembly pathways have been identified along with a large number of uncharacterized accessory proteins. The *nif* system is required for the formation of Fe-S clusters in the nitrogenase enzyme complex although *nif* homologues can be found in organisms that lack nitrogenase [95]. The *isc* system works as a general pathway for the maturation of multiple Fe-S proteins in both bacteria and the mitochondria of eukaryotes [65, 96, 97]. The third system, named *suf*, mediates Fe-S cluster assembly under oxidative stress and iron limitation conditions in *E. coli* [32-35, 98], but is the sole cluster assembly system in other prokaryotes and in the chloroplast of some photosynthetic eukaryotes [14, 25, 35]. All three systems utilize a cysteine desulfurase enzyme (NifS, IscS, and SufS) to liberate sulfide from free cysteine during cluster assembly. In some bacterial phyla, the SufE protein acts in concert with SufS as a sulfur transfer partner for Fe-S cluster assembly. All three systems also contain members of the A-type carrier (ATC-II) family of Fe-S biosynthesis proteins ($IscA^{Nif}$, IscA, and SufA) that contain three conserved cysteine residues involved in Fe-S cluster coordination [13, 65]. Despite some early controversy concerning the role of ATC-II proteins, all recent biochemical and genetic analyses suggest that they bind Fe-S clusters *in vivo* and are able to transfer the clusters to target apoproteins [13, 16, 44].

The model organism *E. coli* carries the *sufABCDSE* operon that is required for

stress-responsive Fe-S cluster assembly. Recently it was shown that *E. coli* SufA, co-expressed with the other Suf proteins, binds a $Fe_2S_2^{2+}$ cluster *in vivo* that can be transferred to target Fe-S apoproteins [16]. However, recent studies have also shown that the SufB can assemble an iron-sulfur cluster *in vitro* [45]. *In vivo* and *in vitro*, SufB forms a stable complex with SufC and SufD (referred to here as $SufBC_2D$) and all three proteins are necessary for *in vivo* Fe-S cluster assembly[23, 33, 34]. Studies in our lab have shown that the $SufBC_2D$ complex can also be reconstituted *in vitro* with an Fe-S cluster similar to SufB alone [99]. Since both SufA and the $SufBC_2D$ complex can assemble Fe-S clusters, this raises the question of how they function in Suf-mediated Fe-S cluster assembly. Do SufA and $SufBC_2D$ work together in a linear assembly pathway, where one protein functions as an Fe-S scaffold and the other as an Fe-S shuttle? Alternatively, do SufA and $SufBC_2D$ work in parallel cluster assembly pathways, where each protein functions as a separate scaffold for particular cluster types or specific target apo-enzymes? In order to answer these questions we analyzed the protein-protein interactions among the Suf proteins and the ability of SufA and $SufBC_2D$ to form Fe-S clusters *in vitro*. Our studies indicate that SufA is an Fe-S cluster shuttle protein that receives its cluster from the $SufBC_2D$ scaffold complex prior to insertion of the cluster into target apoenzymes.

MATERIALS AND METHODS

Strains, plasmids, and growth conditions

SufA was amplified from MG1655 chromosomal DNA as template using the primers 5′- TAAACATATGGACATGCATTCAGGAACCTTTA-3′ and 5′-ATAGGGATCCCTATACCCCAAAGCTTTCGCCACAG-3′. PCR products were

digested with *BamHI* and *NdeI* and cloned into the corresponding sites of pET21a (Novagen), generating plasmid pET21a-SufA. The nucleotide sequences of the plasmid insert was confirmed by DNA sequencing. *E. coli* BL21(DE3) containing the pET21a-SufA expression vector was grown in LB at 30 °C. Isopropyl-1-thio-β-D-galactopyranoside was added at 500 μM final concentration for 6 h to induce SufA expression. The plasmid pGSO164 containing the entire *suf* operon under the control of arabinose-inducible promoter was used to over-express SufABCDSE in the TOP10 strain of *E. coli*. The cells were grown in LB at 37 °C and L-arabinose was added to 0.2% final concentration by weight for 3 h to induce the expression of SufABCDSE. After induction, cells were harvested by centrifugation and cell pellets were frozen at -80 °C.

Protein purification

The $SufBC_2D$ complex was purified as described previously (17), using Phenyl FF, Q-sepharose, and Superdex 200 chromatography resins in sequence. SufA was purified by freeze-thaw method as follows: Briefly, the cell pellet was thawed on ice and resuspended in buffer containing 25 mM Tris-HCl, pH 7.5, 100 mM NaCl, 10 mM βME, 2 X EDTA-free protease inhibitor tablets. The pellet was refrozen at -80 °C for 1 hour. The freeze-thaw cycle was repeated two more times. The freeze-thaw extract was centrifuged at 20,000 X g for 20 min and the clear lysate was loaded onto a Q-sepharose anion exchange column. The protein was eluted with a linear gradient of 25 mM Tris-Cl, pH 7.5, 1 M NaCl, 10 mM βME. The fractions containing SufA were collected and concentrated to 3 mL and loaded onto HiLoad16/60 Superdex 75 gel filtration column equilibrated with 25 mM Tris-Cl, pH 7.5, 150 mM NaCl, and 10 mM βME. Fractions

containing SufA dimer were concentrated and frozen at -80 °C until further use.

Cross-linking and label transfer

Purified SufA was labeled with a trifunctional cross-linker Mts-Atf-biotin (2-[N2-(4- azido-2,3,5,6-tetrafluorobenzoyl)-N6-(6-biotinamidocaproyl)-L-lysinyl]ethyl methanethiosulfonate (Pierce). This crosslinker contains a sulfhydryl-specific methane-thiosulfonate (Mts) moiety that was used to attach Mts-Atf-biotin specifically to cysteine residues in SufA. It also contains a photo-activated tetrafluorophenyl azide moiety (Atf). The Atf moiety will insert into carbon-hydrogen bonds within 11.1 Å of the cross-linker upon exposure to UV light. SufA (50 μM) was mixed with 250 μM Mts-Atf-biotin in a total reaction volume of 300 μL in phosphate-buffered saline (0.1 M, pH 7.2). After 1 h incubation at room temperature, the unreacted Mts-Atf-biotin was removed by Zeba Desalting spin columns (Pierce) according to the manufacturer's protocol. Labeling reactions were carried out in the absence of ambient light to prevent premature activation of the Atf moiety. Addition of reductant to labeled SufA was able to remove the label, indicating that Mts-Atf-biotin binds SufA as expected via reducible disulfide bonds with cysteine residues.

Mts-Atf-biotin-labeled SufA (4 μM) was mixed with the other Suf proteins (2 μM) in 100 μL of phosphate-buffered saline. The reactions were incubated for 1 h at room temperature. Samples were irradiated with UV light for 5 min at a distance of 10 cm using a Spectroline Model BIB-150P UV lamp (312 nm) to initiate cross-linking with the Atf moiety. After UV light exposure, 4 X LDS sample buffer (Invitrogen) with 1.2 M β-mercaptoethanol was added. The samples were separated by denaturing gel electrophoresis on 4–12% Bis-Tris gels and blotted to nitrocellulose membrane.

Horseradish peroxidase-conjugated streptavidin (Pierce) was used to visualize proteins labeled with Mts-Atf-biotin. Where indicated, the relative intensity of labeled bands from the immunoblots was quantified using ImageJ software from NIH.

RESULTS

SufA interacts with SufB and SufC

To determine the stepwise interactions that occur between SufA and the other Suf proteins, we utilized the trifunctional cross-linker Mts-Atf-Biotin in a label transfer reaction as described previously [45]. Briefly, we specifically labeled exposed cysteine residues in SufA with Mts-Atf-Biotin to generate the bait protein, and performed the label transfer reaction with all other Suf proteins (Figure 5.1). Mts-Atf-Biotin specifically senses protein-protein interactions within 11 Å of a labeled cysteine residue. SufA contains three cysteines, all of which are highly conserved [14]. Based on analysis of the SufA crystal structure, two of the three conserved cysteine residues of each SufA monomer (Cys114 and Cys116) are co-localized to the SufA dimmer interface within 3 – 6 Å of each other while the third cysteine (Cys50) is nearby at a distance of approximately 8 - 9 Å from the other cysteines[100]. Therefore, our label transfer assay will detect interactions that occur fairly close to this localized Fe-S cluster-binding site of SufA and may not indicate protein-protein interactions that involve more distant regions of SufA. However, given the importance of the conserved cysteines at the SufA dimer interface for *in vivo* function, protein-protein interactions that occur in the vicinity of that region also must be critical for Suf function.

After activation of protein cross-linking by Mts-Atf-Biotin with UV light, samples

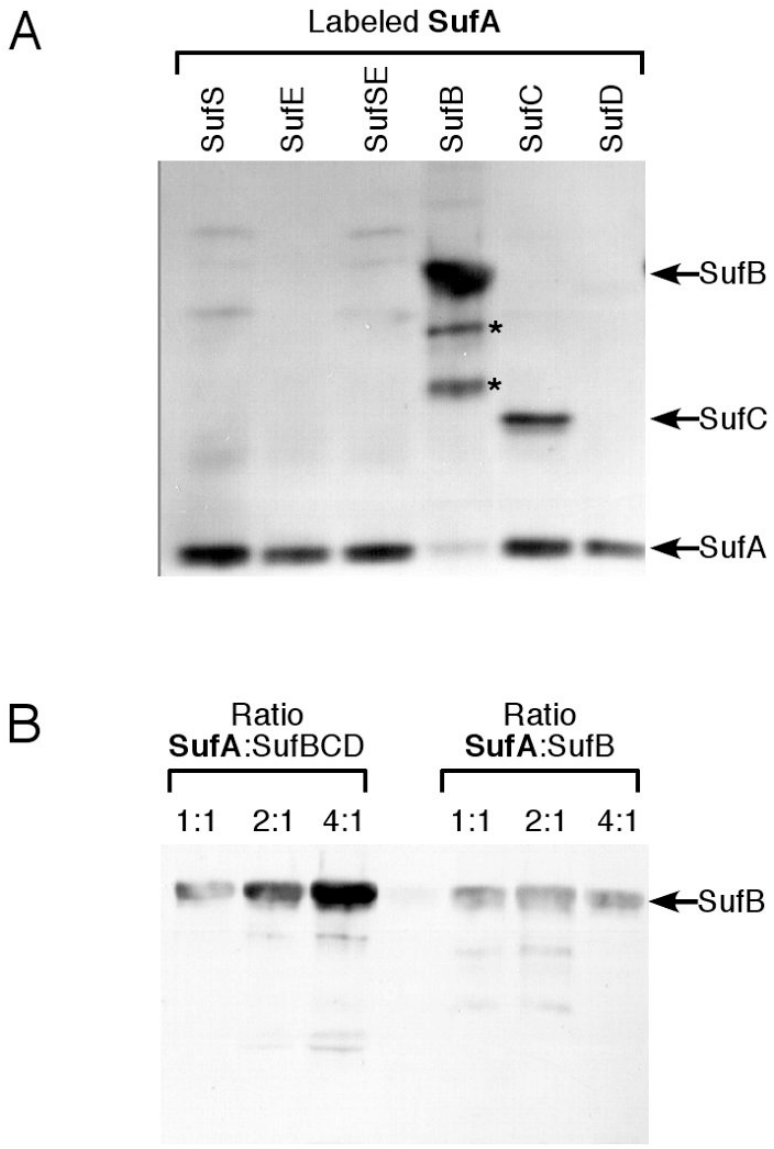

Figure 5.1 Label transfer analysis of SufA interactions with the other Suf proteins. (A) SufA (4 μM) prelabeled with Mts-Atf-Biotin was incubated for 1 h with 2 μM of the other Suf proteins individually or in various combinations. Lower molecular weight bands below SufB (indicated by *) were confirmed by mass spectrometry to be proteolysis products of SufB. (B) Increasing amounts of SufA pre-labeled with Mts-Atf-Biotin were incubated for 1 h with 2 μM of SufB or the SufBCD complex. After UV-light induced cross-linking, samples from (A) and (B) were separated by reducing SDS-PAGE and the location of the biotin tag was determined by immunoblot using streptavidin conjugated to horseradish peroxidase.

were reduced and biotin transfer from SufA to the other Suf proteins was detected via immunoblot (Figure 5.1). SufA interacted with both SufB and SufC, resulting in detectable label transfer to those proteins (Figure 5.1 A). No strong interactions were observed between SufA and the other SufS, SufE, or SufD proteins. Next, increasing concentrations of labeled SufA were mixed with SufB alone or the $SufBC_2D$ complex (Figure 5.1 B). SufA label transfer to SufB increased when SufB was bound as part of the $SufBC_2D$ complex as compared to SufB alone. In contrast, the interaction of SufA with SufC seemed to diminish if SufC is present as part of the $SufBC_2D$ complex (Figure 5.1 B). To further confirm this result, increasing concentrations of labeled SufA were mixed with SufC alone or the $SufBC_2D$ complex. As initially observed, SufA interaction with SufC is diminished if SufC is part of the $SufBC_2D$ complex (Figure 5.2 A). The results from these experiments suggest that the conformation of SufB in the $SufBC_2D$ complex is altered (as compared to SufB alone) to enhance overall SufA binding or to bring the labeled SufA cysteines closer to SufB. Since there is currently no clearly defined functional role for SufC ATPase activity, we also tested if ATP affects the interaction between SufA and $SufBC_2D$. Increasing concentrations of ATP in the label transfer reaction showed no effect on the SufA-$SufBC_2D$ interactions (Figure 5.2 B), indicating that the ATPase activity of SufC is not involved in the SufA and SufB interaction under our *in vitro* conditions.

SufS and SufSE reduce SufA label transfer to $SufBC_2D$

We previously demonstrated that SufE binds to SufB in the $SufBC_2D$ complex in order to donate persulfide sulfur for Fe-S cluster assembly. To determine if the presence of the sulfur donation system SufS and SufE alters the interaction between SufA and

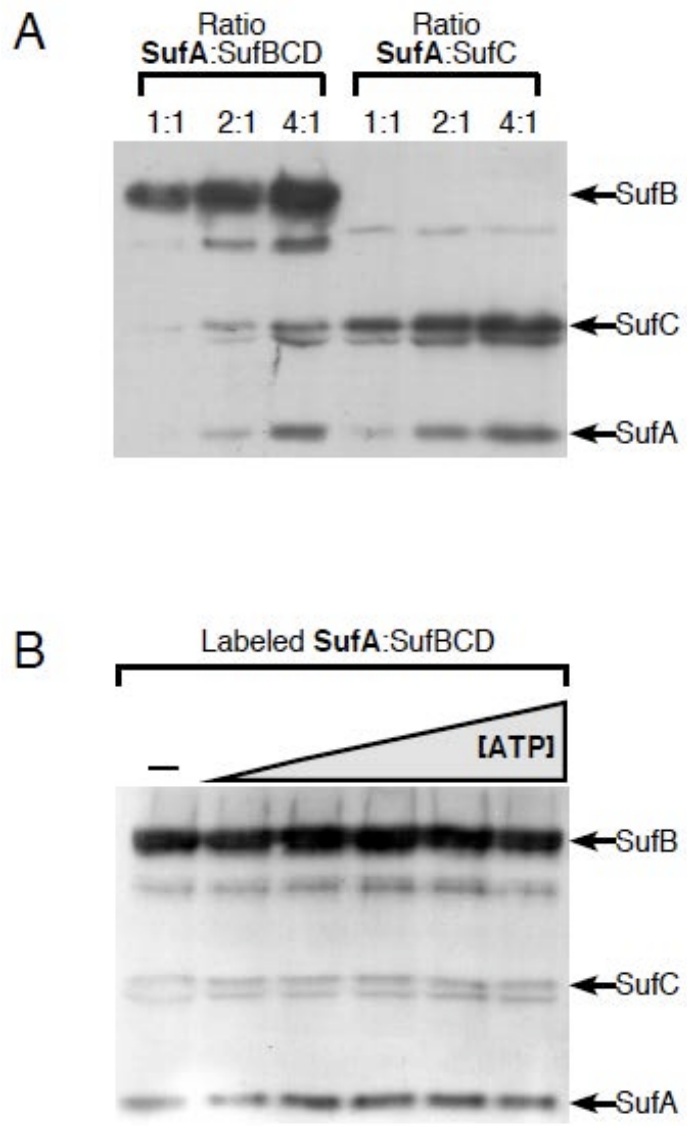

Figure 5.2 Label transfer analysis of SufA interactions with $SufBC_2D$ and SufC. (A) Increasing amounts of SufA pre-labeled with Mts-Atf-Biotin were incubated for 1 hour with 2 μM of SufC or the $SufBC_2D$ complex. (B) Label transfer analysis of SufA interaction with the $SufBC_2D$ complex in the presence of ATP. SufA (4 μM) pre-labeled with Mts-Atf-Biotin was incubated for 1 hr with 2 μM of the $SufBC_2D$ complex. ATP was present at 0, 1, 10, 50, 100, or 300 μM final concentrations during the incubation (increasing concentrations indicated by grey gradient bar above gel). After UV-light induced cross-linking, samples from (A) and (B) were separated by reducing SDS-PAGE and the location of the biotin tag was determined by immunoblot using streptavidin conjugated to horseradish peroxidase.

$SufBC_2D$, we repeated the SufA-$SufBC_2D$ label transfer reaction with unlabeled SufS and SufE added individually or together (Figure 5.3). The label transfer reactions were conducted with a constant amount of labeled SufA and $SufBC_2D$ but increasing concentrations of unlabeled SufS, SufE, or SufSE. The label transfer between SufA and $SufBC_2D$ was slightly diminished if SufE was present at a 4-fold excess over SufA (Figure 5.3A). However, SufS began to block SufA label transfer at equimolar protein ratios and further diminished the label transfer as its concentration increased (Figure 5.3 A). The SufSE complex also blocked label transfer between SufA and $SufBC_2D$ in a manner similar to SufS alone although it was slightly less efficient than SufS alone based on quantification of the relative intensity of the labeled SufB band using ImageJ software (Figure 5.3 B).

There are two interpretations of these results. First, it is possible that both SufA and SufSE interact with $SufBC_2D$ at a common binding site or at two binding sites that at least partially overlap. Such a common binding site would preclude simultaneous binding by both SufA and SufSE. Alternatively, SufS or SufSE may interact with SufA and block SufA binding to SufB. However, if SufS and SufA do interact, the site of interaction must be distant from the labeled SufA cysteines since we see no label transfer from SufA to SufS or SufSE (Figure 5.1). To test these possibilities we further analyzed the interactions between SufA and SufS using surface plasmon resonance. SufA was covalently immobilized while SufS was added in solution. SufA and SufS did interact in this assay. The K_D for the SufA-SufS interaction (1.4 μM) was calculated using observed k_{on} and k_{of} and was approximately three orders of magnitude higher than the K_D for the strong SufE-SufS interaction (1.1 nM) measured under similar conditions. To determine

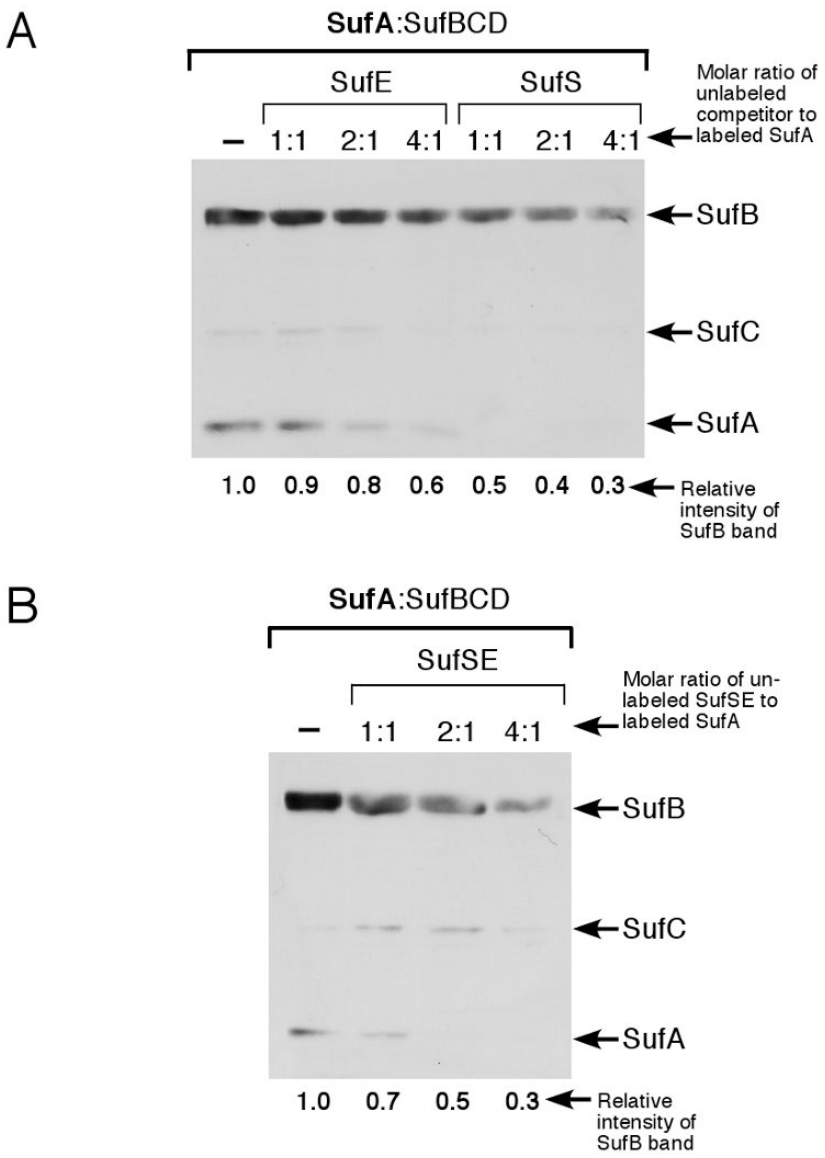

Figure 5.3 Label transfer analysis of SufA interactions with the $SufBC_2D$ complex in the presence of SufS and SufE. (A) Increasing amounts of unlabeled SufE or SufS or SufSE complex (B) were added to a mixture of 4 μM pre-labeled SufA and 2 μM $SufBC_2D$ complex. (B) Increasing amounts of unlabeled SufSE complex were added to a mixture of 4 μM pre-labeled SufA and 2 μM $SufBC_2D$ complex. After UV-light induced cross-linking, samples were separated by reducing SDS-PAGE and the location of the biotin tag was determined by immunoblot using streptavidin conjugated to horseradish peroxidase. The relative intensity of the SufB band in each blot was quantified by ImageJ software and normalized to lane 1 of each blot.

if the SufSE complex interacts with SufA, we immobilized SufA while SufSE (pre-mixed prior to injection) were added in solution. We found that the weak interaction between SufA and SufS was completely abrogated as concentrations of SufE were increased (Figure 5.2 A). Even a 1:1 ratio of SufE:SufS was enough to block binding of SufS to immobilized SufA. SufE itself did not interact with immobilized SufA (data not shown), in good agreement with the label transfer results shown in Figure 1 and with our previous studies.

The sum of the label transfer and surface plasmon resonance experiments indicate that SufS can weakly interact with SufA but that this interaction does not take place in the vicinity of the labeled cysteines in SufA (Figure 5.1). The reduction of SufA label transfer to $SufBC_2D$ in the presence of SufS (Figure 5.3 A) may result from direct SufA-SufS interactions or from competition between SufA and SufS for a common binding site on $SufBC_2D$. With the data in hand we cannot directly distinguish between those two possibilities. In contrast, both label transfer and surface plasmon resonance methods show that the SufSE complex does not interact with SufA (Figure 5.1 and Figure 5.2 A). Therefore, the disruption of SufA label transfer to $SufBC_2D$ in the presence of SufSE logically results from competition between SufA and SufSE for a common binding site on $SufBC_2D$ (rather than from SufSE binding and sequestration of SufA). While a subtle point, this distinction has important implications for establishing the step-wise progression of the Suf Fe-S cluster assembly pathway. Our results indicate that SufA interacts with the $SufBC_2D$ complex and not with the physiological SufSE sulfur transfer system. In fact, SufA and SufSE seem to compete for a common binding site on the $SufBC_2D$ complex.

DISCUSSION

Implications of protein-protein interactions for Suf-mediated Fe-S cluster assembly

Our label transfer results show that the labeled cysteines in the active site of SufA interact closely with $SufBC_2D$ and SufB alone but do not interact with SufS, SufE or SufSE. While SufA can interact with SufB alone, the interaction is enhanced when SufB is present in the $SufBC_2D$ complex (Figure 5.1 B). We previously reported that SufE interaction with SufB for sulfur transfer is also enhanced for the $SufBC_2D$ complex compared to SufB alone, further confirming that the $SufBC_2D$ complex is at the core of the Suf pathway[45]. The SufSE complex reduces SufA binding to apo-$SufBC_2D$ (Figure 5.1 B) but does not directly interact with SufA (Figure 5.3), suggesting that SufSE and SufA share an overlapping binding site on $SufBC_2D$. The mutual exclusivity of SufSE and SufA interactions with $SufBC_2D$ supports a model where SufA functions with the $SufBC_2D$ complex to mediate a step downstream of the SufSE sulfur donation step during cluster assembly (Figure 5.4). In this model SufA would not function as a scaffold and would carry out a function subsequent to *de novo* Fe-S cluster assembly. Such a model is consistent with previously published results showing that SufE and SufA do not interact [49] and that SufA does not enhance SufS or SufSE cysteine desulfurase activity [23].

In vivo the Suf pathway must limit release of sulfide and/or oxidation of reactive sulfur species under oxidative stress. The *in vivo* sensitivity of the Fe-S cluster assembly process to oxidative stress necessitates tight protein-protein interactions to shield reactive sulfur species from the cellular milieu, a proposition supported by the crystal structures of SufS and SufE, in which their cysteine active sites are at least partially solvent excluded [21, 48]. The label transfer assays conducted here show that neither SufS nor SufE come

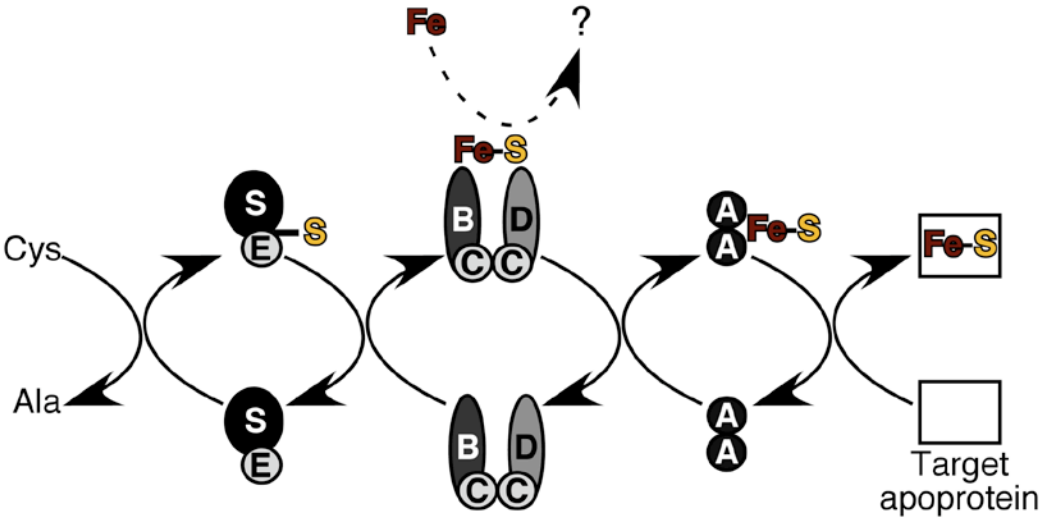

Figure 5.4 Current model of Suf-mediated Fe-S cluster assembly. Interactions and processes detailed in this work or previous studies are shown with bold arrows. The unknown process of iron donation is shown as a dashed arrow.

within 11 Å of the labeled cysteines on SufA (Figure 5.1). This result does contradict other *in vitro* studies that seem to show direct sulfur transfer from SufSE to SufA [15]. At present we have no explanation for this discrepancy, although it may reflect non-physiological sulfur transfer under *in vitro* conditions. Although we observed weak interaction between SufS and SufA using surface Plasmon resonance, this interaction was abolished in the presence of SufE. Both SufS and SufE are coexpressed from the same polycistronic message and both are required *in vivo* for Suf function [34, 59]. SufE also is necessary to elevate SufS cysteine desulfurase activity to levels comparable to other cysteine desulfurases (such as IscS) [23, 43]. Therefore the SufSE complex is the physiological sulfur transfer pathway and it is unlikely that SufA interacts with SufS alone for sulfur transfer *in vivo* since SufE will also be present. Possibly weak SufS-SufA interactions are relevant in the context of stabilizing a larger macromolecular complex that includes $SufBC_2D$ and SufE at some step of Fe-S cluster assembly. Resolving these mechanistic details will require co-structures of the Suf protein complexes.

We also found that SufA can interact with SufC alone but that SufA interaction with SufC is reduced in the $SufBC_2D$ complex (Figure 5.2). This may indicate a direct role for SufC in recruiting SufA to the $SufBC_2D$ complex. Such an interaction must be short-lived since SufA only transfers label to SufB in the $SufBC_2D$ complex (at least under the steady state conditions used in our assays). Possibly after initial binding to SufC, SufA quickly migrates to a more stable binding site that places its active site cysteines closer to SufB. Clearly the ATPase activity of SufC is not required and does not affect SufA protein-protein interactions with $SufBC_2D$. The exact role of SufC in mediating the SufA and SufB interaction remains to be clarified at the structural level.

Chapter 6

The Study of Function Divergence of $SufBC_2D$ and $SufB_2C_2$

ABSTRACT

The putative model for Suf iron-sulfur cluster assembly proposed by our lab suggests $SufBC_2D$ is an intermediate for iron requisition during iron-sulfur cluster assembly and $SufB_2C_2$ is the scaffold complex for final cluster assembly and transfer. Initial results indicated that a linear Fe_3S_4 cluster might be an intermediate during Fe_4S_4 assembly on SufB. To test this hypothesis, I systematically compared the cluster reconstitution and transfer efficiency between these two complexes. Preliminary results did not provide conclusive evidence for a linear Fe_3S_4 cluster present on SufB. Cluster transfer experiments indicated that ATPase activity of SufC might not be involved in the Fe_4S_4 cluster transfer from $SufBC_2D$ and $SufB_2C_2$ to AcnA. Repeated experiments indicated that the clusters on both $SufBC_2D$ and $SufB_2C_2$ were stable under aerobic conditions. Experiments comparing cluster reconstitution with TCEP or without reductant showed that $SufB_2C_2$ may be a better sulfur acceptor from SufSE. Alkylation of cysteines on SufB prevented $SufBC_2D$ from using SufSE and L-Cysteine as a sulfur source for cluster assembly. These studies may help us locate the cluster binding cysteines on SufB. However, most of the results in this chapter are preliminary and further studies are needed.

INTRODUCTION

In vivo biosynthesis of Fe-S clusters requires dedicated biosynthetic machinery to prevent oxidation of both iron and sulfide building blocks, as well as protein cysteinyl ligands, by oxygen or reactive oxygen species. The *sufABCDSE* operon works for de novo Fe-S cluster biogenesis under iron starvation and oxidative stress conditions in *Escherichia coli*. The SufS cysteine desulfurase and SufE sulfur transfer protein together mobilize sulfur from free cysteine as a protein-bound persulfide (R-S-SH) and are more resistant to oxidative stress than IscS. The mobilized sulfur atom is ultimately incorporated into the Fe-S cluster in SufB as sulfide during assembly. The SufA protein is a member of the A-type Fe-S carrier protein (ATC) family that transfers Fe-S clusters to target apoenzymes. The remaining proteins, SufB, SufC, and SufD, form a stable $SufBC_2D$ complex when purified under anaerobic conditions after co-expression of the whole operon [12].

Both SufB and the $SufBC_2D$ complex can form a Fe_4S_4 cluster after in vitro reconstitution suggesting that SufB is the specific Fe-S scaffold protein in the complex. These Fe_4S_4 clusters convert to Fe_2S_2 clusters upon exposure to oxygen [71]. In vitro the cluster on the $SufBC_2D$ complex can be transferred either to the SufA carrier protein or directly to a target apoenzyme, such as aconitase B. These in vitro studies suggest that the $SufBC_2D$ complex is a novel type of Fe-S scaffold system distinct from the well-characterized IscU scaffold proteins. SufC is an ATPase with homology to ATPase subunits of membrane transporters, although the $SufBC_2D$ complex is cytosolic. The basal activity of SufC alone is atypically low, but SufC ATPase activity is enhanced by interacting with SufB or SufD separately or as part of $SufBC_2D$ complex [101]. The

C-terminal half of SufD shares significant homology with the same region in SufB (45% sequence similarity over the C-terminal 150 residues for each protein). Even though SufB alone can form Fe-S clusters in vitro, deletion of any of the three components (SufB, SufC, or SufD) abolishes cluster formation on SufB in vivo.

My colleague Dr. Saini later found that SufD and SufC ATPase activity are required for iron acquisition but not for sulfur acquisition during in vivo Fe-S cluster formation on SufB [99]. When he purified a polyhistidine tagged form of SufB after co-expression with SufCDSE, he found that SufB, SufC, and SufD form at least two distinct complexes in vivo: $SufBC_2D$ and $SufB_2C_2$, which had different amounts of Fe-S cluster and cofactor $FADH_2$ content. These two complexes may have different functions during in vivo cluster assembly. Based on these result, a model for in vivo Suf Fe-S cluster assembly was proposed (Figure 6.1).

To delineate the functional differences between $SufBC_2D$ and $SufB_2C_2$, I purified native $SufBC_2D$ and $SufB_2C_2$ complexes under anaerobic and aerobic conditions. $SufBC_2D$ was purified from *E. coli* cells overexpressing the whole *sufABCDSE* operon. $SufB_2C_2$ was purified from the cells overexpressing *sufBC*. I tried to compare the reconstitution and cluster transfer efficiency between $SufBC_2D$ and $SufB_2C_2$ as well as to track the intermediates during the cluster assembly. I studied the oxidation sensitivity of these two complexes. I also attempted to purify these two complexes under anaerobic conditions after in vivo expression (without any in vitro cluster reconstitution). The results below are preliminary but lay the groundwork for further study.

Fe-S cluster assembly on IscU, the house keeping cluster scaffold protein, has been carefully characterized. Both Fe_2S_2 and Fe_4S_4 can be formed on the IscU dimer. Fe_2S_2

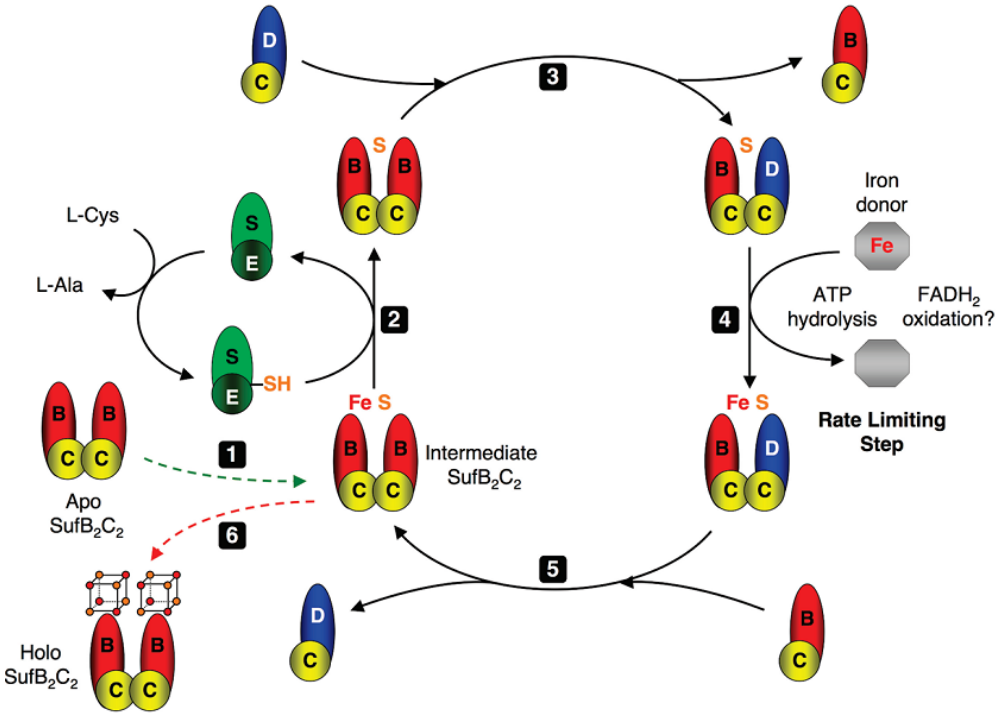

Figure 6.1 Putative model for in vivo Suf-mediated Fe-S cluster assembly [99]. Sulfur is mobilized from L-cysteine by SufSE and transferred to apo $SufB_2C_2$ (steps 1 and 2). SufBC interact with SufCD in the $SufBC_2D$ complex for iron acquisition, ATP hydrolysis, and possibly for $FADH_2$ oxidation (steps 3 and 4). A $SufB_2C_2$ intermediate containing sub-stoichiometric iron and sulfide begins another cycle (step 5). After multiple cycles, $SufB_2C_2$ forms 2 X Fe_4S_4 clusters and exits the cycle for cluster transfer (step 6). The exact mechanism of SufD/SufB association and dissociation during the reaction cycle is unknown but we show the cycle proceeding through exchange of $SufB_1C_1$ and $SufC_1D_1$ heterodimer intermediates. A second interlocking cycle could be occurring simultaneously with exchange of $SufB_1C_1$ and $SufC_1D_1$ intermediates connecting the two cycles (not shown for simplicity). Green arrow shows entry of apo $SufB_2C_2$ into the cycle. The red arrow indicates maturation of $SufB_2C_2$ into the 2 X Fe_4S_4 form.

and Fe_4S_4 clusters assemble sequentially on IscU. These two types of clusters can also interconvert under different conditions and can be transferred to different target proteins. Reductive coupling of 2 X Fe_2S_2 generates a Fe_4S_4 cluster while oxidative degradation of Fe_4S_4 forms Fe_2S_2. Interestingly, we never observe stable Fe_2S_2 forms of $SufBC_2D$ during cluster reconstitution although the Fe_4S_4 form of $SufBC_2D$ will decompose to Fe_2S_2 upon air exposure. Dr. Saini also obtained preliminary evidence for the presence of a linear Fe_3S_4 cluster bound during anaerobic purification but based on the initial data we cannot assign this cluster type specifically to the $SufBC_2D$ and/or $SufB_2C_2$ complex and also cannot determine if this cluster is a degradation product or a bona fide intermediate during cluster assembly.

MATERIALS AND METHODS

Strains, plasmids, and growth conditions

The plasmid pGSO164 [45] containing the entire *suf* operon under the control of an arabinose inducible promoter was used to over-express SufABCDSE in the Top10 strain of *E. coli*. The cells were grown in LB at 37 °C and L-Arabinose was added to 0.2% final concentration by weight for 3 h to induce the expression of SufABCDSE. Recombinant His6-$SufB_2C_2$ was co-expressed with SufSE using expression vector pFWO469 in *E. coli* strain BL21(DE3) [99]. Cultures were grown in LB at 37 °C and induced with 100 μM of iso-propyl-1-thio-β-D-galactopyranoside (IPTG) when OD600 was 0.5–0.6 followed by overnight induction at 18 °C. After induction, cells were harvested by centrifugation and cell pellets were frozen at−80 °C. AcnA was expressed using expression vector pET-21a_AcnA in *E. coli* strain BL21(DE3). Cultures were grown in LB at 37 °C and

induced with 100μM of iso-propyl-1-thio-β-D-galactopyranoside (IPTG) when OD600 was 0.5–0.6 followed by overnight induction at 18 °C.

Protein Purification

The $SufBC_2D$ complex was purified as described previously[45], using Phenyl FF, Q-sepharose, and Superdex 200 gel chromatography resins in sequence at aerobic condition on BioLogic DuoFlow system (BioRad) or at anaerobic condition on ÄKTA system (GE Healthcare). His_6−$SufB_2C_2$was purified aerobically using a Ni^{2+} -NTA column as described previously[99]. For AcnA purification, harvested cells were lysed in 25 mM Tris, pH 7.5, 100 mM NaCl, 5 mM DTT, 1 mM phenylmethylsulfonyl fluoride, and 1× EDTA-free protease inhibitor tablet via sonication. Following centrifugation at 20,000 × g for 30 min, lysate was filtered before loading on columns. AcnA was purified using Q-sepharose, Phenyl FF, and Superdex 200 chromatography resins in sequence. The Q-sepharose column utilized a linear gradient from 25 mM Tris-HCl, pH 7.5, 10 mM βME to 25 mM Tris-HCl, pH 7.5, 1 M NaCl, 10 mM βME. The Phenyl FF column used a linear gradient of 25 mM Tris-HCl, pH 7.5, 100 mM NaCl, 1 M $(NH_4)_2SO_4$, 10 mM βME to 25 mM Tris-HCl, pH 7.5, 10 mM βME. The Superdex column was run with 25 mM Tris-HCl, pH 7.5, 150 mM NaCl, and 5 mM DTT. All the purified proteins were concentrated, frozen as drops in liquid nitrogen, and stored at -80°C until further use.

Iodoacetamide alkylation of cysteines in $SufBC_2D$

0.5mM stock of protein $SufBC_2D$ were in buffer 25 mM Tris-HCl, 150mM NaCl, 10 mM BME, pH7.4. Before iodoacetamide(IAA) treatment, replace 2-mercaptoethanol(BME) with tris(2-carboxyethyl)phosphine(TCEP) using 5 ml

desalting column (GE Health care). Then incubate SufBC$_2$D with 200 fold of IAA in the dark for 30 min. Remove TCEP and IAA using 5 ml desalting column (GE Health care) and keep alkylated protein SufBC$_2$D$_{alk}$ in 25 mM Tris-HCl, 150mM NaCl, 10 mM, pH7.4

Quantification of free thiols in SufBC$_2$D

The number of free thiols in SufBC$_2$D before and after alkylation, was determined by 5,5'-dithio-bis(2-nitrobenzoic) (DTNB) acid assay (Thermo Scientific Ellman's reagent). based on molar absorptivitiy. Prepare 30 μM SufBC$_2$D or SufBC$_2$D$_{alk}$ in native reaction buffer 0.1 M sodium phosphate, pH 8.0, containing 1 mM EDTA or denatured reaction buffer buffered 6M guanididne hydrocholoride. Incubate 12.5 μL protein with 2.5 ul 10mM DTNB in 125 μL reaction buffer at room temperature for 15 minutes. For blank, add 12.5 μL reaction buffer with DTNB and extra reaction buffer. Recard the sample absorbace at 412 nm. Calculate the amount and concentration of sulfhydryls in the sample from the molar extinction coefficient of 2-nitro-5-thiobenzoic acid (TNB). For native protein, use 14,150 $M^{-1}cm^{-1}$ for calculation. For denatured protein, use 13,800 $M^{-1}cm^{-1}$ for calculation.

In Vitro Fe-S Cluster Reconstitution

Both SufBC$_2$D and SufB$_2$C$_2$ were incubated separately in an anaerobic glove box (Coy) in reconstitution buffer containing 25 mM Tris (pH 7.5), 100 mM NaCl, and 5 mM dithiothreitol (DTT), with a 10-fold excess of L-cysteine and ferrous ammonium sulfate (FAS) and 4 μM SufS and SufE (molar ratio of SufSE : Scaffold = 1 : 250). The 25 mM Tris (pH 7.5), 100 mM NaCl was purged with Nitrogen for 2 hours and equilibrated in

the chamber for overnight. After 2.5-3 hours, the proteins were purified by anaerobic anion exchange chromatography using a Hitrap Q FF 1mL column (GE Healthcare). If using 5 ml HiTrap desalting columns (GE Healthcare) purification, incubate the reconstitution mixture was incubated with EDTA equal to the iron concentration for 15 min and centrifuged at 10 X 1000 g for 5 min. After loading the supernatant on to the 5 ml desalting column, fractions containing $SufBC_2D$ and $SufB_2C_2$ were collected and concentrated for analysis. Iron content of purified proteins was determined calorimetrically using ferrozine as described previously (Riemer, J 2004 colorimeetric ferrozine-based). The acid-labile sulfide content of purified proteins was determined by a previously reported method [100].

For $SufBC_2D$ and $SufBC_2D_{alk}$ reconstitution,with SufS-SufE-L-cys as sulfur source, incubate 50 µM $SufBC_2D$ or $SufBC_2D_{alk}$ with 2 mM DTT, 0.2 µM SufS, 0.2 µM SufE, and 300 µM ferrous ammonium sulfate (FAS). Before recording the UV-Vis absorbance (200-800 nm),add 650 µM L-cys.. For reconstitution with Na_2S as sulfur source incubate 50 µM $SufBC_2D$ or $SufBC_2D_{alk}$ with 2 mM DTT and 300 µM ferrous ammonium sulfate (FAS). Before recording the UV-Vis absorbance (200-800 nm),add 650 µM Na_2S. Record UV-Vis during the reconstitution every 10 min. for 2 hours.

Aconitase Activity Assay

The Fe-S cluster transfer experiments were performed anaerobically at 25 ºC. For activation of AcnA, the following components were added in 50 µl of activation buffer (50 mM Tris pH 7.5, 2 mM DTT, 100 mM NaCl), 20 µM apo-AcnA and either 40 µM [4Fe-4S] $SufBC_2D$ (to provide one equivalent of Fe and S) or 5-fold molar excess of free iron (FAS) and sulfide (Na_2S) to fully activate the apo-AcnA. For the Fe-S cluster

experiment in presence of ATP, 2mM of ATP and 10mM of $MgCl_2$ were added. Aconitase activity was assayed every 10 min for 1h. Assays were carried out in sealed anoxic cuvettes containing 150 µl of 50 mM Tris (pH 8.0) with 0.5 µl of AcnA activation reaction mixture (from above). The reaction was initiated by addition of 50 µl of 80 mM DL-isocitratic acid. AcnA activity was measured at 240 nm at room temperature by following the formation of cis-aconitate (ε_{240} = 3400 M-1 cm-1) from iso-citrate.

For cluster transfer to AcnA from $SufBC_2D$ and $SufB_2C_2$, four different conditions were used including (1) no reductant, (2) with 2 mM DTT, (3) with 2mM DTT, 2mM ATP, 10 mM $MgSO_4$, and (4) with 2mM DTT, 2mM ATP, 10 mM $MgSO_4$, 100 mM KCl. 4 µL cluster transfer mixture were added to the prepared AcnA assay solution at different time points to check the AcnA activity as a function of cluster transfer.

RESULT

Kinetic analysis of cluster reconstitution for $SufBC_2D$ and $SufB_2C_2$

Different types of Fe-S clusters have different UV-Vis absorption spectra. For Fe_2S_2 clusters, the spectrum often has a peak or shoulder at 320 nm and a broad peak at 420 nm. For Fe_3S_4, there is a broad peak at 320nm, a sharper peak at 420 nm and two lower intensity peaks around 500 nm and 600 nm. For Fe_4S_4 clusters, there is just one broad peak at 420 nm [102].

$SufBC_2D$ and $SufB_2C_2$ were each reconstituted with SufS-SufE-L-cysteine as a sulfur source and ferrous ammonium sulfate ($(NH_4)_2Fe(SO_4)_2$) as an iron source. After two hours, $SufBC_2D$ reconstitution was stopped by adding one molar equivalent of EDTA based on iron concentration and purified with a desalting column. In contrast,

$SufB_2C_2$ reconstitution was stopped by loading the sample directly on the anion exchange column and purified by this column. During reconstitution, UV-Vis absorption spectra are different between the two complexes. For $SufBC_2D$, the UV-Vis absorption spectra indicated that $SufBC_2D$ likely did not form a Fe_4S_4 cluster during the 2 hours reconstitution (Figure 6.2 A and B). Instead the UV-Vis absorption spectrum looked like a linear Fe_3S_4 cluster after purification from desalting column (Figure 6.2 B). The UV-Vis spectrum indicated a broad peak at 320 nm and a lower intensity peak at around 600 nm and the intensity of these two peaks increased during reconstitution. After purification from a desalting column, the UV-Vis signal indicated the presence of a linear Fe_3S_4. However, UV-Vis absorption spectrum of the $SufB_2C_2$ reconstitution was more like a Fe_4S_4 cluster from the very beginning of reconstitution (Figure 6.2 C). The UV-Vis spectrum indicated only one broad peak at 420 nm was present at the initial scan of reconstitution and this peak signal increased during reconstitution. After purification from the anion exchange column, the UV-Vis absorption spectrum looked like a Fe_4S_4 cluster which had a broad peak at 420 nm (Figure 6.2 D). The Fe and S content were quantified and labeled in the figure (Figure 6.2 B and D). Both complexes had a higher amount of S than Fe. The desalting column gave a better color and protein recovery efficiency. However, it cannot remove all the junk (non-protein bound Fe-S species). The QFF column did removed the junk species but half of the protein and maybe some of the clusters were lost during the QFF column for both $SufBC_2D$ and $SufB_2C_2$ reconstitution.

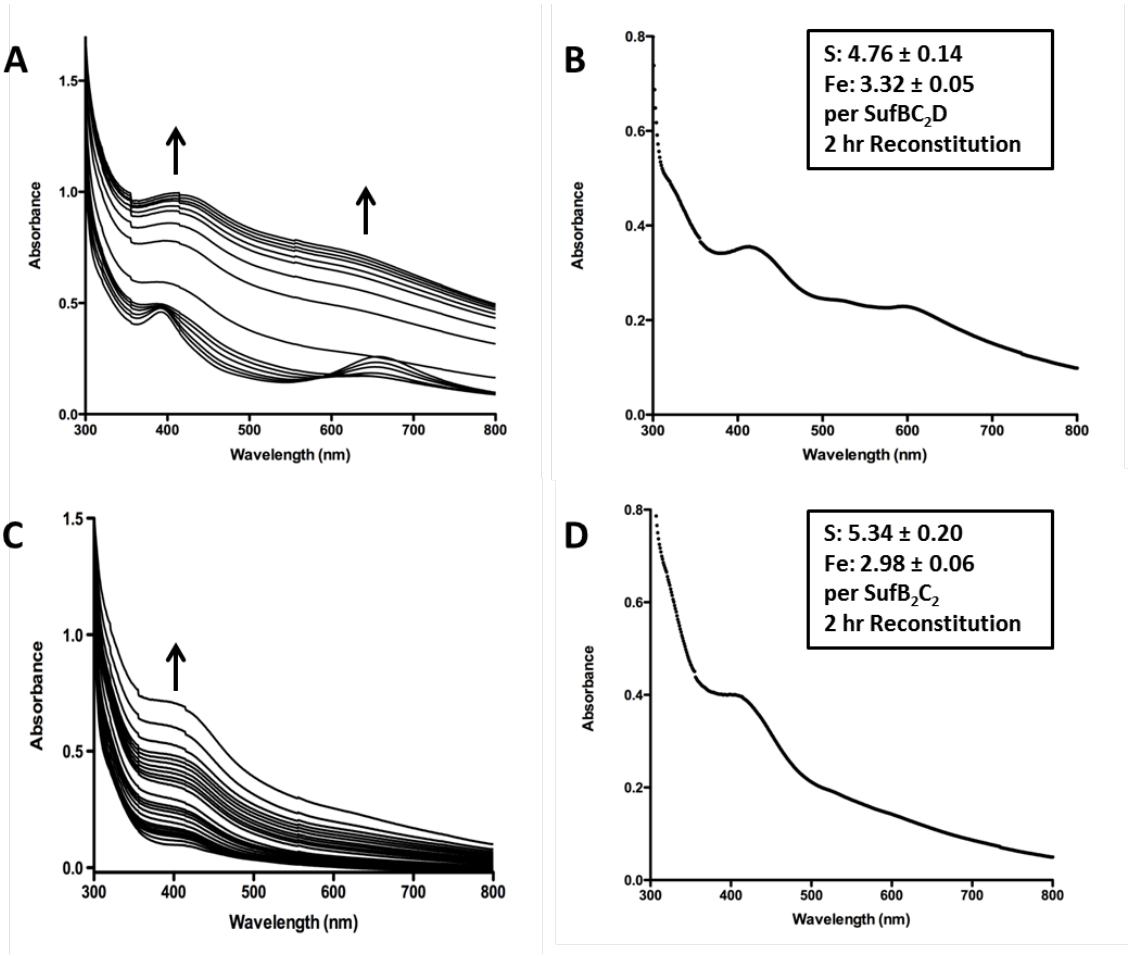

Figure 6.2 UV-Vis absorption spectra change of $SufBC_2D$ and $SufB_2C_2$ during 2 hours cluster reconstitution and after purification. (A) UV-Vis spectrum was recorded from 5 to 10 min until 100 min during cluster reconstitution and (B) UV-Vis spectrum was recorded after desalting column purification. UV-Vis scan of $SufB_2C_2$ (C) UV-Vis spectrum was recorded every 5 min until 120 min during cluster reconstitution during 2 hours cluster reconstitution and (D) UV-Vis spectrum was recorded after anion exchange column purification. The iron and sulfur content of the purified samples were labeled in the imbedded tables. The reconstitution reaction contained 50 μM $SufBC_2D$ or $SufB_2C_2$, 0.2 μM SufSE, 650 μM L-cysteine, 300 μM $Fe^{2+}$and 2 mM DTT. Corresponding UV-Vis spectrum of controls for Figure 6.2 A was shown in Figure 6.3 E. The blank for Figure 6.2 C was shown in Figure 6.3 F.

Alkylation of cysteines on SufB prevented SufBC$_2$D using SufSE-Cys as a sulfur source for cluster assembly.

In the SufBC$_2$D complex, SufB is the actual cluster binding protein [45]. The most common cluster binding residues in proteins are cysteines. There are 13 cysteines on SufB. Those involved in the cluster binding are unknown. To identify those active site cysteines, SufBC$_2$D was alkylated with iodoacetamide. There are 1 cysteine on SufC and 3 on SufD. So there are 18 cysteines in total on one SufBC$_2$D complex. After alkylation, 13 cysteines were alkylated and which left 5 cysteines free on the complex based on the DTNB assay. To test if the alkylation affects the cluster assembly on SufBC$_2$D, I checked cluster reconstitution on SufBC$_2$D$_{alk}$ using different sulfur sources, Na$_2$S as a readily available sulfur source or SufSE and L-cysteine as the physiological sulfur mobilization system. Cluster reconstitution on unmodified SufBC$_2$D was used as a control. We know that SufS can mobilize the sulfur from L-cysteine and transfer it to SufE. Then SufE can transfer the sulfur to SufB for cluster assembly in vivo [45]. Comparing SufBC$_2$D reconstitution using Na$_2$S or SufSE with L-cysteine, we can see the cluster signal after 14 min reconstitution was much higher in the sample using Na$_2$S as sulfur source compared the one using SufSE-L-cys (Figure 6.3 A and B). 14 min was the first time point scanned. The gradually increasing signal in the sample using SufSE-L-cys is logical since SufSE-L-cys is an enzymatic sulfur mobilization system which takes time to transfer sulfur to SufB for cluster assembly.

In contrast, Fe-S clusters cannot be efficiently reconstituted on SufBC$_2$D$_{alk}$ when using SufSE-L-Cys as a sulfur source (Figure 6.3 D). Surprisingly, using Na$_2$S as a sulfur source for SufBC$_2$D$_{alk}$ (Figure 6.3 C), clusters can be assembled. Previous results showed

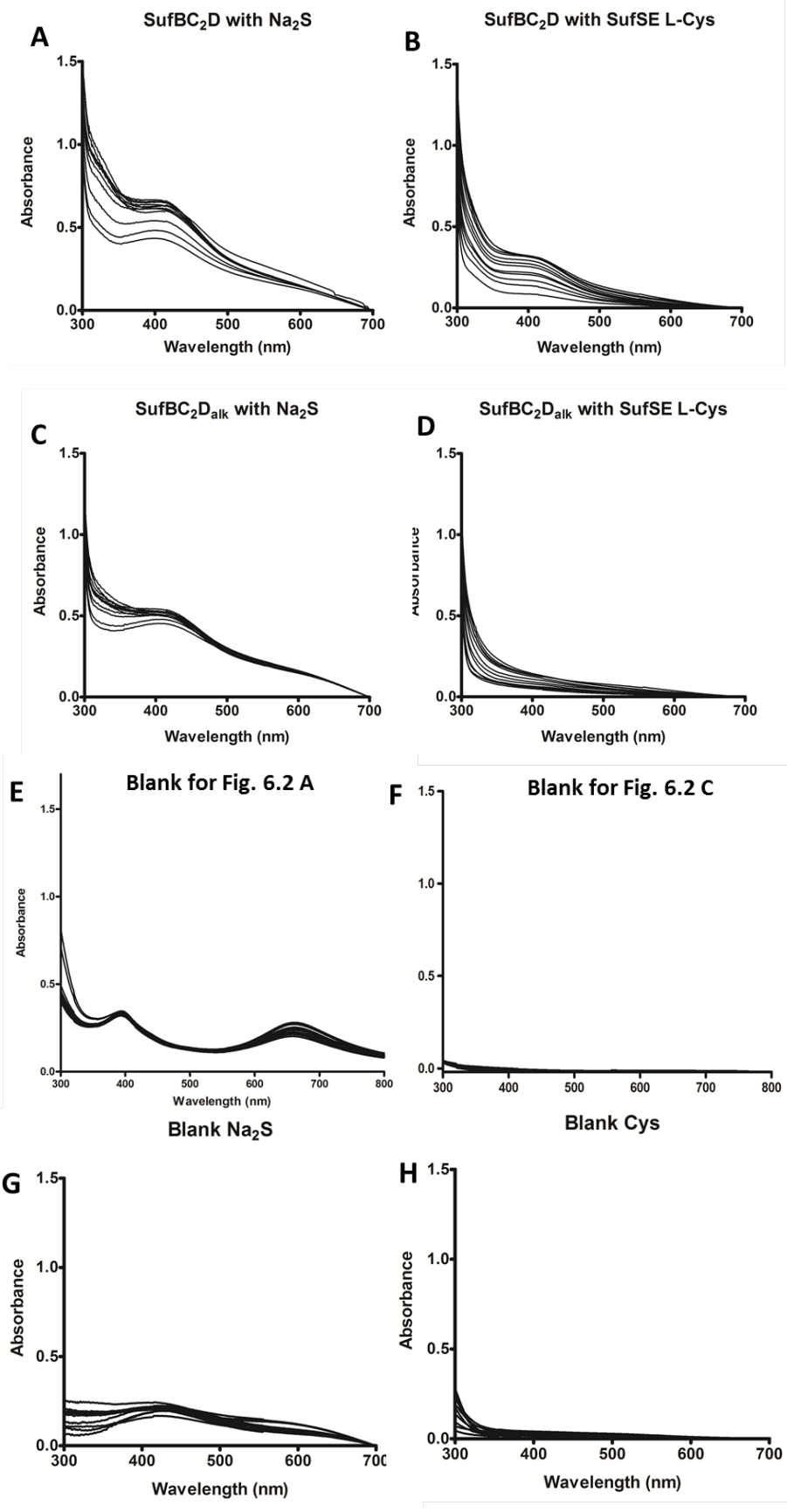
A
SufBC2D with Na2S
Absorbance
Wavelength (nm)
B
SufBC2D with SufSE L-Cys
Absorbance
Wavelength (nm)
C
SufBC2Dalk with Na2S
Absorbance
Wavelength (nm)
D
SufBC2Dalk with SufSE L-Cys
Wavelength (nm)
E
Blank for Fig. 6.2 A
Absorbance
Wavelength (nm)
Blank Na2S
F
Blank for Fig. 6.2 C
Blank Cys
G
Absorbance
Wavelength (nm)
H
Absorbance
Wavelength (nm)

Figure 6.3 UV-Vis absorption spectra change of $SufBC_2D$ and $SufB_2C_2$ during 2 hours cluster reconstitution. The spectrum was recorded every 10 min starting from 14 min to 124 min. (A) $SufBC_2D$ reconstitution with Na_2S as a sulfur source. (B) $SufBC_2D$ reconstitution with SufSE-Cys as a sulfur source. (C) $SufBC_2D_{alk}$ reconstitution with Na_2S as a sulfur source. (D) $SufBC_2D_{alk}$ reconstitution with SufSE-Cys as a sulfur source. The reconstitution reaction contained 50 μM $SufBC_2D$ or $SufB_2C_2$, 0.2 μM SufSE with 650 μM L-cysteine or 650 μM Na_2S , 300 μM $Fe^{2+}$and 2 mM DTT. Figure 6.13 Corresponding UV-Vis spectrum of controls for (E) Figure 6.2 A, (F) Figure 6.2 C, (G) Figure 6.4 A or C and (H) Figure 6.4 B or D. These samples are treated the same way for their corresponding reconstitution sample except with the scaffold protein.

that $SufBC_2D$ can enhance SufS desulfurase activity when SufE is present by removing the persulfide from SufE Cys51. We tested if $SufBC_2D_{alk}$ can still enhance SufSE activity. My colleague Guangchao Dong compared desulfurase activity of SufSE with $SufBC_2D_{alk}$ or unmodified $SufBC_2D$. He found that $SufBC_2D_{alk}$ lost its ability to enhance SufSE. Together these results indicated that alkylation of SufB may prevent its cysteines from receiving sulfur from SufSE, since those cysteines may be exposed to alkylation. The cluster reconstitution results suggest that one or more Cys residues on SufB receive sulfur from SufE and relay it to more protected cysteines that are involved in the clusters binding and are not sensitive to alkylation. $SufBC_2D_{alk}$ was sent for Mass Spectrometry analysis to identify which Cys residues were alkylated. Further mutation studies on the cysteines of $SufBC_2D$ are needed for validation of these results.

$SufB_2C_2$ may be a better sulfur acceptor from SufSE and can be reconstituted without DTT present more efficiently than $SufBC_2D$

TCEP is a stronger reductant than DTT when using sulfur liberation during the desulfurase enzyme reaction [70]. Previous study from the Dos Santos's lab indicated that in the presence of TCEP, sulfur cannot be transferred from SufE to $SufBC_2D$ [70]. Instead, SufE persulfide is directly reduced by TCEP and released as sulfide from SufE into the reaction solution. Reconstitution of the Fe-S cluster on $SufBC_2D$ and $SufB_2C_2$ in the presence of TCEP instead of DTT was performed. In agreement with Dos Santos's data, TCEP prevented the sulfur transferring from SufE to SufB and the reconstitution did not work on $SufBC_2D$ (Figure 6.4 A). However, we can see reconstitution worked on $SufB_2C_2$ even though it was not as efficient compared to reconstitution in the presence of DTT (Figure 6.4 B). This gave us a hint that $SufB_2C_2$

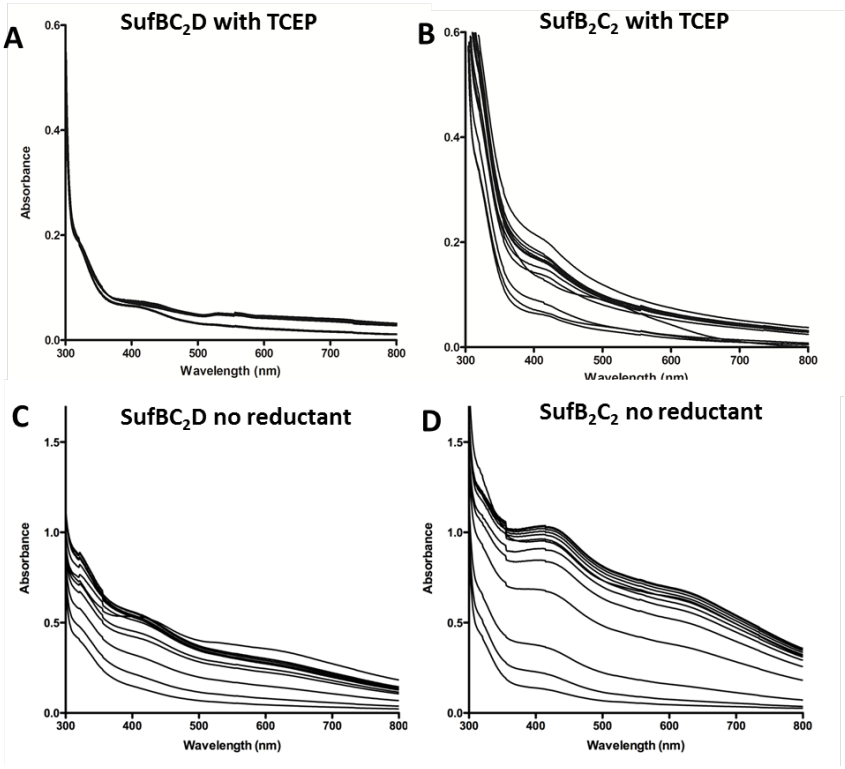

Figure 6.4 UV-Vis absorption spectra of $SufBC_2D$ and $SufB_2C_2$ at different reconstitution conditions. (A) The reconstitution reaction contained 50 μM $SufBC_2D$, 0.2 μM SufSE, 650 μM L-cysteine, 300 μM $Fe^{2+}$and 2 mM TCEP. (B) The reconstitution reaction contained 50 μM $SufB_2C_2$, 0.2 μM SufSE, 650 μM L-cysteine, 300 μM Fe^{2+} and 2 mM TCEP. (C) The reconstitution reaction contained 50 μM $SufBC_2D$, 0.2 μM SufSE, 650 μM L-cysteine and 300 μM Fe^{2+} without reductant. (D The reconstitution reaction contained 50 μM $SufB_2C_2$, 0.2 μM SufSE, 650 μM L-cysteine and 300 μM Fe^{2+} without reductant.

may be a better sulfur acceptor from SufE or that $SufB_2C_2$ is better at binding free S^{2-} released by TCEP than $SufBC_2D$. More surprisingly, both $SufBC_2D$ and $SufB_2C_2$ can be reconstituted with cluster in the absence of any reductant (Figure 6.4 C and D). The reconstitution is more efficient on $SufB_2C_2$ than $SufBC_2D$ in vitro with SufS-SufE-L-cysteine and ferrous ammonium sulfate as sulfur and iron source respectively. This result is consistent with our in vivo Suf Fe-S cluster assembly model. SufBC is needed for sulfur acquisition during assembly and SufD is needed for the iron acquisition [99]. If iron is provided as a readily available form (FAS), SufD becomes dispensable and may even hamper cluster assembly.

The Fe-S Clusters on $SufBC_2D$ and $SufB_2C_2$ are robust and resistant to aerobic conditions

Purified holo-$SufBC_2D$ and $SufB_2C_2$ were exposed to aerobic conditions. The UV-Vis absorption spectra did not change for at least 30 min (Figure 6.5 A and B) and longer times (2 hours) aerobic incubation also did not show significant cluster signal change. This result was in contrast to Wollers' 2010 result [71], which showed that cluster on $SufBC_2D$, was very sensitive to aerobic conditions. The UV-Vis absorption spectra of the cluster changed in 8 min in that study. However, our result is more consistent with the fact that Suf pathway works under oxidative stress conditions in *E. coli*.

Comparison of different purification methods for holo $SufBC_2D$ and $SufB_2C_2$

Anion exchange and desalting columns were both used for purification of holo proteins to remove contaminating iron sulfide species after reconstitution or in vivo expression. Results were published using both methods [45, 102]. For IscU, apo-IscU, Fe_2S_2-

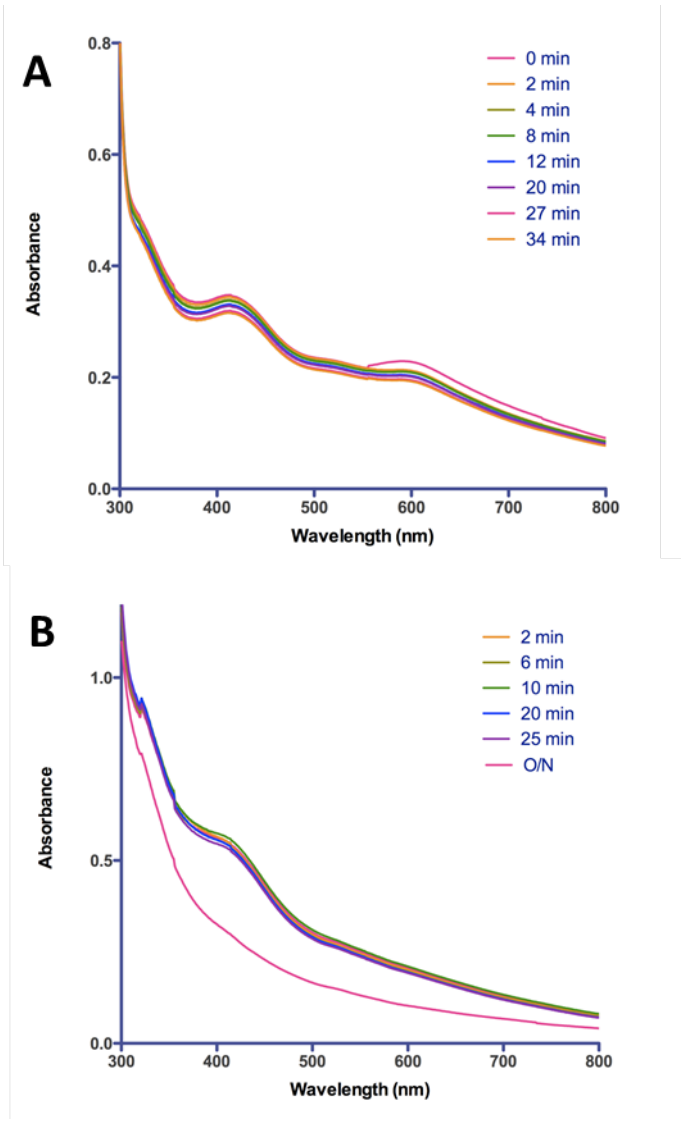

Figure 6.5 Cluster stability on $SufBC_2D$ and $SufB_2C_2$ in aerobic condition. (A) 50 µM holo $SufBC_2D$ was exposed to aerobic condition. And UV-Vis scan was performed in 30 min. (A) 50 µM holo $SufB_2C_2$ was exposed to aerobic condition. And UV-Vis scan was performed in 30 min and after over-night aerobic condition incubation.

-IscU and Fe_4S_4-IscU can be easily separated from each other on an anion exchange column [103]. We tested if anion exchange chromatography can separate the holo $SufBC_2D$ or $SufB_2C_2$ from the apo protein (Figure 6.6 A and 6.6 B). However, there was no separation of holo and apo proteins on the anion exchange column for either $SufBC_2D$ or $SufB_2C_2$. $SufBC_2D$ and $SufB_2C_2$ eluted out as a single peak containing both apo and holo proteins on the anion exchange column after either 2 hours reconstitution or 5 hours reconstitution reactions. I also tried to use the desalting column to separate protein from contaminating iron sulfide species. For this purification method, I first incubated the reconstitution mixture with equal molar EDTA: protein for 15 min and then loaded on the desalting column. Comparing these two methods (Figure 6.7 A and 6.7 B), we could see that desalting column helped protein retain more cluster but could not remove all the non-specific cluster species. However, anion exchange column may be too harsh for clusters on $SufBC_2D$ and $SufB_2C_2$. The cluster content based on UV-vis absorption spectra was much less. It should be noted that UV-visible absorption spectroscopy may not be definitive enough to say that actual cluster content is higher with desalting column purification since some non-specific iron sulfide species have similar features to the holo proteins.

Cluster transfer comparison for $SufBC_2D$ and $SufB_2C_2$ with or without ATP and DTT to AcnA

Through the activity change for AcnA, we can indirectly measure the cluster transfer efficiency from the SufB scaffold complexes. Apo AcnA is inactive while holo Fe_4S_4 AcnA has aconitase activity [104]. For $SufBC_2D$, the transfer efficiency was quite close for the four transfer conditions I tested which are: without DTT, ATP and KCl; with DTT but

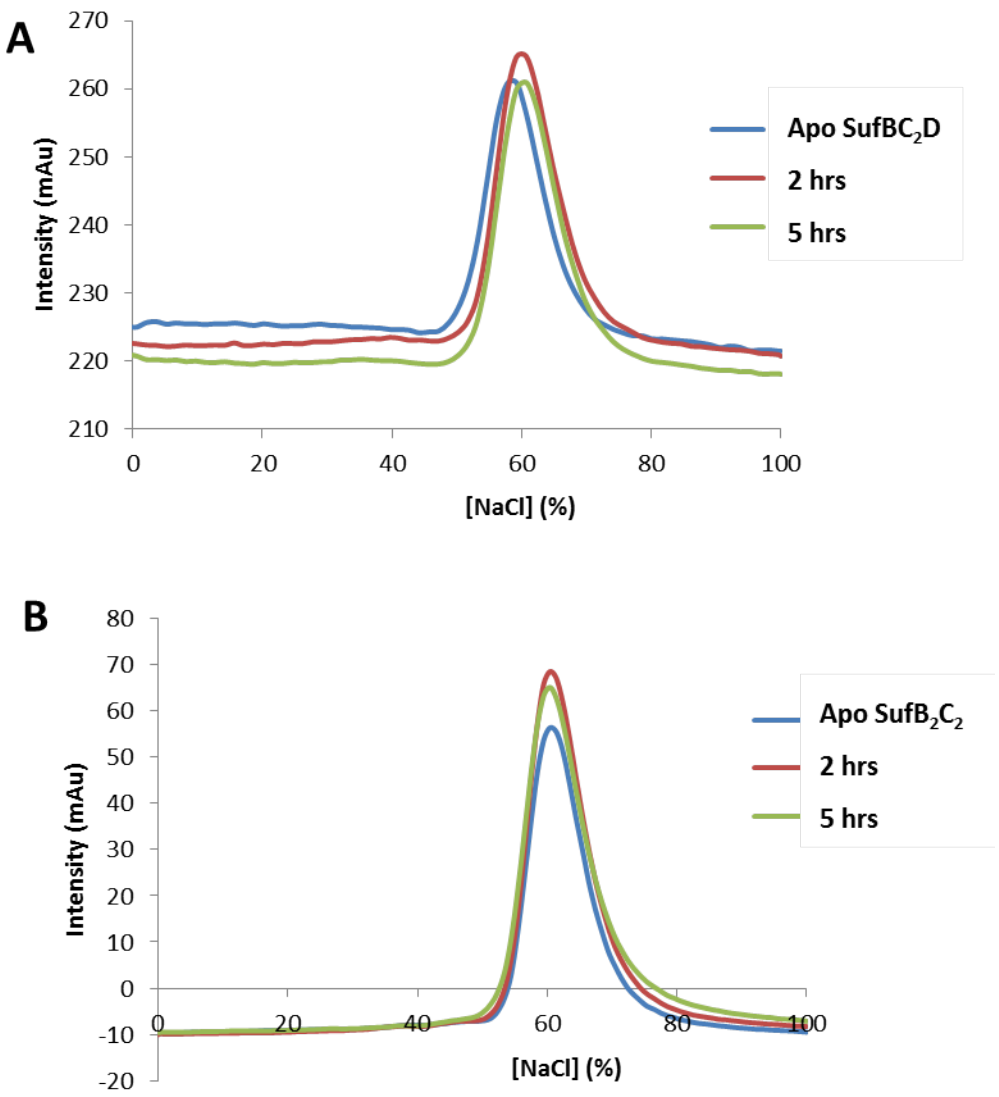

Figure 6.6 Anion exchange column purification profile on cluster reconstitution $SufBC_2D$ (A) and $SufB_2C_2$ (B) at different reconstitution time.

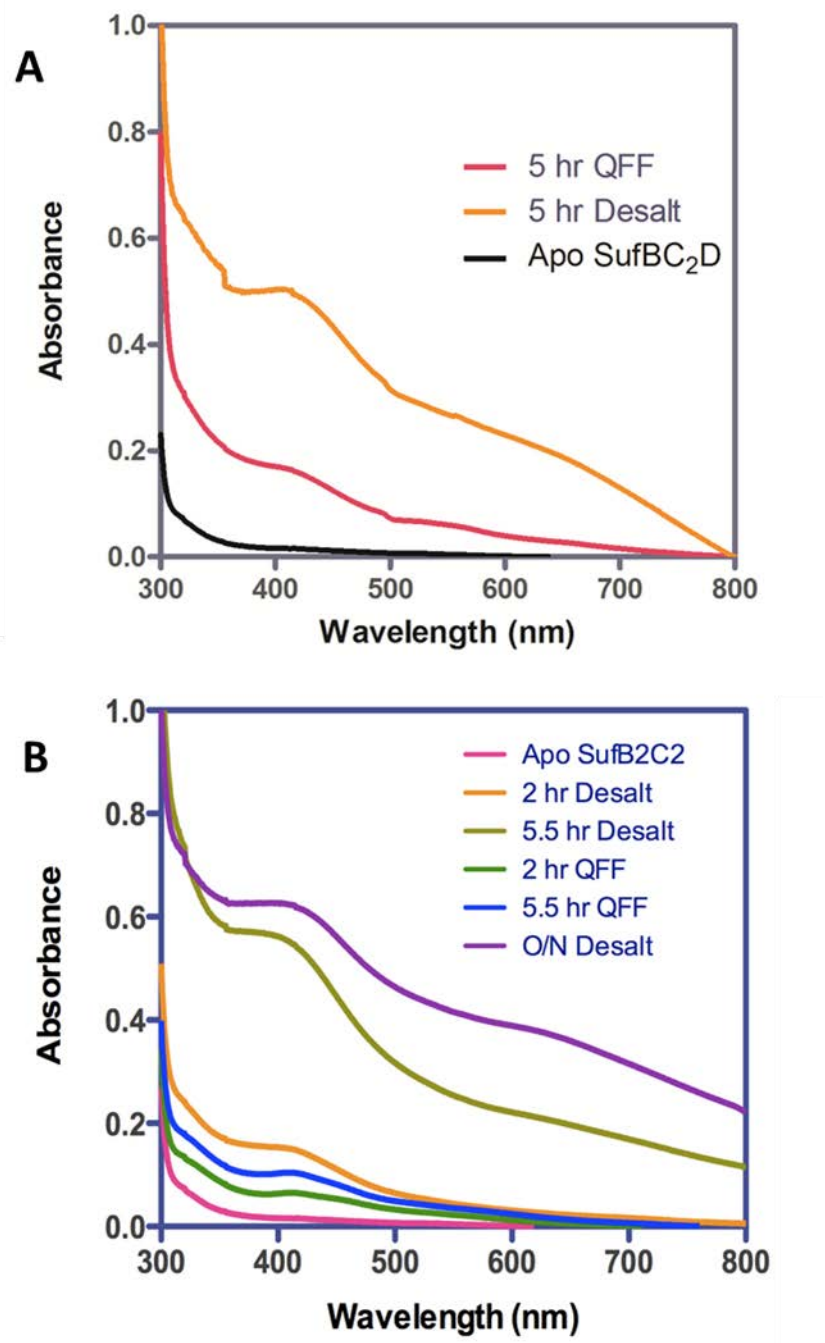

Figure 6.7 UV-Vis absorption spectra of sample from desalting column and anion exchange column purification after cluster reconstitution on $SufBC_2D$ (A) and $SufB_2C_2$ (B).

without ATP and KCl; with DTT and ATP but without KCl; and with DTT, ATP and KCl (Figure 6.8). UV-Vis spectra of holo $SufBC_2D$ and $SufB_2C_2$ used for the cluster transfer assays is shown in Figure 6.9. Both of the holo complexes were purified with anion exchange column after reconstitution to completely remove contaminating species. For $SufB_2C_2$, the transfer efficiency was similar with or without ATP and KCl like $SufBC_2D$. However, DTT did make a difference. $SufB_2C_2$ cannot transfer cluster to AcnA in the absence of DTT (Figure 6.8 B). So the cluster transfer mechanism for $SufBC_2D$ and $SufB_2C_2$ may be different. Overall, the transfer efficiency for $SufBC_2D$ and $SufB_2C_2$ was similar and ATPase activity for SufC had no effect on the cluster transfer from either complex to AcnA.

Efforts to purify holo $SufBC_2D$ in anaerobic chamber

I tried to purify holo native $SufBC_2D$ after overexpressing the whole *sufABCDSE* operon (Figure 6.10 A and B). Early results indicated that apo $SufBC_2D$ and holo $SufBC_2D$ can be separated at the first step using a hydrophobic interaction column (Figure 6.10 A). The protein gel showed $SufBC_2D$ was present in two peaks. These two peaks have different UV-Vis spectra. The peak containing fraction 7 had bright yellow color. Meanwhile, the peak containing fraction 14 had dark green color. In both peaks, SufS co-eluted with $SufBC_2D$ and PLP 420 nm peaks were observed in the UV-vis absorption spectra. Other than the PLP signal, it seemed to have Fe-S cluster signal due to the presence of the 320 nm shoulder and 620 nm shoulder. However, pure holo $SufBC_2D$ could not be purified on the anion exchange column (Figure 6.10 B and Figure 6.11 B). The peak containing $SufBC_2D$ also contained other proteins (Figure 6.12 B). The bands in the holo sample fraction were separated on SDS-PAGE protein gels (Figure 6.12

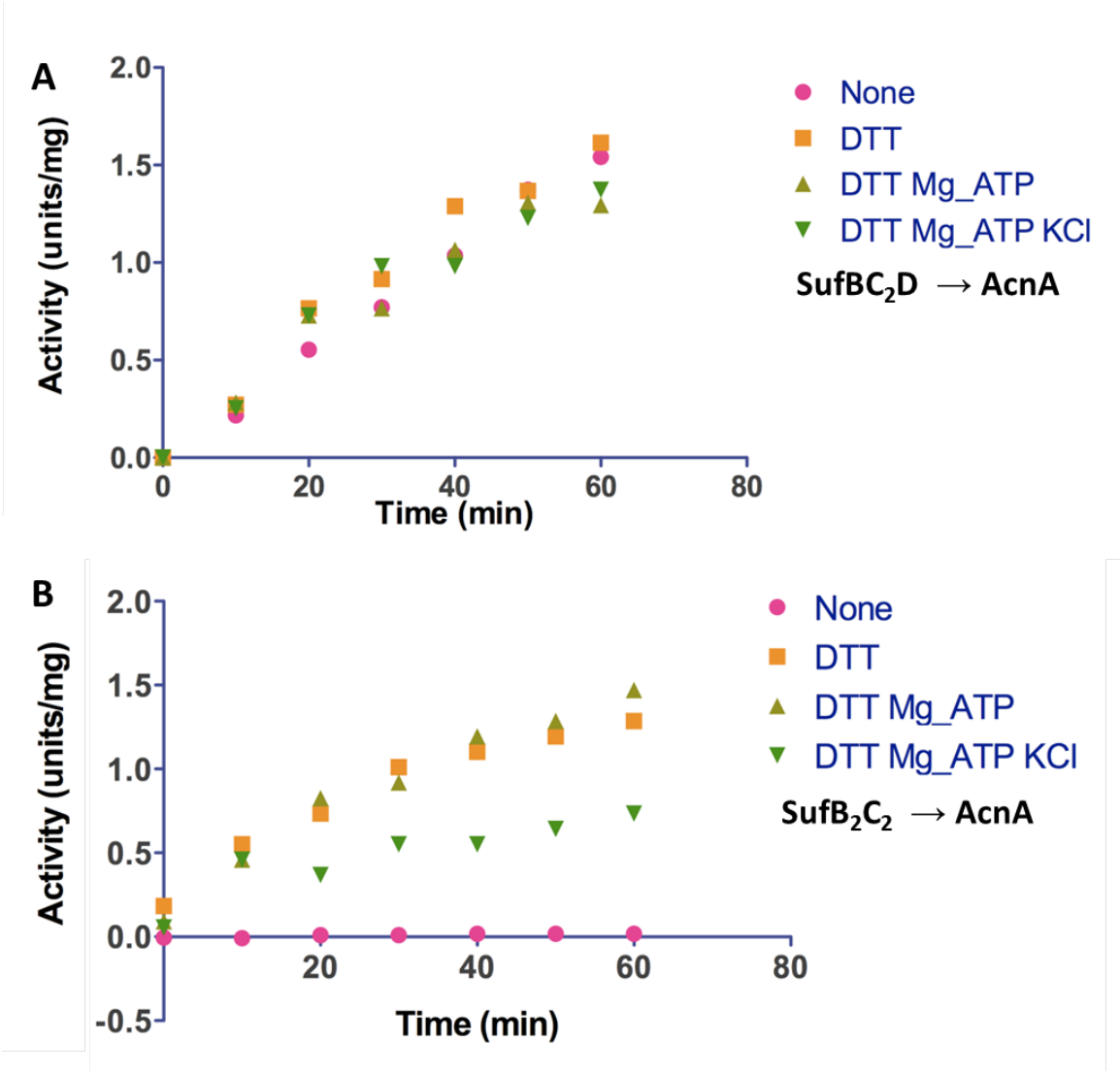

Figure 6.8 Aconitase activity at 0, 10, 20, 30, 40, 50, 60 min after incubating with equal molar ratio (AcnA to Fe_4S_4) of holo-SufBC_2D (A) and SufB_2C_2 (B).

B) and analyzed with MALDI-MS. The top scored candidate of MS1 band is 60 kDa chaperonin 1 (GroL1). This protein prevents misfolding and promotes the refolding and proper assembly of unfolded polypeptides generated under stress conditions. The top scored candidate of MS2 band is elongation factor Tu2. This protein promotes the GTP-dependent binding of aminoacyl-tRNA to the A-site of ribosomes during protein biosynthesis. The specificity of the binding between these two proteins and holo-SufBC$_2$D needs further validation. It may just due protein overexpression that these two translational/folding proteins co-elute on anion exchange column with SufBC$_2$D. We could try to further purify with size exclusion column in the future.

DISCUSSION

Whether the linear Fe_3S_4 cluster is an intermediate for cluster assemble is still an open question.

Previous studies in our lab indicated the presence of a linear Fe_3S_4 cluster on SufB$_2$C$_2$ or SufBC$_2$D [99]. It is possible a Fe_4S_4 degradation product or a biosynthetic precursor for cluster assembly in Suf system. Either possibility makes the Suf system a unique one which is different from the Isc system, since the degradation intermediate or biosynthetic intermediate on IscU is Fe_2S_2[103]. Spectra analysis of the real time cluster reconstitution on SufB$_2$C$_2$ and SufBC$_2$D indicated the possible presence of a linear Fe_3S_4 intermediate on SufBC$_2$D but not on SufB$_2$C$_2$. If this is true, the cluster assembly process is different for these two complexes. Previous studies indicated that SufD and SufC ATPase acitivity are required for iron acquisition during in vivo Fe-S cluster formation on SufB. Since the iron donor in vivo is unknown yet, for our in vitro reconstitution

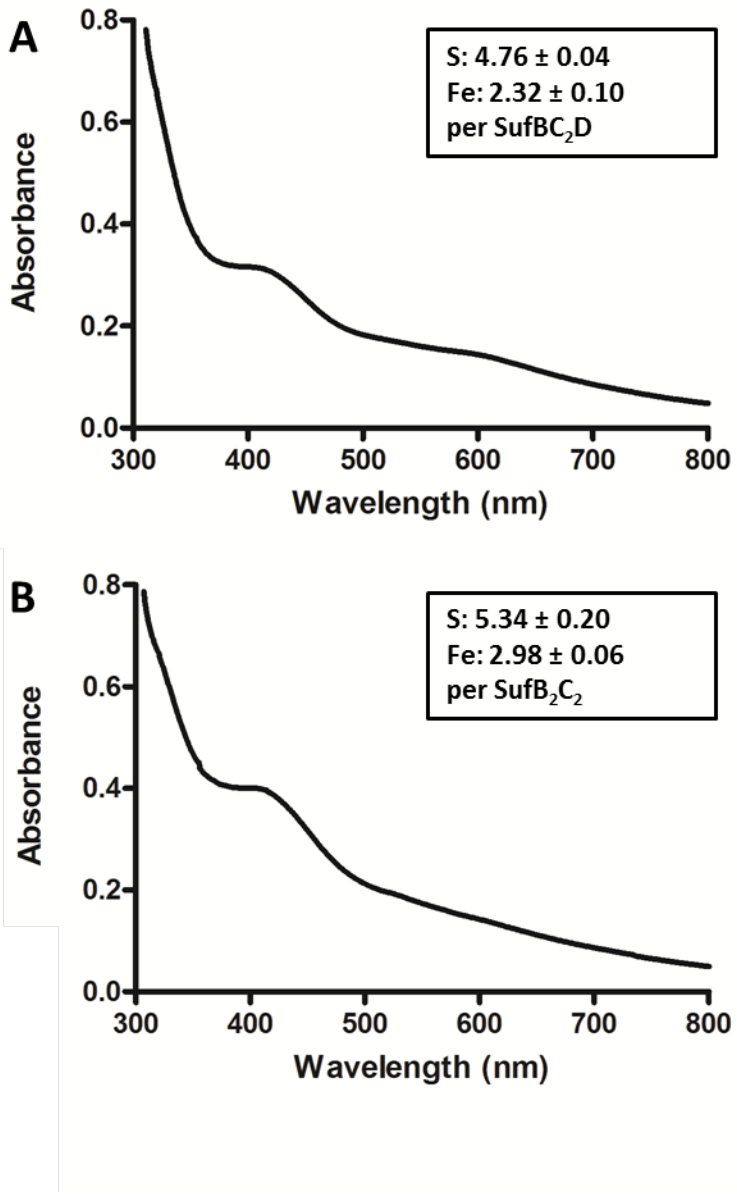

Figure 6.9 UV-Vis absorption spectra of holo $SufBC_2D$ (A) and $SufB_2C_2$ (B) used in the AcnA cluster transfer assay. The iron and sulfur content of the purified samples were labeled in the imbedded tables.

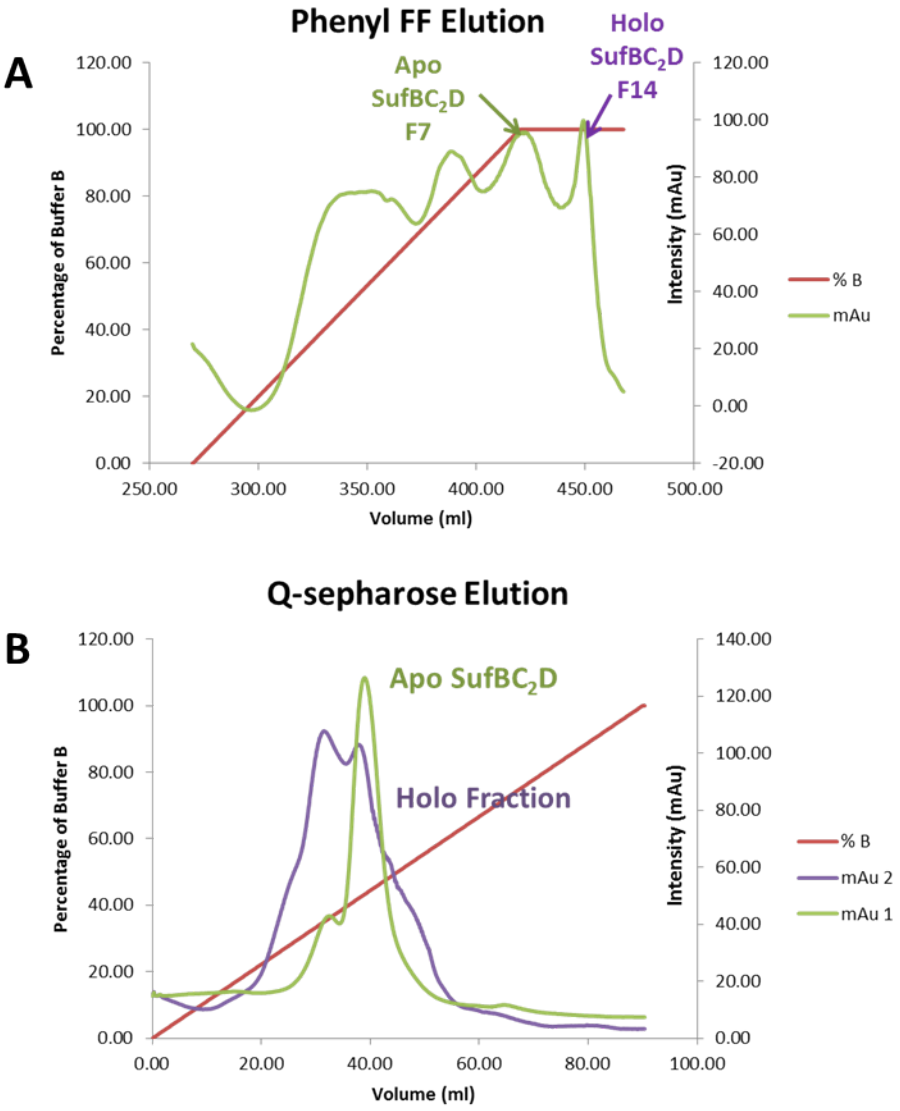

Figure 6.10 Anaerobic purification of $SufBC_2D$. (A) Phenyl column purification profile. (B) UV-Vis absorption spectra of fraction 7 and 14 from phenyl column purification. (B) Anion exchange column purification profile.

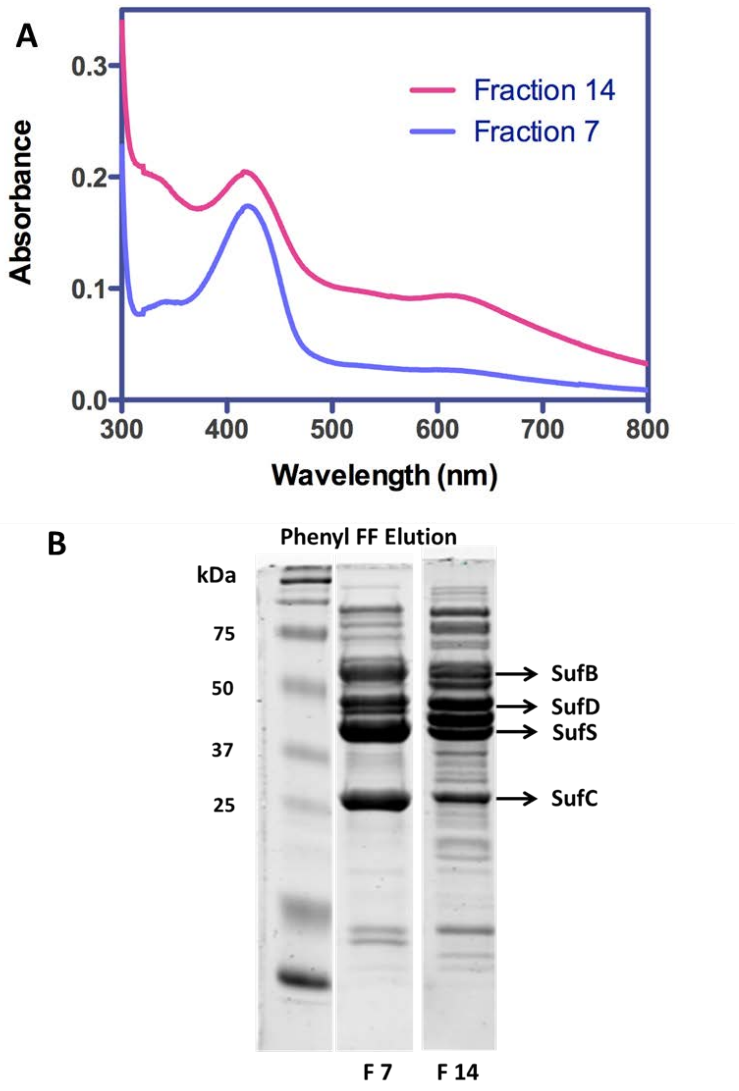

Figure 6.11 (A) UV-Vis absorption spectra of fraction 7 and 14 from phenyl column purification. (B) Protein separation of fraction 7 and 14 from phenyl FF column on a 15% SDS-PAGE reducing gel.

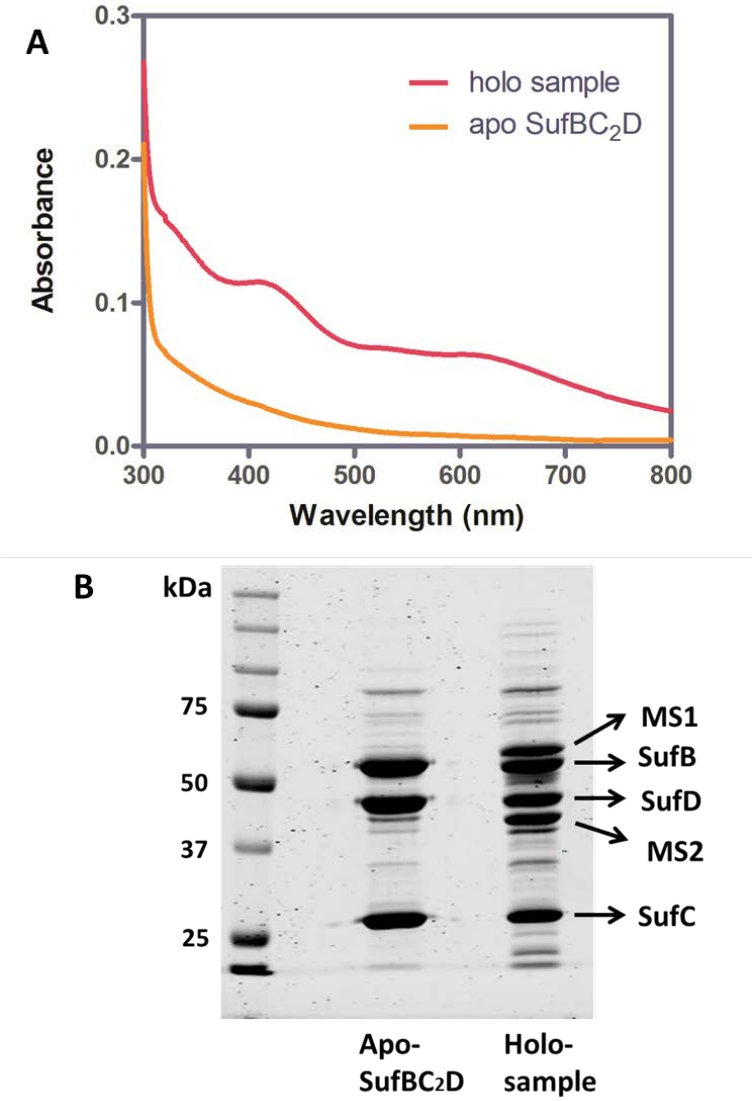

Figure 6.12 (A) UV-Vis absorption spectra of final collection sample from anion exchange column purification. (B) Protein separation of final smaple from anion exchange column on a 15% SDS-PAGE reducing gel. The MS1 and MS2 bands were cut out for mass spectrometry analysis.

experiment we used a readily available iron source Fe^{2+} (ferrous ammonium sulfate). Under this condition, $SufB_2C_2$ did not have any disadvantage for iron incorporation due to lack of SufD. The spectra analysis indicated the Fe_4S_4 cluster after 14 min. Either cluster intermediates happened at earlier time and were missed in our time course or $SufB_2C_2$ preferentially accommodated the intact Fe_4S_4 cluster rather than other cluster intermediates. The latter explanation is consistent with the putative role we proposed for $SufB_2C_2$ that $SufB_2C_2$ is the final cluster scaffold complex that occurs via a $SufBC_2D$ intermediate complex used for iron acquisition. The presence of the linear Fe_3S_4 cluster on $SufBC_2D$ also fits our model for in vivo Suf Fe-S cluster assembly, possibly using "sulfur first and iron second" mechanism for cluster assembly since 4 sulfur atoms were already present in the scaffold complex. However, the results here are preliminary. More techniques like variable temperature magnetic circular dichroism (VT-MCD) and electron paramagnetic resonance (EPR) spectroscopy are needed for the further confirmation of the linear Fe_3S_4 cluster besides the initial UV-vis spectra analysis. The finding of the actual iron donor in vivo also may help us better discriminate the functional difference between $SufBC_2D$ and $SufB_2C_2$.

Functional difference of the cysteines on SufB

There are 13 cysteines on SufB. One Fe_4S_4 cluster only needs 4 cysteines for binding. What are the cluster binding cysteines on SufB? What are the functions of the other cysteines? These questions are always puzzles. Initial testing and mutation analysis were made but no solid conclusion can be made. To answer the question, I first alkylated the $SufBC_2D$ complex. The alkylation separated the cysteines on SufB to two types, one is iodoactemide (IAA) accessible cysteines which may be more exposed and solvent

accessible and the other is IAA inaccessible cysteines which may be more buried or oxidized. Desulfurase activity assays showed that $SufBC_2D_{alk}$ can no longer enhance SufSE activity. This meant that the sulfur receiving cysteine on SufB was alkylated by IAA. However, cluster can still be assembled on $SufBC_2D_{alk}$ using Na_2S as a sulfur source, which indicated that the cluster binding cysteines were still unmodified after iodoacetamide treatment. It also gave us a hint that there may be a sulfur relaying system on SufB. Firstly the more exposed cysteines receive sulfur from SufE and then relay the sulfur to the cluster binding cysteines for cluster assembly. Mass spectrometry analysis of $SufBC_2D_{alk}$ will help us locate the cysteines on SufB which are alkylated and which are unmodified. Further mutation study of cysteines on $SufBC_2D$ is needed for validation of these results.

$SufB_2C_2$ can be reconstituted with Fe-S cluster using SufSE-L-Cys system when TCEP is present and can be reconstituted in the absence of DTT more efficiently than $SufBC_2D$

$SufBC_2D$ cannot be reconstituted with Fe-S cluster using SufSE-L-Cys system when TCEP is present (Figure 6.4 A). However, we know that $SufBC_2D$ can be reconstituted with cluster when using Na_2S as a sulfur source. If TCEP is only involved in sulfide S^{2-} release, then $SufBC_2D$ should assemble the cluster by binding the released sulfide in solution. The unsuccessful reconstitution means that TCEP did more than just S^{2-} release and also made some changes on $SufBC_2D$, like breaking the possible disulfide bonds to change the conformation of $SufBC_2D$, or the cluster binding cysteines is accessible to TCEP which prevents the sulfur binding for cluster assembly (by removing persulfides before they can assemble with iron). However, TCEP pretreatment of $SufBC_2D$ did not

affect the cluster reconstitution. This leaves open the latter possibility. To confirm this, we can do the cluster reconstitution experiments on SufBC$_2$D and SufBC$_2$D$_{alk}$ with Na$_2$S and TCEP together to see whether the reconstitution is successful.

SufB$_2$C$_2$ can be reconstituted with Fe-S cluster using SufSE-L-cys system when TCEP is present but SufBC$_2$D cannot (Figure 6.4 A and B). This gave us a hint that SufB$_2$C$_2$ may be a better sulfur acceptor from SufE or that SufB$_2$C$_2$ is better at binding free S^{2-} released by TCEP than SufBC$_2$D. To test if SufB$_2$C$_2$ still can receive sulfur from SufSE, we can check whether this complex can affect SufSE activity when TCEP is present. We know that TCEP can bypass the sulfur transfer step from SufE to SufB [70]. In SufBC$_2$D, preventing further enhancement of SufSE activity when using TCEP as sulfide releasing reagent instead of DTT. However, the reaction showed slight inhibition for SufSE activity due to the possible interference of SufE and SufBC$_2$D interaction on TCEP reduction [70]. If SufB$_2$C$_2$ can still receive sulfur from SufE, SufB$_2$C$_2$ may further inhibit the desulfurase activity in the presence of TCEP by binding and blocking TCEP access to SufE Cys51. We also can use the radioactive L-cys as the substrate to monitor the sulfur destination in the SufSE, SufB$_2$C$_2$ and TCEP mixture. This may be a more straightforward and easier way to test the hypothesis. The ability of SufB$_2$C$_2$ to accommodate a cluster when TCEP is present indicated the conformation of SufB$_2$C$_2$ may be more compacted and less affected by strong reductant interference. We can also alkylate the SufB$_2$C$_2$ to see its effect on the cluster reconstitution when using SufSE-L-cys or Na$_2$S as sulfur sources.

The reconstitution is more efficient on SufB$_2$C$_2$ than SufBC$_2$D in vitro with SufS-SufE-L-cysteine and ferrous ammonium sulfate as sulfur and iron source

respectively (Figure 6.4 C and D). This result is consistent with our in vivo Suf Fe-S cluster assembly model. SufBC is needed for sulfur acquisition during assembly and SufD is needed for the iron acquisition. If iron is provided as a readily available form (FAS), SufD becomes dispensable and may even hamper cluster assembly. The conformation of SufB in $SufBC_2D$ may be different from it in the $SufB_2C_2$ complex. In the $SufB_2C_2$ complex SufB may be in a better conformation for sulfur incorporation and cluster binding.

The Fe-S Clusters on $SufBC_2D$ and $SufB_2C_2$ are resistant to aerobic conditions

The Fe-S clusters on $SufBC_2D$ and $SufB_2C_2$ are resistant to aerobic conditions (Figure 6.5 A and B). This result helps us understand why the Suf system is better adapted to function under oxidative stress conditions besides the advantage of using SufSE as a sulfur source compared IscU using IscS. We can include holo-IscU in this experiment to carefully compare the oxidative sensitivity of the clusters on the scaffold protein in Suf and Isc system. Since the clusters on $SufBC_2D$ and $SufB_2C_2$ are very robust at aerobic conditions, we can treat the samples with H_2O_2 to monitor a quicker cluster change and may help us detect the possible degradation products.

Phenyl FF column may be used to separate holo-$SufBC_2D$ from its apo form.

The anion exchange column cannot separate holo form from apo form for both $SufBC_2D$ and $SufB_2C_2$ (Figure 6.6 A and B). However, when I tried to purify $SufBC_2D$ anaerobically, I did see a separation of holo-form and apo-form on the phenyl FF column (Figure 6.10 A). This raised the possibility that phenyl FF column may be applied for holo- $SufBC_2D$ purification. I also tried to use a desalting column to purification (Figure

6.7 A and B). However, even though this method had a higher protein recovery compared to the anion exchange column purification, it cannot remove all the non-specific Fe-S species. I recommend that if you use a small amount of scaffold protein, such as under 100 μM, you can use a desalting column for purification to have enough sample for further testing. If you have a large reconstitution sample, you had better used the anion exchange column for purification. The samples from the anion exchange column are better for CD or EPR experiments. Further testing of the phenyl column may also show that hydrophobic interaction chromatography is a good way to purify the proteins after reconstitution.

ATPase activity of SufC is not involved in the cluster transfer from $SufBC_2D$ or $SufB_2C_2$ to AcnA.

SufC has low basal ATPase activity. However, the activity is accelerated by SufB [101]. Including the ATPase enzyme substrate Mg_ATP in the cluster transfer reaction, I did not see a difference in the cluster transfer efficiency to AcnA for either $SufBC_2D$ or $SufB_2C_2$. It seemed ATPase activity of SufC is not involved in the cluster transfer from $SufBC_2D$ or $SufB_2C_2$ to AcnA. However, the highest activity for my AcnA was low which is around 1.76 units/mg. The specific activity for AcnA should be about 15 units/mg [105]. There are several possibilities for the low activity of AcnA here. First possibility is that AcnA itself was damaged during purification or EDTA and potassium ferricyanide treatment. I reconstituted AcnA with Na_2S and FAS and checked its activity. It was 6.59 units/mg. It was still lower than the published value but higher than the activity after cluster transfer from $SufBC_2D$ or $SufB_2C_2$. Secondly, the amount of cluster on $SufBC_2D$ or $SufB_2C_2$ I provided may not be enough for full activation of AcnA. I did

calculate the cluster content and tried to provide an equal Fe_4S_4 molar ratio to AcnA (Figure 6.9). Experiments need to be repeated to fully clarify these questions. There was an interesting finding for $SufB_2C_2$. Holo-$SufB_2C_2$ cannot transfer its clusters to AcnA without DTT (Figure 6.9 B). The requirement for DTT showed that cluster transfer from $SufB_2C_2$ to aconitase may involve intermediate disassembly of the cluster, release of iron and sulfur in solution, and then reassembly in the target AcnA protein. We can have EDTA in the transfer mixture to see if it can inhibit the cluster transfer. Alternatively, DTT may coordinate and remove the intact cluster from SufB forming a small molecular weight cluster in solution, which is then bound and trapped in AcnA. KCl also inhibited cluster transfer from holo-$SufB_2C_2$ to AcnA. The high salt concentration (100 mM KCl) may interfere with the cluster transfer. I am not sure the actual mechanism for this phenomenon but it is consistent with protein/cluster loss from SufB on the anion exchange column, which uses high salt to elute the proteins.

Suf system may work for the newly synthesized protein correctly folding and cluster incorporation under stress conditions.

When I purified the holo-$SufBC_2D$ at anaerobic condition, I found that an elongation factor and a chaperon protein were co-eluted with holo-$SufBC_2D$ (Figure 6.12 B). The chaperon protein is 60 kDa chaperonin 1 (GroL1) which prevents misfolding and promotes the refolding and proper assembly of unfolded polypeptides generated under stress conditions. The elongation factor is Tu2 which promotes the GTP-dependent binding of aminoacyl-tRNA to the A-site of ribosomes during protein biosynthesis. . The specificity of the binding between these two proteins and holo-$SufBC_2D$ needs further validation. However, it raises the possibility that the Suf system may directly bind to the

protein translational machinery and chaperon proteins for the newly synthesized protein to mediate correc folding and cluster incorporation under stress conditions. This may be another advantage using Suf system for cluster assembly under stress conditions.

The data for this chapter is preliminary and opens lots of questions. Solid conclusions cannot yet be made based on these results but lots of interesting hypothesis were proposed. Further experiments to answer those questions should help us understand more about the Suf system.

References

1. Ratledge, C., and Dover, L. G. (2000) Iron metabolism in pathogenic bacteria, *Annual review of microbiology 54*, 881-941.
2. Nunoshiba, T., Obata, F., Boss, A. C., Oikawa, S., Mori, T., Kawanishi, S., and Yamamoto, K. (1999) Role of iron and superoxide for generation of hydroxyl radical, oxidative DNA lesions, and mutagenesis in Escherichia coli, *The Journal of biological chemistry 274*, 34832-34837.
3. Briat, J. F. (1992) Iron assimilation and storage in prokaryotes, *Journal of general microbiology 138*, 2475-2483.
4. Winterbourn, C. C. (1995) Toxicity of iron and hydrogen peroxide: the Fenton reaction, *Toxicology letters 82-83*, 969-974.
5. Amir, A., Meshner, S., Beatus, T., and Stavans, J. (2010) Damped oscillations in the adaptive response of the iron homeostasis network of E. coli, *Molecular microbiology 76*, 428-436.
6. Beinert, H., Holm, R. H., and Munck, E. (1997) Iron-sulfur clusters: nature's modular, multipurpose structures, *Science 277*, 653-659.
7. Rouault, T. A., and Tong, W. H. (2008) Iron-sulfur cluster biogenesis and human disease, *Trends in genetics : TIG 24*, 398-407.
8. Kiley, P. J., and Beinert, H. (1998) Oxygen sensing by the global regulator, FNR: the role of the iron-sulfur cluster, *FEMS microbiology reviews 22*, 341-352.
9. Reeve, J. N., Beckler, G. S., Cram, D. S., Hamilton, P. T., Brown, J. W., Krzycki, J. A., Kolodziej, A. F., Alex, L., Orme-Johnson, W. H., and Walsh, C. T. (1989) A hydrogenase-linked gene in Methanobacterium thermoautotrophicum strain delta H encodes a polyferredoxin, *Proceedings of the National Academy of Sciences of the United States of America 86*, 3031-3035.
10. Furne, J., Saeed, A., and Levitt, M. D. (2008) Whole tissue hydrogen sulfide concentrations are orders of magnitude lower than presently accepted values, *American journal of physiology. Regulatory, integrative and comparative physiology 295*, R1479-1485.
11. Berglin, E. H., and Carlsson, J. (1985) Potentiation by sulfide of hydrogen peroxide-induced killing of Escherichia coli, *Infection and immunity 49*, 538-543.
12. Ayala-Castro, C., Saini, A., and Outten, F. W. (2008) Fe-S cluster assembly pathways in bacteria, *Microbiology and molecular biology reviews : MMBR 72*, 110-125, table of contents.
13. Vinella, D., Brochier-Armanet, C., Loiseau, L., Talla, E., and Barras, F. (2009) Iron-sulfur (Fe/S) protein biogenesis: phylogenomic and genetic studies of A-type carriers, *PLoS genetics 5*, e1000497.

14. Johnson, D. C., Dean, D. R., Smith, A. D., and Johnson, M. K. (2005) Structure, function, and formation of biological iron-sulfur clusters, *Annual review of biochemistry 74*, 247-281.
15. Sendra, M., Ollagnier de Choudens, S., Lascoux, D., Sanakis, Y., and Fontecave, M. (2007) The SUF iron-sulfur cluster biosynthetic machinery: sulfur transfer from the SUFS-SUFE complex to SUFA, *FEBS letters 581*, 1362-1368.
16. Gupta, V., Sendra, M., Naik, S. G., Chahal, H. K., Huynh, B. H., Outten, F. W., Fontecave, M., and Ollagnier de Choudens, S. (2009) Native Escherichia coli SufA, coexpressed with SufBCDSE, purifies as a [2Fe-2S] protein and acts as an Fe-S transporter to Fe-S target enzymes, *Journal of the American Chemical Society 131*, 6149-6153.
17. Hidese, R., Mihara, H., and Esaki, N. (2011) Bacterial cysteine desulfurases: versatile key players in biosynthetic pathways of sulfur-containing biofactors, *Appllied Microbiology and Biotechnology 91*, 47-61.
18. Mihara, H., Fujii, T., Kato, S., Kurihara, T., Hata, Y., and Esaki, N. (2002) Structure of external aldimine of Escherichia coli CsdB, an IscS/NifS homolog: implications for its specificity toward selenocysteine, *Journal of biochemistry 131*, 679-685.
19. Mihara, H., Kato, S., Lacourciere, G. M., Stadtman, T. C., Kennedy, R. A., Kurihara, T., Tokumoto, U., Takahashi, Y., and Esaki, N. (2002) The iscS gene is essential for the biosynthesis of 2-selenouridine in tRNA and the selenocysteine-containing formate dehydrogenase H, *Proceedings of the National Academy of Sciences of the United States of America 99*, 6679-6683.
20. Mihara, H., Maeda, M., Fujii, T., Kurihara, T., Hata, Y., and Esaki, N. (1999) A nifS-like gene, csdB, encodes an Escherichia coli counterpart of mammalian selenocysteine lyase. Gene cloning, purification, characterization and preliminary x-ray crystallographic studies, *The Journal of biological chemistry 274*, 14768-14772.
21. Lima, C. D. (2002) Analysis of the E. coli NifS CsdB protein at 2.0 A reveals the structural basis for perselenide and persulfide intermediate formation, *Journal molecular biology 315*, 1199-1208.
22. Kaiser, J. T., Bruno, S., Clausen, T., Huber, R., Schiaretti, F., Mozzarelli, A., and Kessler, D. (2003) Snapshots of the cystine lyase C-DES during catalysis. Studies in solution and in the crystalline state, *The Journal of biological chemistry 278*, 357-365.
23. Outten, F. W., Wood, M. J., Munoz, F. M., and Storz, G. (2003) The SufE protein and the SufBCD complex enhance SufS cysteine desulfurase activity as part of a sulfur transfer pathway for Fe-S cluster assembly in Escherichia coli, *The Journal of biological chemistry 278*, 45713-45719.
24. Jang, S., and Imlay, J. A. (2010) Hydrogen peroxide inactivates the Escherichia coli Isc iron-sulphur assembly system, and OxyR induces the Suf system to compensate, *Molecular microbiology 78*, 1448-1467.
25. Huet, G., Daffe, M., and Saves, I. (2005) Identification of the Mycobacterium tuberculosis SUF machinery as the exclusive mycobacterial system of [Fe-S] cluster assembly: evidence for its implication in the pathogen's survival, *Journal of bacteriology 187*, 6137-6146.

26. Meyer, J. (2008) Iron-sulfur protein folds, iron-sulfur chemistry, and evolution, *Journal of biological inorganic chemistry : JBIC : a publication of the Society of Biological inorganic chemistry 13*, 157-170.
27. Sheftel, A., Stehling, O., and Lill, R. (2010) Iron-sulfur proteins in health and disease, *Trends in endocrinology and metabolism: TEM 21*, 302-314.
28. Shepard, E. M., Boyd, E. S., Broderick, J. B., and Peters, J. W. (2011) Biosynthesis of complex iron-sulfur enzymes, *Current opinion in chemical biology 15*, 319-327.
29. Xu, X. M., and Moller, S. G. (2011) Iron-sulfur clusters: biogenesis, molecular mechanisms, and their functional significance, *Antioxidants & redox signaling 15*, 271-307.
30. Rouault, T. A. (2012) Biogenesis of iron-sulfur clusters in mammalian cells: new insights and relevance to human disease, *Disease models & mechanisms 5*, 155-164.
31. Imlay, J. A. (2006) Iron-sulphur clusters and the problem with oxygen, *Molecular microbiology 59*, 1073-1082.
32. Nachin, L., El Hassouni, M., Loiseau, L., Expert, D., and Barras, F. (2001) SoxR-dependent response to oxidative stress and virulence of Erwinia chrysanthemi: the key role of SufC, an orphan ABC ATPase, *Molecular microbiology 39*, 960-972.
33. Nachin, L., Loiseau, L., Expert, D., and Barras, F. (2003) SufC: an unorthodox cytoplasmic ABC/ATPase required for [Fe-S] biogenesis under oxidative stress, *The EMBO journal 22*, 427-437.
34. Outten, F. W., Djaman, O., and Storz, G. (2004) A suf operon requirement for Fe-S cluster assembly during iron starvation in Escherichia coli, *Molecular microbiology 52*, 861-872.
35. Takahashi, Y., and Tokumoto, U. (2002) A third bacterial system for the assembly of iron-sulfur clusters with homologs in archaea and plastids, *The Journal of biological chemistry 277*, 28380-28383.
36. Kambampati, R., and Lauhon, C. T. (1999) IscS is a sulfurtransferase for the in vitro biosynthesis of 4-thiouridine in Escherichia coli tRNA, *Biochemistry 38*, 16561-16568.
37. Takahashi, Y., and Nakamura, M. (1999) Functional assignment of the ORF2-iscS-iscU-iscA-hscB-hscA-fdx-ORF3 gene cluster involved in the assembly of Fe-S clusters in Escherichia coli, *Journal of biochemistry 126*, 917-926.
38. Agar, J. N., Zheng, L., Cash, V. L., Dean, D. R., and Johnson, M. K. (2000) Role of the IscU Protein in Iron-Sulfur Cluster Biosynthesis: IscS-mediated Assembly of a 2Fe-2S Cluster in IscU, *Journal of the american chemical society 122*, 2136-2137.
39. Mihara, H., Kurihara, T., Yoshimura, T., and Esaki, N. (2000) Kinetic and mutational studies of three NifS homologs from Escherichia coli: mechanistic difference between L-cysteine desulfurase and L-selenocysteine lyase reactions, *Journal of biochemistry 127*, 559-567.
40. Schwartz, C. J., Djaman, O., Imlay, J. A., and Kiley, P. J. (2000) The cysteine desulfurase, IscS, has a major role in in vivo Fe-S cluster formation in Escherichia

coli, *Proceedings of the National Academy of Sciences of the United States of America 97*, 9009-9014.
41. Smith, A. D., Agar, J. N., Johnson, K. A., Frazzon, J., Amster, I. J., Dean, D. R., and Johnson, M. K. (2001) Sulfur transfer from IscS to IscU: the first step in iron-sulfur cluster biosynthesis, *Journal of the american chemical society 123*, 11103-11104.
42. Urbina, H. D., Silberg, J. J., Hoff, K. G., and Vickery, L. E. (2001) Transfer of sulfur from IscS to IscU during Fe/S cluster assembly, *The Journal of biological chemistry 276*, 44521-44526.
43. Loiseau, L., Ollagnier-de-Choudens, S., Nachin, L., Fontecave, M., and Barras, F. (2003) Biogenesis of Fe-S cluster by the bacterial Suf system: SufS and SufE form a new type of cysteine desulfurase, *The Journal of biological chemistry 278*, 38352-38359.
44. Ollagnier-de-Choudens, S., Lascoux, D., Loiseau, L., Barras, F., Forest, E., and Fontecave, M. (2003) Mechanistic studies of the SufS-SufE cysteine desulfurase: evidence for sulfur transfer from SufS to SufE, *FEBS letters 555*, 263-267.
45. Layer, G., Gaddam, S. A., Ayala-Castro, C. N., Ollagnier-de Choudens, S., Lascoux, D., Fontecave, M., and Outten, F. W. (2007) SufE transfers sulfur from SufS to SufB for iron-sulfur cluster assembly, *The Journal of biological chemistry 282*, 13342-13350.
46. Allison, W. S. (1976) Formation and Reactions of Sulfenic Acids in Proteins, *Accounts of chemical research 9*, 293-299.
47. Everett, S. A., and Wardman, P. (1995) Perthiols as antioxidants: radical-scavenging and prooxidative mechanisms, *Methods in enzymology 251*, 55-69.
48. Goldsmith-Fischman, S., Kuzin, A., Edstrom, W. C., Benach, J., Shastry, R., Xiao, R., Acton, T. B., Honig, B., Montelione, G. T., and Hunt, J. F. (2004) The SufE sulfur-acceptor protein contains a conserved core structure that mediates interdomain interactions in a variety of redox protein complexes, *Journal of molecular biology 344*, 549-565.
49. Iannuzzi, C., Adinolfi, S., Howes, B. D., Garcia-Serres, R., Clemancey, M., Latour, J. M., Smulevich, G., and Pastore, A. (2011) The role of CyaY in iron sulfur cluster assembly on the E. coli IscU scaffold protein, *PloS one 6*, e21992.
50. Ramelot, T. A., Cort, J. R., Goldsmith-Fischman, S., Kornhaber, G. J., Xiao, R., Shastry, R., Acton, T. B., Honig, B., Montelione, G. T., and Kennedy, M. A. (2004) Solution NMR structure of the iron-sulfur cluster assembly protein U (IscU) with zinc bound at the active site, *Journal of molecular biology 344*, 567-583.
51. Chahal, H. K., Dai, Y., Saini, A., Ayala-Castro, C., and Outten, F. W. (2009) The SufBCD Fe-S scaffold complex interacts with SufA for Fe-S cluster transfer, *Biochemistry 48*, 10644-10653.
52. Park, S., and Imlay, J. A. (2003) High levels of intracellular cysteine promote oxidative DNA damage by driving the fenton reaction, *Journal of bacteriology 185*, 1942-1950.

53. Cook, P. F., and Wedding, R. T. (1976) A reaction mechanism from steady state kinetic studies for O-acetylserine sulfhydrylase from Salmonella typhimurium LT-2, *The Journal of biological chemistry 251*, 2023-2029.
54. Lee, J. H., Yeo, W. S., and Roe, J. H. (2004) Induction of the sufA operon encoding Fe-S assembly proteins by superoxide generators and hydrogen peroxide: involvement of OxyR, IHF and an unidentified oxidant-responsive factor, *Molecular microbiology 51*, 1745-1755.
55. Tokumoto, U., Kitamura, S., Fukuyama, K., and Takahashi, Y. (2004) Interchangeability and distinct properties of bacterial Fe-S cluster assembly systems: functional replacement of the isc and suf operons in Escherichia coli with the nifSU-like operon from Helicobacter pylori, *Journal of biochemistry 136*, 199-209.
56. Winterbourn, C. C., and Metodiewa, D. (1999) Reactivity of biologically important thiol compounds with superoxide and hydrogen peroxide, *Free radical biology and medicine 27*, 322-328.
57. Zhang, N., Schuchmann, H. P., and Vonsonntag, C. (1991) The Reaction of Superoxide Radical-Anion with Dithiothreitol - a Chain Process, *Journal of physical chemistry 95*, 4718-4722.
58. Kato, S., Mihara, H., Kurihara, T., Takahashi, Y., Tokumoto, U., Yoshimura, T., and Esaki, N. (2002) Cys-328 of IscS and Cys-63 of IscU are the sites of disulfide bridge formation in a covalently bound IscS/IscU complex: implications for the mechanism of iron-sulfur cluster assembly, *Proceedings of the National Academy of Sciences of the United States of America 99*, 5948-5952.
59. Zheng, M., Wang, X., Templeton, L. J., Smulski, D. R., LaRossa, R. A., and Storz, G. (2001) DNA microarray-mediated transcriptional profiling of the Escherichia coli response to hydrogen peroxide, *Journal of bacteriology 183*, 4562-4570.
60. Blanchard, J. L., Wholey, W. Y., Conlon, E. M., and Pomposiello, P. J. (2007) Rapid changes in gene expression dynamics in response to superoxide reveal SoxRS-dependent and independent transcriptional networks, *PloS one 2*, e1186.
61. Ohtsu, I., Wiriyathanawudhiwong, N., Morigasaki, S., Nakatani, T., Kadokura, H., and Takagi, H. (2010) The L-cysteine/L-cystine shuttle system provides reducing equivalents to the periplasm in Escherichia coli, *The Journal of biological chemistry 285*, 17479-17487.
62. Sauve, V., Bruno, S., Berks, B. C., and Hemmings, A. M. (2007) The SoxYZ complex carries sulfur cycle intermediates on a peptide swinging arm, *The Journal of biological chemistry 282*, 23194-23204.
63. Rohwerder, T., and Sand, W. (2003) The sulfane sulfur of persulfides is the actual substrate of the sulfur-oxidizing enzymes from Acidithiobacillus and Acidiphilium spp, *Microbiology 149*, 1699-1710.
64. Quentmeier, A., and Friedrich, C. G. (2001) The cysteine residue of the SoxY protein as the active site of protein-bound sulfur oxidation of Paracoccus pantotrophus GB17, *FEBS letters 503*, 168-172.
65. Zheng, L., Cash, V. L., Flint, D. H., and Dean, D. R. (1998) Assembly of iron-sulfur clusters. Identification of an iscSUA-hscBA-fdx gene cluster from Azotobacter vinelandii, *The Journal of biological chemistry 273*, 13264-13272.

66. Fontecave, M., and Ollagnier-de-Choudens, S. (2008) Iron-sulfur cluster biosynthesis in bacteria: Mechanisms of cluster assembly and transfer, *Archives of biochemistry and biophysics 474*, 226-237.
67. Tokumoto, U., and Takahashi, Y. (2001) Genetic analysis of the isc operon in Escherichia coli involved in the biogenesis of cellular iron-sulfur proteins, *Journal of biochemistry 130*, 63-71.
68. Fontecave, M., Choudens, S. O., Py, B., and Barras, F. (2005) Mechanisms of iron-sulfur cluster assembly: the SUF machinery, *Journal of biological inorganic chemistry 10*, 713-721.
69. Dai, Y., and Outten, F. W. (2012) The E. coli SufS-SufE sulfur transfer system is more resistant to oxidative stress than IscS-IscU, *FEBS letters 586*, 4016-4022.
70. Selbach, B. P., Pradhan, P. K., and Dos Santos, P. C. (2013) Protected sulfur transfer reactions by the Escherichia coli Suf system, *Biochemistry 52*, 4089-4096.
71. Wollers, S., Layer, G., Garcia-Serres, R., Signor, L., Clemancey, M., Latour, J. M., Fontecave, M., and Ollagnier de Choudens, S. (2010) Iron-sulfur (Fe-S) cluster assembly: the SufBCD complex is a new type of Fe-S scaffold with a flavin redox cofactor, *The Journal of biological chemistry 285*, 23331-23341.
72. Fujii, T., Maeda, M., Mihara, H., Kurihara, T., Esaki, N., and Hata, Y. (2000) Structure of a NifS homologue: X-ray structure analysis of CsdB, an Escherichia coli counterpart of mammalian selenocysteine lyase, *Biochemistry 39*, 1263-1273.
73. Behshad, E., and Bollinger, J. M., Jr. (2009) Kinetic analysis of cysteine desulfurase CD0387 from Synechocystis sp. PCC 6803: formation of the persulfide intermediate, *Biochemistry 48*, 12014-12023.
74. Busenlehner, L. S., and Armstrong, R. N. (2005) Insights into enzyme structure and dynamics elucidated by amide H/D exchange mass spectrometry, *Archives of biochemistry and biophysics 433*, 34-46.
75. Engen, J. R. (2009) Analysis of protein conformation and dynamics by hydrogen/deuterium exchange MS, *Analytical chemistry 81*, 7870-7875.
76. Mandell, J. G., Falick, A. M., and Komives, E. A. (1998) Identification of protein-protein interfaces by decreased amide proton solvent accessibility, *Proceedings of the National Academy of Sciences of the United States of America 95*, 14705-14710.
77. Tawfik, D. S. (2002) Modification of Sulfhydryl Groups with DTNB, In *The Protein Protocols Handbook* (Walker, J. M., Ed.), pp 483-484, Humana Press.
78. Singh, H., and Busenlehner, L. S. (2014) Probing Backbone Dynamics With Hydrogen/Deuterium Exchange Mass Spectrometry, In *Protein Dynamics: Methods and Protocols* (Livesay, D. R., Ed.), Humana Press, New York.
79. Mandell, J. G., Baerga-Ortiz, A., Croy, C. H., Falick, A. M., and Komives, E. A. (2005) Application of amide proton exchange mass spectrometry for the study of protein-protein interactions, *Current protocols in protein science Chapter 20*, Unit20 29.
80. Ehring, H. (1999) Hydrogen exchange/electrospray ionization mass spectrometry studies of structural features of proteins and protein/protein interactions, *Analytical biochemistry 267*, 252-259.

81. Tirupati, B., Vey, J. L., Drennan, C. L., and Bollinger, J. M., Jr. (2004) Kinetic and structural characterization of Slr0077/SufS, the essential cysteine desulfurase from Synechocystis sp. PCC 6803, *Biochemistry 43*, 12210-12219.
82. Engen, J. R., Gmeiner, W. H., Smithgall, T. E., and Smith, D. L. (1999) Hydrogen exchange shows peptide binding stabilizes motions in Hck SH2, *Biochemistry 38*, 8926-8935.
83. Mandell, J. G., Baerga-Ortiz, A., Akashi, S., Takio, K., and Komives, E. A. (2001) Solvent accessibility of the thrombin-thrombomodulin interface, *Journal of molecular biology 306*, 575-589.
84. Busenlehner, L. S., Alander, J., Jegerscohld, C., Holm, P. J., Bhakat, P., Hebert, H., Morgenstern, R., and Armstrong, R. N. (2007) Location of substrate binding sites within the integral membrane protein microsomal glutathione transferase-1, *Biochemistry 46*, 2812-2822.
85. Kim, S., and Park, S. (2013) Structural changes during cysteine desulfurase CsdA and sulfur-acceptor CsdE interactions provide insight into the trans-persulfuration, *Journal of biological chemistry 288*, 27172-27180.
86. Selbach, B., Earles, E., and Dos Santos, P. C. (2010) Kinetic analysis of the bisubstrate cysteine desulfurase SufS from Bacillus subtilis, *Biochemistry 49*, 8794-8802.
87. Loiseau, L., Ollagnier-de Choudens, S., Lascoux, D., Forest, E., Fontecave, M., and Barras, F. (2005) Analysis of the heteromeric CsdA-CsdE cysteine desulfurase, assisting Fe-S cluster biogenesis in Escherichia coli, *The Journal of biological chemistry 280*, 26760-26769.
88. Shi, R., Proteau, A., Villarroya, M., Moukadiri, I., Zhang, L., Trempe, J. F., Matte, A., Armengod, M. E., and Cygler, M. (2010) Structural basis for Fe-S cluster assembly and tRNA thiolation mediated by IscS protein-protein interactions, *PLoS Biology 8*, e1000354.
89. Liu, G., Li, Z., Chiang, Y., Acton, T., Montelione, G. T., Murray, D., and Szyperski, T. (2005) High-quality homology models derived from NMR and X-ray structures of E. coli proteins YgdK and Suf E suggest that all members of the YgdK/Suf E protein family are enhancers of cysteine desulfurases, *Protein science : a publication of the Protein Society 14*, 1597-1608.
90. Bolstad, H. M., Botelho, D. J., and Wood, M. J. (2010) Proteomic analysis of protein-protein interactions within the Cysteine Sulfinate Desulfinase Fe-S cluster biogenesis system, *Journal of proteome research 9*, 5358-5369.
91. Singh, H., Dai, Y., Outten, F. W., and Busenlehner, L. S. Escherichia coli SufE Sulfur Transfer Protein Modulates the SufS Cysteine Desulfurase through Allosteric Conformational Dynamics, *The Journal of biological chemistry 288*, 36189-36200.
92. Singh, H., Dai, Y., Outten, F. W., and Busenlehner, L. S. (2013) Escherichia coli SufE Sulfur Transfer Protein Modulates the SufS Cysteine Desulfurase through Allosteric Conformational Dynamics, *The Journal of biological chemistry 288*, 36189-36200.
93. Beinert, H. (2000) Iron-sulfur proteins: ancient structures, still full of surprises, *Journal of biological inorganic chemistry 5*, 2-15.

94. Kiley, P. J., and Beinert, H. (2003) The role of Fe-S proteins in sensing and regulation in bacteria, *Current opinion in microbiology 6*, 181-185.
95. Jacobson, M. R., Cash, V. L., Weiss, M. C., Laird, N. F., Newton, W. E., and Dean, D. R. (1989) Biochemical and genetic analysis of the nifUSVWZM cluster from Azotobacter vinelandii, *Molecular & general genetics 219*, 49-57.
96. Kispal, G., Csere, P., Prohl, C., and Lill, R. (1999) The mitochondrial proteins Atm1p and Nfs1p are essential for biogenesis of cytosolic Fe/S proteins, *The EMBO journal 18*, 3981-3989.
97. Schilke, B., Voisine, C., Beinert, H., and Craig, E. (1999) Evidence for a conserved system for iron metabolism in the mitochondria of Saccharomyces cerevisiae, *Proceedings of the National Academy of Sciences of the United States of America 96*, 10206-10211.
98. Patzer, S. I., and Hantke, K. (1999) SufS is a NifS-like protein, and SufD is necessary for stability of the [2Fe-2S] FhuF protein in Escherichia coli, *Journal of bacteriology 181*, 3307-3309.
99. Saini, A., Mapolelo, D. T., Chahal, H. K., Johnson, M. K., and Outten, F. W. (2010) SufD and SufC ATPase activity are required for iron acquisition during in vivo Fe-S cluster formation on SufB, *Biochemistry 49*, 9402-9412.
100. Beinert, H. (1983) Semi-micro methods for analysis of labile sulfide and of labile sulfide plus sulfane sulfur in unusually stable iron-sulfur proteins, *Analytical biochemistry 131*, 373-378.
101. Eccleston, J. F., Petrovic, A., Davis, C. T., Rangachari, K., and Wilson, R. J. (2006) The kinetic mechanism of the SufC ATPase: the cleavage step is accelerated by SufB, *The Journal of biological chemistry 281*, 8371-8378.
102. Chahal, H. K., and Outten, F. W. (2012) Separate FeS scaffold and carrier functions for SufB(2)C(2) and SufA during in vitro maturation of [2Fe2S] Fdx, *Journal of inorganic biochemistry 116*, 126-134.
103. Agar, J. N., Krebs, C., Frazzon, J., Huynh, B. H., Dean, D. R., and Johnson, M. K. (2000) IscU as a scaffold for iron-sulfur cluster biosynthesis: sequential assembly of [2Fe-2S] and [4Fe-4S] clusters in IscU, *Biochemistry 39*, 7856-7862.
104. Varghese, S., Tang, Y., and Imlay, J. A. (2003) Contrasting sensitivities of Escherichia coli aconitases A and B to oxidation and iron depletion, *Journal of bacteriology 185*, 221-230.
105. Jordan, P. A., Tang, Y., Bradbury, A. J., Thomson, A. J., and Guest, J. R. (1999) Biochemical and spectroscopic characterization of Escherichia coli aconitases (AcnA and AcnB), *The Biochemical journal 344 Pt 3*, 739-746.

Appendix A

Mass Spectrometry Analysis of SufS, SufE, IscS and IscU

Cysteine residues condition in proteins based on the crystal structure and DTNB assay

IscS

There are 3 cysteine residues in IscS, which are Cys 111 170 and 328. Acitive site Cys 328 is located on the disordered loop (Ala 327 to Leu 333) in crystal structure. Cys 170 and 111 both are not near the dimmer face. They located at α-helix and points to a β sheet core. They are in similar environment. And they are unlikely can form disulfide bond with Cys 328 based on the distance unless large conformation change. And in the IscS-IscU complex crystal structure, they are both far away from IscU.

2 cysteines per monomer were detected by DTNB in native IscS protein, while 3 cysteines per monomer were detected by DTNB at denature protein.

IscU

There are 3 cysteine residues in IscU, which are Cys 37, 63 and 106. Cys 37 located on a loop. Cys 63 located on one end of α-helix and Cys 106 located at center of a α-helix. All the SH groups on those cysteines pointed to one empty center which were proposed for the cluster binding site. Cys 63 and 106 are potential residue coordinated

with cluster.

All these 3 cysteines can be detected by DTNB both at native and denature state.

SufS

There are 4 cysteine residues in SufS, which are Cys 134, 217, 363 and 377. Cys 363 is the active site cysteine. Cys 134 located at a α-helix, at the edge of the crystal, which may be in a hydrophilic environment. Cys 217 located at a loop. Cys 363 also located on a loop. Cys 377 located at β-sheet. Both of Cys 363 and 377 may be located on the dimer inner surface.

2 cysteine residues were detected by DTNB assay at native state, which all 4 cysteine residues were detected at denature state by DTNB assay.

SufE

There are 2 cysteine residues in SufE, which are Cys 17 and 51. And Cys 51 is the active site cysteine. Both of them located at loops. The SH group on Cys 17 pointed out while Cys 51 pointed inward. In the crystal structure, Cys 17 binds BME. Both of them were detected by DTNB ssay at native and denature state.

Phosphorylation

For SufS, SufE, IscS and IscU, all the proteins have phosphoryltate modifications on Serine (S), Threonine (T) and Tyrosine (Y). These modifications reduce the ionization efficiency of peptides, which will affect the mass spec result. This is the reason we treat our proteins with Lamda phosphatase to remove these modifications.

Modification amino acid collection (p): file refers to 06-27-12 Cys oxidation ID_results_summary and 06-27-12 Cys oxidation data Quantitation summary

Modification label list:

M* = +16

C# = +57 IAA treatment

STY@ = +80

C^ = +16

C~ = +32

C$ = +48

Amino acids phosphate modified summary:

IscU_C1 K.IHC#S (p) ILAEDAIK.A

R.NVGS (p) FDNNDENVGS (p) GMVGAPAC#GDVM*K.L

IscU_C2 K.IHC#S (p) ILAEDAIK.A

R.NVGSFDNNDENVGS (p) GM*VGAPAC#GDVM*KLQIK.V

K.T (p) YGC^GS (p) AIAS (p) S (p) S (p) LVTEWVK.G

IscU_O1 K.MMQFMT (p) MDGT (p) FGNPASR.S

R.VAEKMMQFMT (p) MDGTFGNPASR.S

IscU_O2 K.IHC#S (p) ILAEDAIK.A

R.NVGSFDNNDENVGS (p) GM*VGAPAC^GDVM*K.L

K.TY (p) GC^GS (p) AIAS (p) S (p) SLVTEWVK.G

IscU_O3 R.FKT (p) YGC$GS (p) AIAS (p) S (p) SLVTEWVKGK.S

K.IHC#S (p) ILAEDAIK.A

R.NVGSFDNNDENVGS (p) GMVGAPAC#GDVM*K.L

K.T (p) YGC^GSAIAS (p) S (p) S (p) LVT (p) EWVK.G

IscS_C1 K.MMQFMT (p) MDGT (p) FGNPASR.S

K.T (p) EHKAVLDT (p) CR.Q

IscS_C2 K.MMQFMT (p) MDGT (p) FGNPASR.S

K.T (p) EHKAVLDT (p) CR.Q

IscS_O1 K.DLAVSSGS (p) AC#T (p) SASLEPSYVLR.A

K.MMQFMT (p) MDGT (p) FGNPASR.S

IscS_O2 K.DLAVS (p) S (p) GS (p) AC~T (p) S (p) ASLEPSYVLR.A

K.MMQFMT (p) MDGT (p) FGNPASR.S

Isc_O3 K.DLAVSS (p) GS (p) AC^T (p) SASLEPSYVLR.A

K.MMQFMT (p) MDGT (p) FGNPASR.S

IscSU_O1 IscS R.VAEKMMQFMT (p) MDGTFGNPASR.S

IscSU_O2 IscU K.T (p) Y (p) GC#GS (p) AIASSSLVTEWVKGK.S

IscS K.DLAVS (p) S (p) GS (p) AC~T (p) SASLEPSYVLR.A

K.MMQFMT (p) MDGT (p) FGNPASR.S

IscSU_O3 IscS -.M*KLPIY (p) LDY (p) S (p) ATTPVDPRVAEK.M

K.MMQFMT (p) MDGTFGNPASR.S

SufE_C1

SufE_C2

SufE_O1

SufE_O2

SufE_O3 R.LPELRDEDRSPQNS (p) IQGCQS (p) QVWIVM*R.Q

SufSE_O1

SufSE_O2 SufS ANS (p) WGNS (p) HEEVDRLVTGLQRIHR.L

SufSE_O3 SufS R.AS (p) LAMY (p) NT (p) HEEVDRLVTGLQRIHR.L

SufS_C1

SufS_C2 R.ASLAMYNT (p) HEEVDRLVTGLQR.I

SufS_O1 R.SAEELVFVRGTTEGINLVANS (p) WGNS (p) NVR.A

R.T (p) GHHCAMPLMAY (p) Y (p) NVPAM*C$R.A

R.VGAELRVIPLNPDGTLQLET (p) LPT (p) LFDEKT (p) R.L

SufS_O2 R.SAEELVFVRGTTEGINLVANS (p) WGNS (p) NVR.A

R.T (p) GHHCAMPLMAY (p) Y (p) NVPAM*C$R.A

SufS_O3 R.GIHT (p) LS (p) AQATEKM*ENVR.K

K.VLVDGAQAVMHHPVDVQALDCDFY (p) VFSGHK.L

R.SAEELVFVRGTTEGINLVANS (p) WGNS (p) NVR.A

R.T (p) GHHCAMPLMAY (p) Y (p) NVPAM*C$R.A

Oxidation (First Trial)

The oxidation data were collected in this table (**Table B. 1**). To be noted, the control data also have certain oxidation and some even higher than oxidized samples and the results are not quite consistent, which can be tell from the big standard deviation. But still, from this data, we can tell active site C364 on SufS is resistant to H_2O_2 treatment and C63 and 106 on IscU is quite sensitive to H_2O_2 treatment. And the data collected for IscU is quite consistent and the sensitivity rank for all its cysteines is C63 > C106 > C37.

Table A.1 Occupancy percent of active site cysteines oxidation in SufS, SufE, IscS and IscU.

Mass shift	Occupancy Percent (%)				
	SufS	SufE	IscS	IscU	
(+ Da)	**C364**	**C51**	**C328**	**C63**	**C106**
0	100	7.6±13.1	58.7±52.2	8.4±2.2	68.1±7.1
16	0	29.9±41.5	13.9±24.0	7.6±0.1	2.3±3.2
32	0	0	8.0±13.8	0	2.2±0.2
48	0	62.5±54.5	19.5±33.7	84.0±2.1	28.2±9.0

Methionine Oxidation

All the proteins we tracked have Met oxidation after treated them with H_2O_2. So Met in those proteins may function as an oxidation buffering system, which can consume some H_2O_2. We have no idea so far whether this has any physiological meaning for our system. The data were recorded in tables below (Table B. 1 – 5).

Table A. 2 Occupancy percent of methionine oxidation in IscS alone and IscS with IscU.

Residue #	IscS	IscS/IscSU
M1	35.6±15.7	16.0±1.7
M23	32.9±41.2	3.2±4.6
M24	46.2±33.0	6.9±10.0
M27	9.5±4.3	6.6±5.0
M29	18.9±15.9	14.0±8.9
M141	12.1±20.9	0
M151	0	15.9±27.5
M169	32.5±28.9	13.1±6.0
M200	39.7±28.9	8.2±3.8
M230	0	0
M252	25.2±10.2	9.9±0.4
M263	0.9±1.6	0.1±0.1
M267	2.2±2.3	7.2±12.2
M315	9.7±14.1	0
M389	31.0±12.7	16.4±4.3
Overall	26.2±15.1	9.0±1.4

Table A.3 Occupancy percent of methionine oxidation in IscU alone and IscU with IscS.

Residue #	IscU	IscU/IscSU
M31	7.1±4.6	12.3±6.8
M41	12.2±9.5	19.1±9.6
Overall	9.7±3.3	15.7±1.5

Table A.4 Occupancy percent of methionine oxidation in SufS alone and SufS with SufE.

Residue #	SufS	SufS/SufSE
M1	0	0
M69	0	0
M121	13.2±18.7	0
M132	15.9±9.4	5.2±8.9
M186	28.0±18.6	16.7±11.4
M206	22.2±4.9	34.5±56.8
M246	5.7±9.9	7.0±12.1
M255	26.3±27.3	33.3±3.8
M366	100.0±0	50.0±70.7
M369	100.0±0	50.0±70.7
M377	0	0
M384	19.1±3.6	17.0±5.2
Overall	24.0±9.9	16.9±5.8

Table A.5 Occupancy percent of methionine oxidation in SufE alone and SufE with SufS.

Residue #	SufE	SufE/SufSE
M59	13.9±5.7	26.2±11.5
M92	17.4±10.8	27.6±7.4
M109	8.6±4.3	8.6±7.4
M126	5.3±4.4	9.7±2.3
Overall	10.6±6.3	10.6±3.1

Appendix B

Permission to Reprint

Elsevier user license for Chapter 2: The *E.coli* SufS-SufE Sulfur Transfer System is more Resistant to Oxidative Stress than IscS-IscU

Author rights:

Authors can use their articles for a wide range of scholarly, non-commercial purposes as outlined below. These rights apply for all Elsevier authors who publish their article as either a subscription article or an open access article. Cite the article using an appropriate bibliographic citation (i.e. author(s), journal, article title, volume, issue, page numbers, DOI and the link to the definitive published version on ScienceDirect)

Authors can use either their accepted author manuscript or final published article for:

- Use at a conference, meeting or for teaching purposes
- Internal training by their company
- Sharing individual articles with colleagues for their research use
- Use in a subsequent compilation of the author's works
- Inclusion in a thesis or dissertation
- Reuse of portions or extracts from the article in other words
- Preparation of derivative words.
- Link: http://www.elsevier.com/journal-authors/author-rights-and-responsibilities

Journal of Biological Chemistry copyright permission for Chapter 3: *Escherichia coli* SufE Sulfur Transfer Protein Modulates the SufS Cysteine Desulfurase through Allosteric Conformational Dynamics

For authors reusing their own material:

Authors need NOT contact the journal to obtain rights to reuse their own material. They are automatically granted permission to do the following:

- Reuse the article in print collections of their own writing.
- Present a work orally in its entirety.
- Use an article in a thesis and/or dissertation.
- Reproduce an article for use in the author's courses. (If the author is employed by an academic institution, that institution also may reproduce the article for teaching purposes.)
- Reuse a figure, photo and/or table in future commercial and noncommercial works.
- Post a copy of the paper in PDF that you submitted via BenchPress.
- Link to the journal site containing the final edited PDFs created by the publisher.
- Link: http://www.jbc.org/site/misc/Copyright_Permission.xhtml

Biochemistry journal copyright permission for Chapter 5: The SufBCD Fe-S scaffold complex interacts with SufA for Fe-S cluster transfer

Purpose: reuse in a thesis/dissertation

Requestor type: author (original work)

Portion: 50% or more of original article

Format: electronic and print

ERMISSION/LICENSE IS GRANTED FOR YOUR ORDER AT NO CHARGE

This type of permission/license, instead of the standard Terms & Conditions, is sent to you because no fee is being charged for your order. Please note the following:

- Permission is granted for your request in both print and electronic formats, and translations.
- If figures and/or tables were requested, they may be adapted or used in part.
- Appropriate credit for the requested material should be given as follows: "Reprinted (adapted) with permission from (The SufBCD Fe-S scaffold complex interacts with SufA for Fe-S cluster transfer). Copyright (2014) American Chemical Society."
- One-time permission is granted only for the use specified in your request. No additional uses are granted (such as derivative works or other editions). For any other uses, please submit a new request.
- Link: https://s100.copyright.com/AppDispatchServlet#formTop